Fenestrae alterations can play a critical role in disease including atherosclerosis and cirrhosis (DeLeve *et al*., 2004; Malarkey *et al*., 2005).

Kuppfer cells: They constitute approximately the 8-12% of the liver cells. They are specialized macrophages derived from monocytes, that assimilate particulated material via phagocytosis (Van Amersfoort *et al*., 2003; Parker and Picut, 2005), as well as all kinds of old, unnecessary or damaged material from the circulation (such as immune complexes, erythrocytes, tumor cells, cell debris and apoptotic cells).

Stellate cells (Ito or fat-storing cells): Represent the 5-8% of the total liver cells. They are located in the space of Disse, the interstitial space between the parenchymal and endothelial cells. Their main functions are storage of viatmin A (which comprises the 80% of the vitamin A stored in the body), synthesis of extracellular matrix and secretion of growth factors (Friedman *et al*., 1985; Michalopoulos and DeFrances, 1997).

Pit cells: They constitute a specialized type of Natural Killer cell in the liver. They have the ability to kill some tumor cells and some virus-infected cells (Sherlock and Dooley, 2007).

5.1.2. Functions of the liver

The liver participates in most of the metabolic processes in the organism. It receives all the final products from protein absorption, carbohydrates and lipids, and it transforms this products in more complex or simpler substances indispensable for the normal function of the living beings. At the same time it is fundamental in the elimination of toxic products, hormones and drugs. Some of the multiple functions that the liver performs will be described below.

In protein metabolism the liver participates in the deamination and transammination of aminoacids that enter into the liver, and by removing the toxic ammonia from the body by transforming it into urea. It participates in the synthesis of non-essential aminoacids and hepatocytes are responsible for synthesis of most of the plasma proteins (albumin, fibrinogen, haptoglobin, transferrin, etc...)(Sherlock and Dooley, 2007).

In carbohydrate metabolism liver is involved in the storage and depolimerization of of glycogen (glycogenesis, glycongenolysis). It is also responsible of gluconeogenesis. Taking it altogether, it is critical in the maintenance of normal blood glucose levels

(Sherlock and Dooley, 2007). The liver is also central to lipid (cholesterol, phospholipid and triglycerides) and lipoprotein metabolism (Sherlock and Dooley, 2007). Bile is critical for digestion, fat absorption and in the removal of waste products. Hepatocytes are responsible fot bile secretion into the canaliculi, from which it flows into bile ducts (Sherlock and Dooley, 2007).

Moreover, liver enzymes play critical roles in the metabolism of endogenous chemicals, process natural products (terpenes, steroids, vitamins, etc…) and metabolize external chemicals such as drugs, pollutants and other xenobiotics (Sherlock and Dooley, 2007). These compounds are generally lipophilic and thus difficult to eliminate. The elimination of these products very often involves their transformation into water-soluble molecules, which enables the elimination through feces or urine. This process is known as biotransformation, and it is mediated by two groups of enzymes Phase I and Phase II enzymes (Sherlock and Dooley, 2007). Phase I reactions involve oxidation, reduction or hydrolisis, which result in an increase in the hydrophilicity of the compound. The main enzyme block within this group is comprised by cytochromes p450 (CYP450), which metabolize most part of the known drugs and many natural products (Table 5.1.) (Guengerich, 2004; Guengerich, 1991). In pharmacology, these enzymes, many times affect to the pharmacokinetics (PK) and pharmacodynamics (PD) of the drug. The reaction products may be more or less effective than the drug itself. Many drugs act as inhibitors or inducers of the enzymes, affecting to the PK/PD parameters. Therefore the study of interaction of the drug (specially new chemical entities) and CYP450 enzymes essential in the drug discovery process. CYP450 enzymes can also be useful in the study of drug-drug interactions (Guengerich, 2004; Guengerich, 1991).

Table 5.1. Classification of human CYP450 based on major substrate class, adapted from (Guengerich, 2004)

Sterols	Xenobiotics	Fatty acids	Eicosanoids	Vitamins	Unknown
1B1	1A1	2J2	4F2	24	2A7
7A1	1A2	4A11	4F3	26A1	2R1
7B1	2A6	4B1	4F8	26B1	2S1
8B1	2A13	4F12	5A1	27B1	2U1
11A1	2B6		8A1		2W1
11B1	2C8				3A43
11B2	2C9				4A22
17	2C18				4F11
19	2C19				4F22
21A2	2D6				4V2
27A1	2E1				4X1
39	2F1				4Z1
46	3A4				20
51	3A5				26C1
	3A7				27C1

This classification is somewhat arbitrary (e.g., P450 1B1 and 27A1 could be grouped in two different categories.

On the other hand, Phase II enzymes, normally involve glucuronidation, acetylation, methylation and conjugation with gluthatione or aminoacids, etc… With the exception of acetylation and methylation, these modifications result in a strong increase in hydrophilicity. These groups are either added directly through a reactive group present in the drug, or through a functional group introduced in a Phase I reaction (327).

5.1.3. Recreation of the liver microenvironment *in vitro*

The obtention of completely functional hepatic *in vitro* systems would represent a very powerful tool in the drug discovery process as well as in the study of liver pathophysiology. These could serve for example in the evaluation of drug uptake and metabolism, microsomal cytochrome P450 induction, the study of drug interactions, hepatotoxicity, among others. The difficulty to achieve these *in vitro* systems lies in the process of hepatocyte isolation, in which the cells lose their surrounding microenvironement which comprises the extracellular matrix and the interaction with the other hepatic cell types, resulting in a de-differentiation process and a rapid loss of liver-specific functions (LeCluyse *et al*., 1996). Apparently, it is the disruption of the

normal tissue architecture during liver perfusions, the responsible of many of the alterations in gene expression observed in cultured hepatocytes (LeCluyse *et al*., 1996). Consequently, the development of methods of culturing hepatocytes whereby primary hepatocytes can be maintained without de-differentiating in long-term cultures with their liver-specific functions intact has been pursued for decades. These studies cover many different aspects of the culture system:

- Medium formulation
- Extracellular matrix
- Cell-cell contacts

Indeed, there is extensive research (reviewed by Le Cluyse and co-workers (328)) of the effect of different medium formulations on hepatocyte cultures in order to elucidate the nutrient, hormonal requirements and other components needed for enhancing hepatocyte gene expression and function as well as survival in long term cultures. For example, it is has been concluded that the presence of serum leads to a dedifferented state of the hepatocytes, allowing the survival of the cells but inducing a lost of liver-specific functions in terms of gene expression as well as a reduction of protein and other metabolite synthesis. It also has been shown that different basal media formulations containing different aminoacid and trace element formulations promote different cell performance in culture. Therefore, improved media formulations have been developed replacing serum with purified and defined hormones (such as insulin), glucocorticoids (such as dexamethasone), growth factors, trace elements and chemical modulatros such as pyruvate.

It is also known that one of the most important influences on the maintenance of normal hepatic structure and function *in vitro* is the interaction with the extracellular matrix. Simple cultures in regular tissue culture plates coated or not with different proteins (laminin, collagen, fibronectin) were soon abandoned because of the loss of hepatocyte viability, phenotype, gene expression and function. Then the protein coating process was substituted for the use of extracellular matrices as subtrates for hepatocyte culture, which is still today a widely employed resource (LeCluyse *et al*., 1996). Matrigel, collagen or liver-derived basement membrane matrices have been the most used materials leading to very promising results (Ben Ze'ev *et al*., 1988; Dunn *et al*., 1989; Dunn *et al*., 1991; Berthiaume *et al*., 1996; Silva *et al*., 1998; Wang *et al*., 2004; Zeisberg *et al*., 2006). These studies demonstrate the importance of the ECM in mantaining the differentiation status of the, such as the restoration of hepatocyte polarity, synthesis of liver-specific proteins and mRNA. Moreover the use of a sandwich

configuration culture, in which additional ECM is overlayed on top of the cultured hepatocytes, has resulted in an enhancement of their viability, phenotype and function, in terms of protein and mRNA synthesis as well as the restorement of bile acid transport and superior cytochrome P450 induction response (LeCluyse *et al*., 1996; Berthiaume *et al*., 1996; Wang *et al*., 2004; Barth and Schwarz, 1982; Dunn *et al*., 1991; Dunn *et al*., 1989).

Finally, the importance of cell-cell contacts (homotypic or heterotypic) is also a point to bear in mind. For example, the use of co-cultures with non-parenchymal cells (NPC) such as biliary epithelial cells, stellate cells or a unpurified NPC fraction, seems to also provide an advance in the establishment of a functional liver tissue construct (Bhatia *et al*., 1999; Uyama *et al*., 2002; Kan *et al*., 2004; Auth Marcus *et al*., 2005), probably because it resembles in a higher degree the cellular composition of the liver. In addition, cultures in which homotypic cell-cell interactions are enhanced have also been developed. The formation of hepatocyte spheroids (with or without the presence of NPC), is a technique that is being used and that has been shown to rescue the hepatocytes from the de-differentiation process (LeCluyse *et al*., 1996).

Most recently there has been an approach towards the use of synthetic biomaterials, in the form of hydrogels, porous membranes or foams, addressed to the obtantion of long-term functional hepatocyte cultures (De Bartolo *et al*., 2004; Sudo *et al*., 2005). The achievement of this goal with synthetic and defined models would be a major advance, as many problems related to the use of materials derived from natural sources would be overcome. Furthermore, the coupling of these materials with perfusion bioreactors, where physical parameters such as oxygen concentration or medium flow rate can be perfectlly controlled (Powers *et al*., 2002; De Bartolo *et al*., 2006; Schmitmeier *et al*., 2006).

In this part of the work, RAD16-I peptide scaffold has been used to build a hepatocyte culture system based on the collagen sandwich cultures, considered today as the gold standard for hepatocyte culture *in vitro* (Berthiaume *et al*., 1996; Wang *et al*., 2004) which recreates the hepatic architechture. RAD16-I has also been combined with modified self-assembling peptide scaffolds containing the integrin-binding sequence RGD, the 67 KDa laminin receptor binding sequence YIGSR (YIG), or the heparing binding sequence present in collagen IV TAGSCLRKFSTM (TAG) in order to create a microenvironement that has features of the extracellular matrix *in vivo* (Genove *et al*., 2005). We have compared the mantainance of some liver specific functions of this sandwich systems to the results obtained using a collagen sandwich

counterpart. Liver-specific or liver-enriched gene expression has been analyzed of using quantitative PCR; as well as albumin and urea secretion to determine liver functionality. In the same direction, the expression of several cellular proteins of interest and the secreted proteome have been analyzed. It has been shown that, hepatocytes cultured in a peptide sandwich configuration maintain similar levels of differentiation as in collagen sandwich cultures, as observed by comparable levels of the liver-specific functions studied. It has also been demonstrated, that CYP3A2, one of the key Phase I drug-metabolizing enzymes in rat hepatocytes can be induced to the same levels of that in collagen sandwiches. This peptide culture system presents the advantage of being completely synthetic and defined, fact that overrules the problems associated with the use of a naturally-derived matrix, such as the batch to batch deviations and the possible carryover of pathogens. Moreover, peptide sequences can be added to the matrix in a facil manner by direct solid phase synthesis allowing systematic variation of molecular cues in the extracellular microenvironment and tailoring that environment to promote specific activities.

5.2. RESULTS

The use of peptide scaffolds for long-term hepatic cultures were evaluated by determining liver-specific functions of hepatocytes cultured in such systems. We wanted to study the suitability of RAD16-I peptide scaffold to build a hepatocyte culture system *in vitro.* Firstly, the attachment of the hepatocytes to the synthetic hydrogel was assessed, as well as the survival of the cells on top of the matrix. The results obtained were compared to hepatocytes attached to a layer of collagen as a control.

Gels were prepared as explained in Chapter 7, and then hepatocytes were added on top of the peptide and collagen monolayers. Cultures were followed for 2 weeks in which it was observed that cells seeded on collagen cultures formed a monolayer, whereas in peptide cultures hepocytes tended to aggregate into spheroid-like structures (Figure 5.4.). This fact could have been due to the fact that collagen-I is a highly instructive protein that is present in liver ECM, and has adhesive sequences, whereas RAD16-I is a short synthetic peptide that does not contain any signalling peptide within its sequence. A viability test was performed by staining cells in culture with a Live/Dead analysis kit (Molecular Probes, L-3224), and it was observed that many of the cells were dead in both collagen and RAD16-I cultures. Several facts could have been the reason for such a bad viability, it could be due a bad perfusion, added to the fact that unattached cells were not washed away after the first incubation period,

and that the medium was changed every other day, when it is highly recommendable to change the medium daily, due to the high metabolic activity of the hepatocytes.

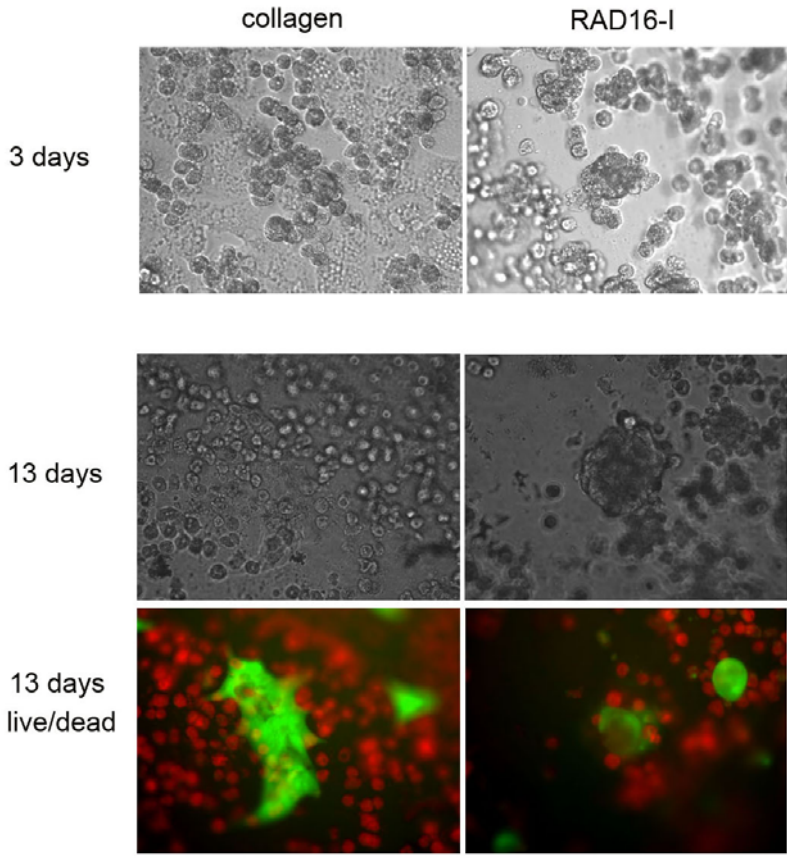

Figure 5.4. Hepatocytes cultured on a collagen/peptide RAD16-I hydrogel monolayer after 3 days and 13 days. Cells were stained with the Live/Dead analysis kit (Molecular Probes, L-3224). Fluorescence microscopy images show in green live cells and in red dead cells.

It has previously shown that hepatocytes cultured on a monolayer of collagen or a tissue culture plate coated with collagen dedifferentiate rapidly, whereas in the case of collagen sandwich cultures hepatocyte polarity and liver-specific functions are restored and supported long-term (Dunn *et al*., 1989; Dunn *et al*., 1991; Berthiaume *et al*., 1996). Therefore, we decided to change the culture system to the sandwich system. The collagen sandwich configuration was adapted into self-assembling peptide scaffold sandwich configuration. Collagen or RAD16-I peptide hydrogel hepatocyte sandwich cultures were prepared as shown in Figure 1 (Chapter 7). Matrix substrates were prepared first. For collagen sandwiches, a collagen solution (2 mg/mL in PBS)

was prepared and gelled for 30 min at 37 ºC. In the case of peptide sandwich cultures, a 0.5% peptide solution ((w/v) in 10% sucrose), containing or not the functionalized peptide sequence (95:5 RAD16-I:functionalized peptide, Table 5.2), was gellified by getting it in contact with a buffer or culture medium through the tissue culture insert membrane as explained in the Materials and Methods section (Figure 5.5., A). Then freshly isolated hepatocytes were added and incubated overnight at 37ºC (Figure 5.5., B). Dead and non-adherent cells were washed away from the cultures using a isotonic but non-ionic solution of 10% sucrose, and finally another layer of gel was added to entrap the cells in a sandwich fashion. In collagen cultures, the collagen solution was added on top of the cells, and was gellified in the incubator for 30 min at 37 ºC. For peptide hydrogel matrices, the solution was allowed to gellify in contact with the cells for 30 min and then very gently, culture media was added to equilibrate the sandwich with the media. The media was removed and the operation was repeated one more time (Figure 5.5.,C). Cultures were monitored for 10 days and they were cultured with defined media containing fatty-acid free bovine serum albumin (FAF-BSA), insulin, hydrocortisone, epidermal growth factor (EGF), transferrin, and ascorbic acid (Hepatocyte Culture Media, HCM, Cambrex, CC-3198). The media was changed daily.

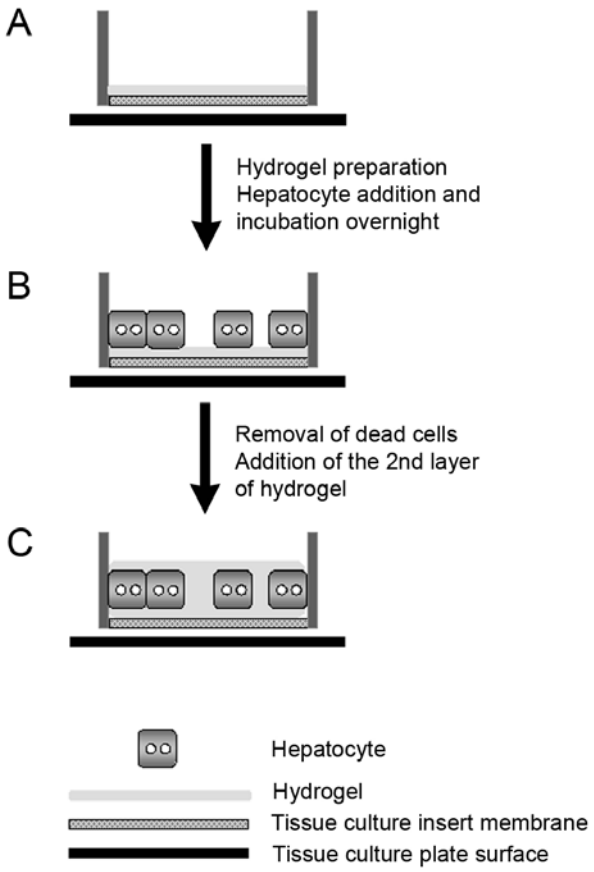

Figure 5.5. Assembly of the sandwich cultures. A) Collagen ot peptidic layers were prepared as it is explained in Materials and Methods. B) Hepatocytes were added and incubated overnight at 37ºC. The following day, dead cells were washed away C) Finally,a second layer of hydrogel was added in top of the hepatocytes.

Table 5.2. Peptide sequences used for the culture of rat hepatocytes

Peptide name	Peptide sequence
RAD16-I	AcN-RADARADARADARADA-$CONH_2$
RGD	AcN-GRGDSPY-GG-RADARADARADARADA-$CONH_2$
YIG	AcN-YIGSR-GG-RADARADARADARADA-$CONH_2$
TAG	AcN-TAGSCLRKFSTM-GG-RADARADARADARADA-$CONH_2$

Cells were monitored daily, the morphology and phenotype of hepatocytes cultured in both collagen and peptide hydrogel sandwiches were similar (Figure 5.6., A). In all cases, including cultures with functionalized peptide hydrogels, hepatocytes

became flattened, adopted a *in vivo*-like polygonal shape, established many cell-cell contacts with a reorganization of bile canaliculilar-like structures. To assess the functionality of the canaliculi-like structures 7-day cultures were incubated with a solution of media containing 2.5 μg/ml of flurorescein diacetate (FD). FD is a weakly fluorescent probe which is internalized in the cell (uptaken from the culture medium) and metabolized by cellular estearases into the fluorescent molecule fluorescein. Therefore, the excretion of the probe can be easily monitored under a fluorescent microscope (Barth and Schwarz, 1982; LeCluyse *et al*., 1994). For the peptide hydrogel sandwich cultures, the bile canaliculi proved to be functional as hepatocytes were able to metabolize and transport FD from the cytoplasm through the canaliculi-like structures, as it can be clearly seen by fluorescence microscopy (Figure 5.6., B). This behavior is comparable to what has been demonstrated before for collagen sandwich cultures (Barth and Schwarz, 1982; LeCluyse *et al*., 1994) as it is shown in the fluorescence microscopy image in Figure 5.7.

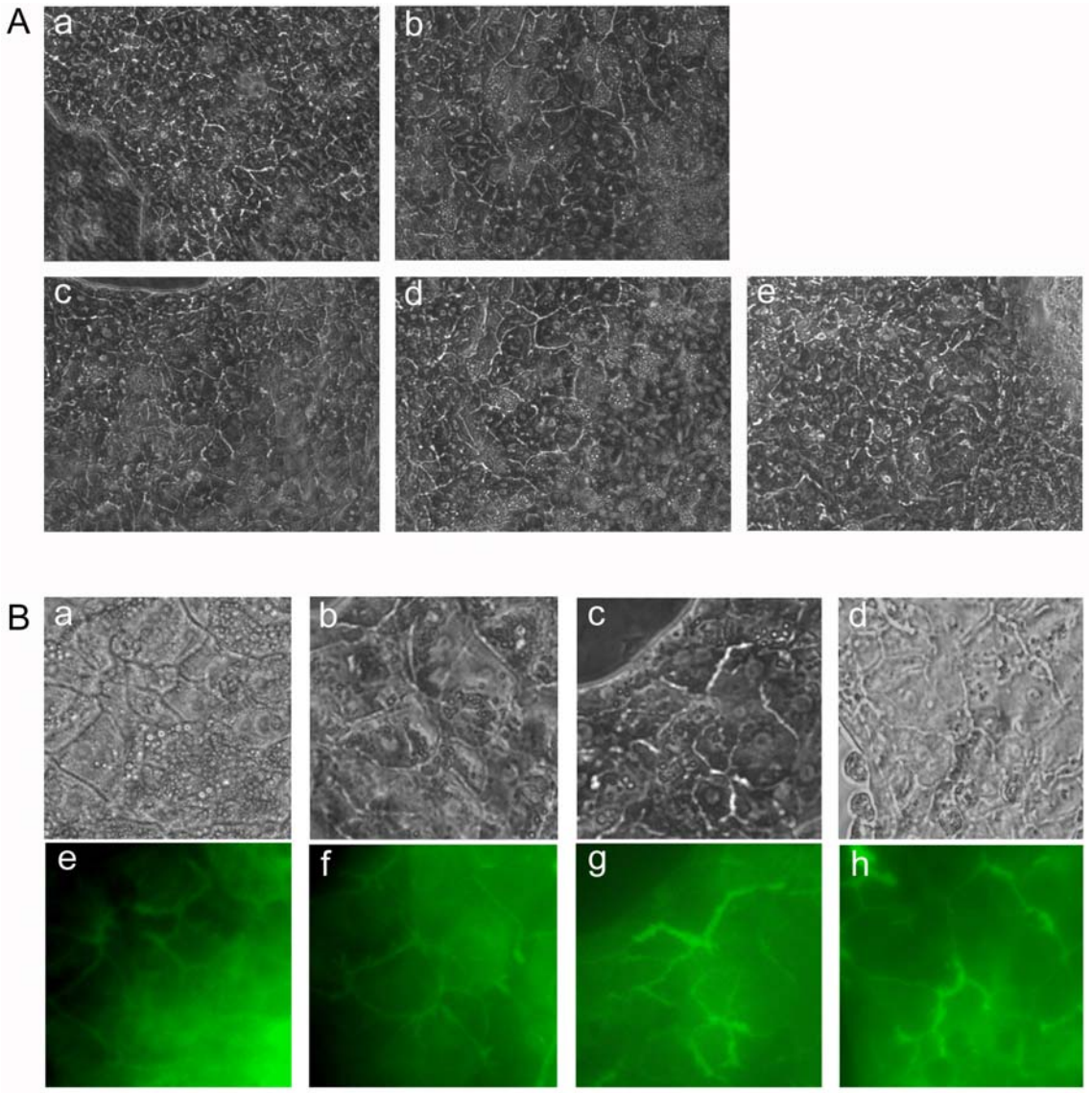

Figure 5.6. A) Morphology of hepatocytes in a sandwich culture for 7 days a) collagen, b) RAD16-I c) YIG, d) RGD and e) TAG. B) Presence of an extensive network of bile canaliculi-like structures in prototypic and functionalized peptide hydrogel sandwich cultures. a-d) phase contrast images and, e-f) fluorescence microscopy images which show the transport of metabolized fluorescein diacetate through the bile canaliculi-like structures. a,e) RAD16-I; b,f) YIG; c,g) RGD and d,h) TAG.

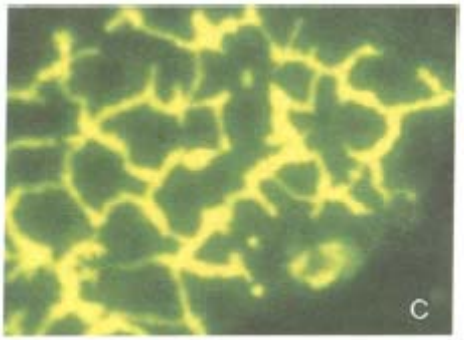

Figure 5.7. Fluorescein transport through bile canaliculi-like structures in collagen sandwich cultures, picture taken fron Barth *et al.* (Barth and Schwarz, 1982)

Moreover, gene expression of the hepatocytes cultured in our systems was assessed by means of quantitative PCR (Figure 5.9.). In this case, freshly isolated hepatocytes were chosen to perform a relative analysis of the gene expression profile, which means that gene expression in the collagen or peptide sandwich cultures were calculated relative to the gene expression of the hepatocytes from the same perfusion just after being isolated. The retrieval of RNA just after every perfusion leads to an accurate and representative value of the levels of expression of the specific hepatocytes at the time of the isolation. To prepare an RNA sample of the freshly isolated hepatocytes, a small aliquot of the hepatocytes were lysated using TRIZOL reagent (Invitrogen, CA, 15596-026) just after the perfusion. The sample was properly stored until needed to isolate the RNA and perform the RT-PCR.

In addition, to test wether the matrix thickness might influence nutrient and oxygen transport (mass transfer effect), and therefore cell function (Li *et al*., 1996), cultures composed of two layers of 1 mm or 0.5 mm-thick gels were prepared (see Materials and Methods). Herein, expression levels of albumin as a hepatocyte differentiation marker, the hepatic transcription factor HNF4-α, one hepatic metabolic enzyme, tyrosine aminotransferase (TAT), and MDR2 as a canalicular membrane marker transporter (Muller and Jansen, 1997) were examined in all culture systems on day 7 and day 10. Albumin is the major plasma protein that circulates in the bloodstream, and it is essential for maintaining the oncotic pressure in the vascular system. It is only produced in the liver, and therefore is one of the main markers to assess hepatocyte differentiation and function. HNF4-α is a transcription factor that has been found to be essential in early development as well as in the adult liver (Hatzis and Talianidis, 2001; Watt *et al*., 2003). It is highly expressed in liver, pancreas, instestines and kindney in mammals. In the adult liver it is one of the most important transcription

factors, it is considered to be at the top of a cascade of transcription regulating many genes involved in several metabolic pathways including glucose and lipids (Watt *et al*., 2003; Hayhurst *et al*., 2001). Thus, a normal expression of HNF4-α in the peptide cultures would be indicative of a differentiated state of the hepatocytes.

The expression of a tyrosine aminotransferase (TAT) was also analyzed. TAT is a liver-specific enzyme essential in tyrosine catabolism, catalizing the transamination with a-ketoglutarate to form p-hydroxyphenylpyruvate and glutamate. Finally we focused also on an hepatobiliary transport protein, multi-drug resistant protein (MDR2). The generation of a bile flow is basic in metabolism, it is a regulated process dependent of a coordinated action of a number transporter proteins present in the sinusoidal or canalicular membranes of the hepatocyte. Disfunction of these proteins leads to retention of the substrates and therefore to a number of different diseases. Figure 5.8. depicts several rodent transport proteins, their membrane localization and their substrates. MDR2, which is located in the canalicular membrane of hepatocytes was chosen in this study. This particular protein has been previously shown to be crucial in liver physiology, as it is involved in the transport of phospholipids (Hooiveld *et al*., 2001; Muller and Jansen, 1997).

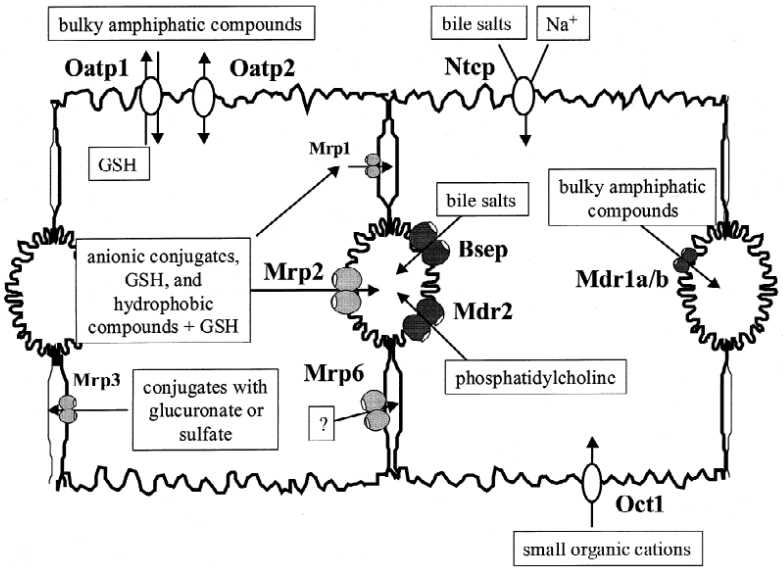

Figure 5.8. Transport proteins and polarity in rat hepatocytes and their substrates (Hooiveld *et al*., 2001). Of special interest relative to this work is MDR2 which is involved in the transport of phosphatidylcholine. Picture taken from Hoovield *et al*. (2001).

Real time PCR (quantitative PCR) was used to assess gene expression. The results obtained showed that, compared with the 1 mm-hydrogel cultures, the use of the 0.5 mm-collagen and peptide matrices resulted in a higher expression of all the genes studied, suggesting that mass transfer through the hydrogel is affected by the gel thickness (Figure 5.9., A). Therefore, we decided to use the 0.5 mm-thick gels for the rest of experiments. Despite the downregulation of most of the genes studied in the 1 mm-thick gels experiment (Figure 5.9., A), it can be observed that the gene expression profile was similar in the collagen and the peptide hydrogel sandwiches. The functionalized YIG-containing matrix exhibited the highest levels of gene expression for all genes studied. Nevertheless, the gene expression for MDR2 remained strongly downregulated as compared to freshly isolated hepatocytes over the entire culture period (Figure 5.9., A). Looking deeper into the gene expression analysis for the 0.5 mm gels, it can be observed that in general, peptide hydrogel and collagen cultures remained mainly in the same levels of expression. Relative expression values that fell between -1 and 1 were cosidered the same as fresh hepatocytes (Sivaraman Anand, 2004). In all conditions tested it was observed that albumin and HNF4-α have already reached the expression levels of freshly isolated hepatocytes, which was maintained until the end of the test (day 10). In addition, MDR2 remained downregulated in almost all conditions tested, except for YIG, which by day 10 reached the relative levels of freshly isolated hepatocytes (Figure 5.9., B). However, RAD16-I and TAG presented a slight upregulation in MDR2 compared to collagen (Figure 5.9., B). Moreover, TAT in collagen cultures remained somehow downregulated by day 7, but its expression was comparable to the positive control (freshly isolated hepatocytes) by day 10 (Figure 5.9., B). Furthermore, in peptide hydrogel sandwich cultures, TAT was maintained in control expression levels in all cases except for the matrix containing the integrin binding sequence RGD, in which it remains slightly downregulated. Figure 5.10. shows a typical amplification plot, showing amplification curves for HNF4-a in different conditions. After the PCR amplification protocol a melting curve analysis of the PCR products formed was always performed, in order to ensure that the analysis was correct and just one PCR product was formed (Figure 5.10.). In this case only one peak was detected, indicative of a adequate amplification. Moreover, the purity of the PCR products was checked running an agarose gel, detecting just one band with the expected molecular weight, therefore confirming that only one PCR product was formed (Figure 5.11.).

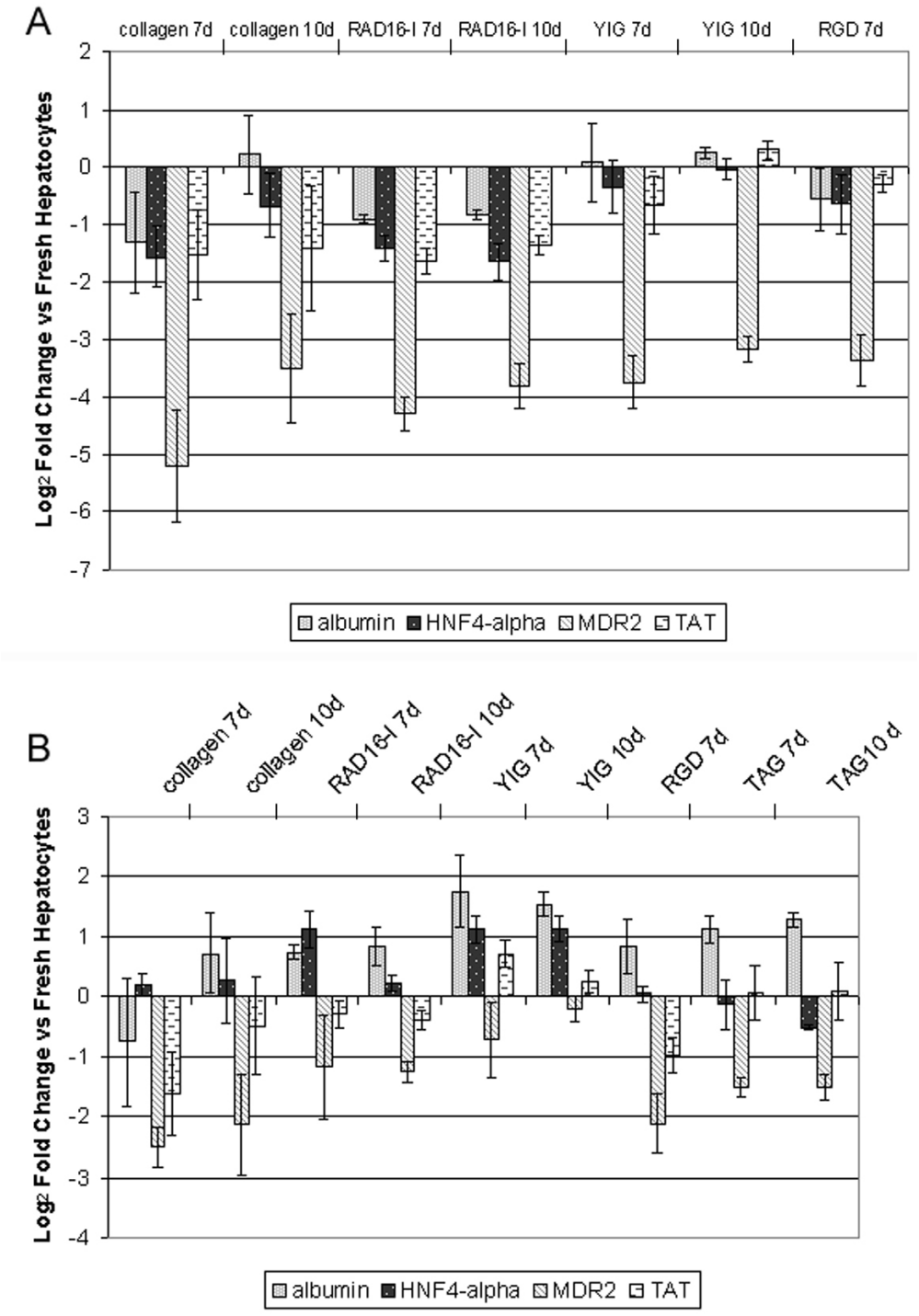

Figure 5.9. Gene expression profile analyzed by quantitative-PCR. A) Hepatocytes cultured in sandwich cultures using hydrogel layers of 1 mm thick. B) Hepatocytes cultured in sandwich conditions using 0.5 mm-thick hydrogel layers.

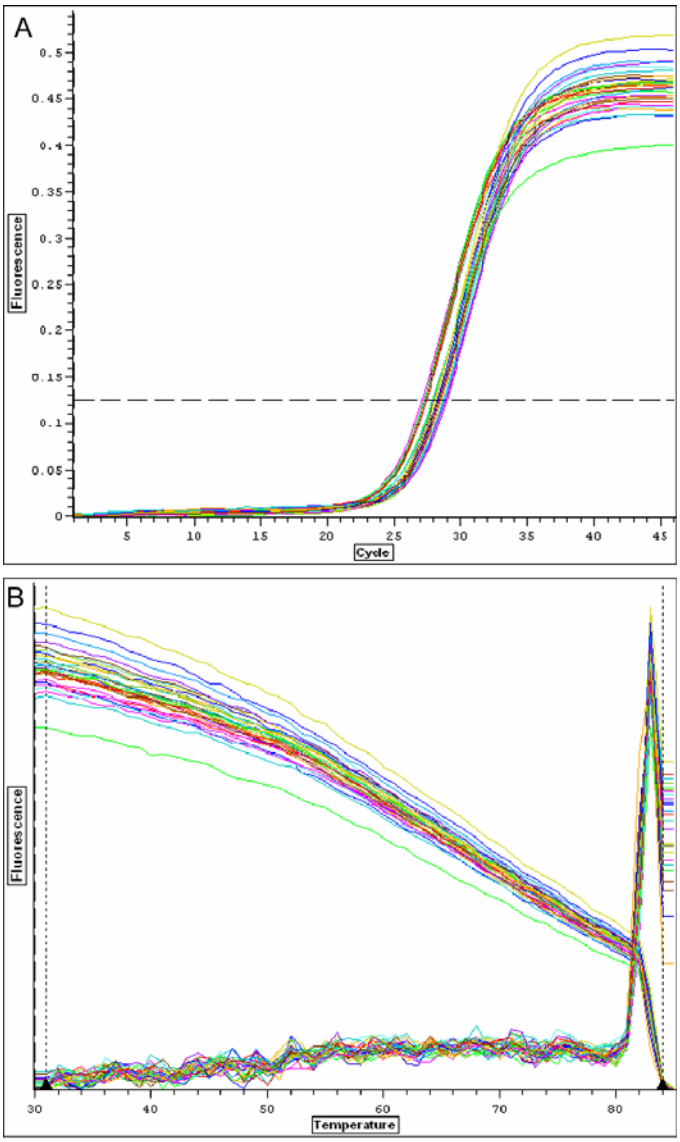

Figure 5.10. A) q-PCR amplification plot for HNF4-α. The dotted line shows the Ct selected to perform the calculations. B) Melting curve

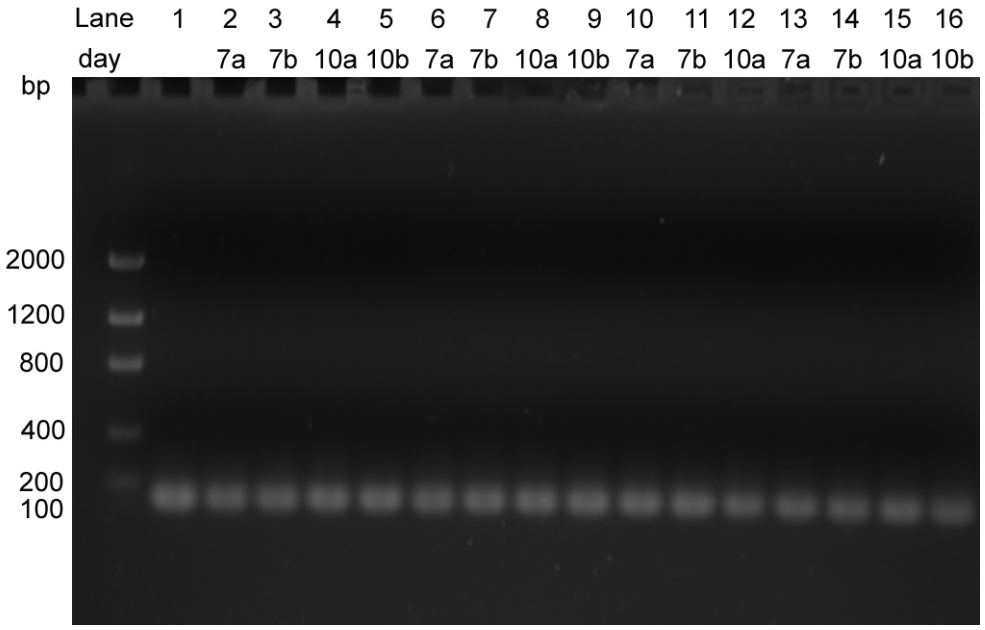

Figure 5.11. DNA gel of the q-PCR products for HNF4-α. Lane 1: Fresh Hepatocytes.; 2-5: collagen; 6-9 RAD16-I; 10-12 RGD; 13-16 YIG.

The effect of peptide hydrogels on hepatocyte-specific functionality was evaluated and compared with the collagen sandwich system by assessing cell-specific albumin and urea secretion over the entire culture period. Figure 5.12. A, shows the amount of albumin secreted normalized by the total cellular protein measured using an ELISA assay specific for rat albumin (see Materials and Methods). It can be observed that in all culture systems, the albumin secretory capacity gradually increased between culture days 3 and 7 and remained stable thereafter (Figure 5.12., A). Figure 5.12., B-C shows a western blot against rat albumin for cellular lysates, in which it can be observed a similar amount of albumin protein expression for all the conditions tested. Membranes were probed against actin to ensure equivalent protein loading per lane.

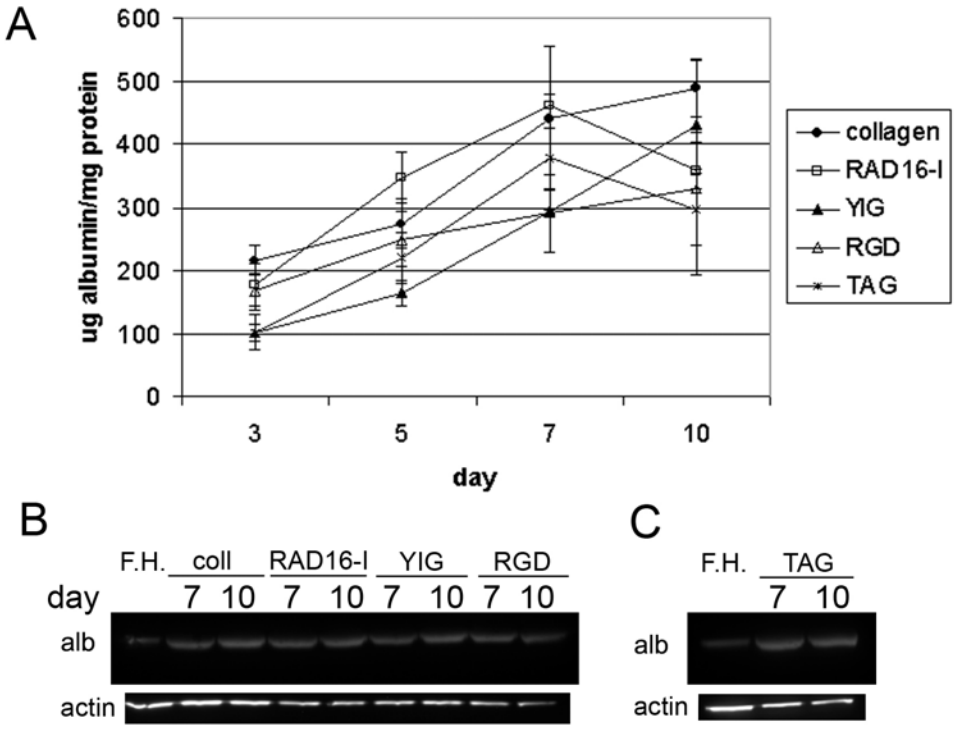

Figure 5.12. A) Secreted albumin present in the media normalized by total protein content in the cellular lysate. B and C) Albumin western blot of the cellular lysate. F.H: Fresh Hepatocytes, coll: collagen.

Furthermore, urea present in the media, (indicative of aminoacid catabolism) was analyzed. Figure 5.13., A shows the urea secretion profile normalized by the total cellular protein. Under all culture conditions, the urea concentration slightly decreased between days 3 and 5 of culture and did not change thereafter. Similarly to albumin, levels of urea production in were comparable in the collagen sandwich and peptide scaffold cultures. Western blot analysis of the transcription factor HNF4-α, demonstrated that it is expressed in all the culture conditions tested (Figure 5.13, B). However, compared to the result obtained for the fresh isolated hepatocytes control, an additional band of higher molecular weight was detected in all the culture conditions, suggesting that the *in vitro* system might be synthesizing another isoform also recognized by the antibody anti HNF4-α used. Additionally, we detected biotin-dependent carboxylases, which are enzymes highly expressed in liver (Jitrapakdee and Wallace, 1999; Baumgartner *et al*., 2001; Jiang *et al*., 2005). In mammals, only four different biotin-dependent carboxylases have been detected so far, acetyl-CoA carboxylase (ACC, MW 270 kDa), pyruvate carboxylase (PC, MW 125 kDa), 3-methyl-crotonyl-CoA carboxylase (MCC, MW 75 kDa) and propionyl-CoA carboxylase (PPC, MW 72 kDa). These enzymes, are involved in the oxidation of odd-chain fatty acids,

catabolism of branched aminoacids such as leucine, lipogenesis and gluconeogenesis (Jitrapakdee and Wallace, 1999; Baumgartner *et al*., 2001; Jiang *et al*., 2005). Using an assay based on the biotin-avidin interaction (see Chapter 7: Materials and Methods), we were able to detect three biotin-dependent carboxylases also present in freshly isolated hepatocytes (Figure 5.13., C). These enzymes were present in all peptide hydrogel cultures, but, interestingly collagen sandwich cultures did not appear to express PPC.

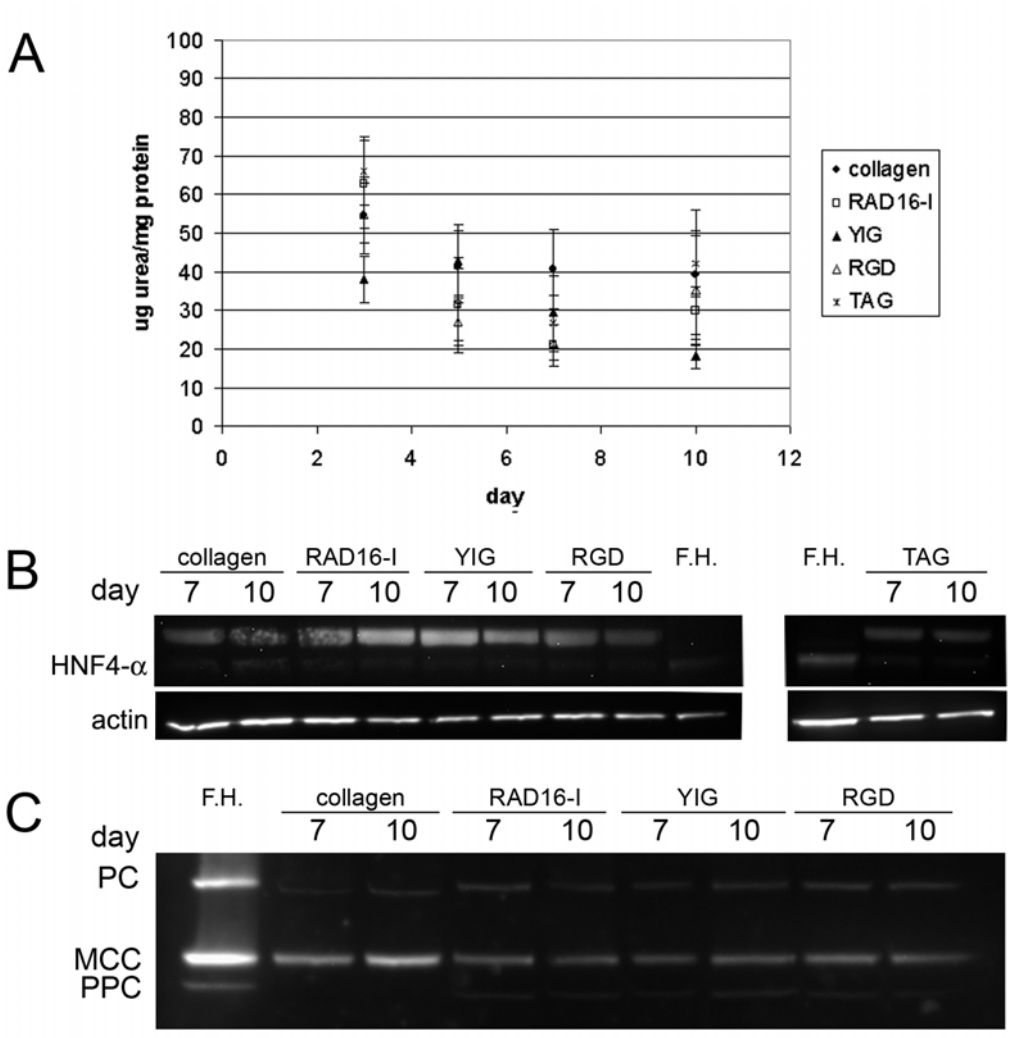

Figure 5.13. A) Urea present in the media at different time points. The results are normalized against total cellular protein content. B) HNF4-α western blots. C) Biotin dependent carboxylases present in the cellular lysate, PC: pyruvate carboxylase, MCC: methylcrotonyl-CoA carboxylase, and PCC: propionyl-CoA carboxylase. F.H.: Fresh hepatocytes.

Moreover, the secreted proteome of hepatocytes was examined and analyzed. This is a very interesting approach, since hepatocytes secrete a large amount of plasma proteins and some of them can be used as markers for diagnosting diseases (Farkas *et al*., 2005). Therefore, protein gels of culture media samples obtained at day 7 and day 10 for collagen and RAD16-I peptide hydrogel were ran and coomassie blue-stained (Figure 5.14.). Control medium (hepatocyte culture medium, HCM) was included in one lane, in order to differentiate medium-conatining proteins from the ones secreted into the medium by the hepatocytes. Four differential bands that were present in the medium form collagen and RAD16-I cultures, but were absent from the control culture medium (HCM) were identified and were excised from the gel for both collagen and RAD16-I peptide cultures. Then, the proteins contained in each band were tryptic digested and the remaining peptides were separated and analyzed as explained in the Materials and Methods section.

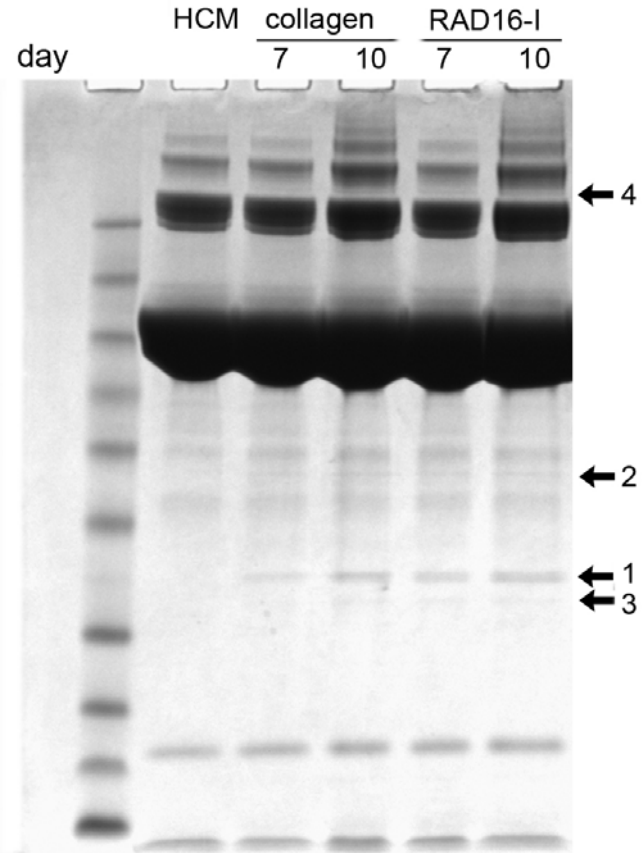

Figure 5.14. SDS protein gel of media obtained at day 7 and day 10 collagen and peptide hydrogel sandwich cultures. HCM represents control medium. Four differential bands were observed and named 1-4.

A brief report of the proteins obtained and their function is showed in Table 5.1. (Ajees *et al*., 2006; Frank and Marcel, 2000; Barter and Rye, 2006; Abraham *et al*., 1990; Alper *et al*., 1965; Braciak *et al*., 1988; Calero *et al*., 1999; Eichner *et al*., 2002; Falkenberg *et al*., 1990; Kapron *et al*., 1997; Logdberg *et al*., 2000; Min *et al*., 1998; Rouet *et al*., 1998; Ship *et al*., 2005; Soprano *et al*., 1986; Tamkun and Hynes, 1983; Tsuji *et al*., 1994). Several proteins were identified in both matrix systems (collagen and RAD16-I), which were mainly plasma proteins or protease inhibitors which were in concordance with proteins observed also in other proteomic studies (Farkas *et al*., 2005). For example, several apolipoproteins were detected (ApoA1, ApoE and ApoJ) (Frank and Marcel, 2000; Ajees *et al*., 2006; Barter and Rye, 2006; Eichner *et al*., 2002; Kapron *et al*., 1997; Min *et al*., 1998; Calero *et al*., 1999); these proteins are of a remarkable importance in reverse cholesterol transport, and its deficiency could lead to atherosclerosis. Haptoglobin, another plasma protein is involved in iron turnover, by binding to free hemoglobin resulting form red cell lysis (Ship *et al*., 2005). Retinol binding protein was also detected in both conditions. This protein, which is specifically synthesized and stored in the liver, is involved in the transport of retinol (vitamin A) by plasma to peripheral target tissues (Soprano *et al*., 1986). Other proteins identified in the culture medium were protease inhibitors such as α-1-microglobulin/bikunin precursor, α-1-macroglobulin, and α-1 inhibitor III. In some other cases, protein function is still unknown such as hypothetical protein Q4FZU2, and some other proteins such as α-1-macroglobulin were found in a zone of lower molecular weight than expected, which could be due to proteolysis during the culture period (Table 5.3.).

Table 5.3. Secreted proteins found in collagen and RAD16-I peptide hydrogel culture medium

Protein	Band	MW	Function	References
Apolipoprotein A1 (ApoA1)	1	30 kDa	Involved in reverse cholesterol transport	(Frank and Marcel, 2000; Ajees *et al*., 2006; Barter and Rye, 2006)
α-1-microglobulin/bikunin precursor (AMBP)	1	39 kDa	α-1-microglobulin has immunoregulatory properties. Binds to IgGA. Bikunin is a serine protease inhibitor	(Falkenberg *et al*., 1990; Rouet *et al*., 1998; Logdberg *et al*., 2000)
Apolipoprotein E (ApoE)	2	36 kDa	Lipid transport. Formation of VLDL and cholymicrons	(Eichner *et al*., 2002)
Haptoglobin	2	38.5 kDa	Free hemoglobin turnover	(Alper *et al*., 1965; Ship *et al*., 2005)
Apolipoprotein J (ApoJ, clusterin)	2	51 kDa	Immune regulation, lipid transport, remodeling, apoptosis	(Kapron *et al*., 1997; Min *et al*., 1998; Calero *et al*., 1999)
Q4FZU2	2	59 kDa	Hypothetical protein. Unknown	
α-1-macroglobulin*	2	167 kDa	Protease inhibitor	(Tsuji *et al*., 1994)
Retinol binding protein (RETBP)	3	23 kDa	Transports retinol from liver	(Soprano *et al*., 1986)
Fibronectin	4	272 kDa	Extracellular matrix and plasma protein	(Tamkun and Hynes, 1983)
α-1 inhibitor III	4	165 kDa	Protease inhibitor	(Abraham *et al*., 1990; Braciak *et al*., 1988)

Finally, an induction experiment using dexamethasone 10 μM was performed, in order to assess cytochrome CYP3A2 inducibility and responsiveness of the culture system as it has been previously described (Silva *et al*., 1998; Turncliff *et al*., 2004; Abu-Absi *et al*., 2005). Figure 5.15 shows the CYP3A2 relative expression to freshly isolated hepatocytes in peptide hydrogel and collagen sandwich configuration at day 7. It can be seen that the cytochrome CYP3A2 is highly downregulated in all conditions

(Figure 5.15., A). However, when cultures were incubated for 24 h with dexamethasone 10 μM (Figure 5.15., panel B), the expression was upregulated in both collagen and peptide sandwiches indicating that hepatocyte in sandwiched cultures have to ability to repond to external inductive stimuli (Figure 5.15., B).

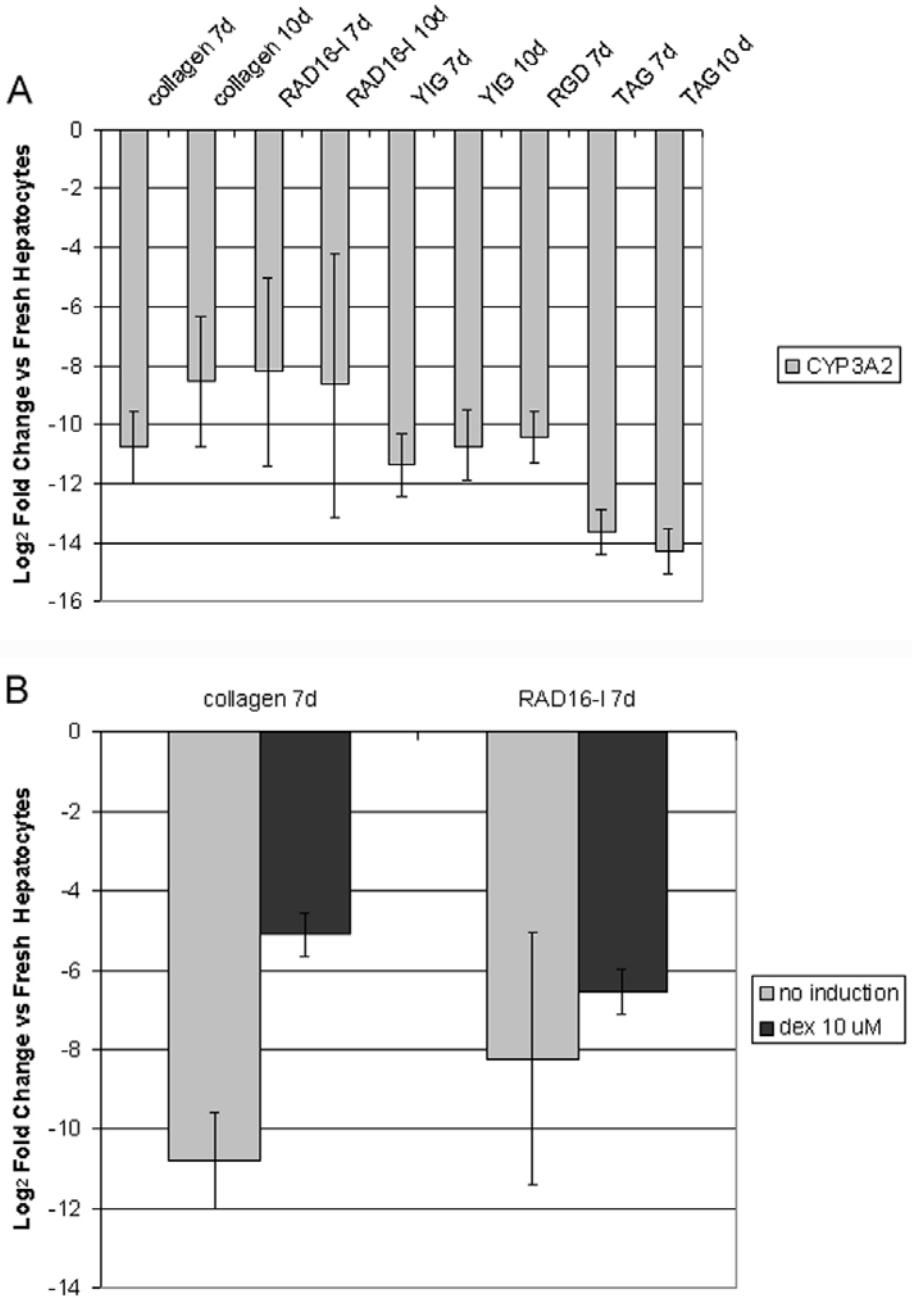

Figure 5.15. A) CYP3A2 expression relative to fresh hepatocytes by Real-time PCR at different time points. B) CYP3A2 expression after a 24 h induction with dexamethasone 10 μm.

5.3. DISCUSSION

Tissue architecture and parenchymal cell morphology reflect the functional differentiation of the liver. Hepatocytes are arranged as monolayer plates *in vivo*, an organization which allows the cells to be highly vascularized. The establishment of a long-term primary hepatocyte *in vitro* culture has been long sought, and many efforts are being made to achive this goal. Sandwiching hepatocytes between two layers of collagen has shown to provide the cells with an *in vivo*-like environment that enables the cells to preserve their specific functionality for several weeks. In this part of the thesis completely synthetic extracellular matrix analogs have been used in order to recreate the most commonly used hepatocyte culture system *in vitro*, the collagen sandwich (Berthiaume *et al*., 1996; Dunn *et al*., 1989; Dunn *et al*., 1991). We suggest that the geometrical factor in combination with the use of an artificial extracellular matrix may give the hepatocytes a unique microenvironment which will allow them to retain important liver-specific functions. In this study, all experiments were performed in parallel to the same sandwich system built of a rat tail collagen gel, which is considered today, as the gold standard for the culture of hepatocytes *in vitro* (Berthiaume *et al*., 1996; Dunn *et al*., 1989; Dunn *et al*., 1991).

It was observed that in peptide cultures, hepatocyte morphology appears to be polygonal and with a vast network of bile canaliculi as it happens in the control collagen cultures (Figure 5.6. and Figure 5.7.). These canaliculi proved to be functional by the fact that they were able to metabolize and transport fluorescein diacetate through them (Figure 5.6., B), as it had been previously shown for collagen sandwich cultures (Barth and Schwarz, 1982; LeCluyse *et al*., 1994). In terms of gene expression, the levels of relative expression of the genes studied was comparable, except for hepatocytes cultured in peptide hydrogel sandwiches containing the peptide YIG, which presented some degree of upregulation specially in MDR2 and TAT. Generally speaking for all the functional experiments tested, hepatocytes in peptide sandwich cultures behaved correspondingly similar to collagen sandwich cultures. The same happened in terms of gene and protein expression, and in relation to the proteomic profile secreted to the culture medium.

However, many efforts have to be performed in order to address the system to fully express liver-specific genes, and to perform liver-specific functions. For example, it would be essential for the implementation of the system in drug screening and drug discovery applications, the expression of cytochromes P450, Phase I and Phase II enzymes in the biotransformation of drugs and other xenobiotics. In particular, rat

CYP3A2 (CYP3A4 in humans), which represents the 30% of the total cytochromes P450, metabolizes the 50% of the marketed drugs. CYP P450, especially CYP3A2, are lost rapidly after hepatocyte isolation and its expression is difficultly recoverd. As it can be seen in Figure 5.15., CYP3A2 appears to be highly downregulated. Even though, CYP3A2 can be induced in this system by using common cytochrome inducers such as dexamethasone (Figure 5.15., B). To overcome this drawback different strategies can be addressed to better recreate the hepatocyte microenvironement, as the use of a hepatocyte-non-parenchymal cell coculture, or the integration of the hydrogel sandwich into a bioreactor that will allow better oxygen and mass transfer as previously described for other systems (De Bartolo *et al*., 2005; De Bartolo *et al*., 2006; Powers *et al*., 2002; Schmitmeier *et al*., 2006; Sudo *et al*., 2005). Nevertheless, this peptide sandwich model represents an enormous advance, meaning that defined and synthetic extracellular matrix analogs are being used, obtaining a truly comparable system to what is considered the gold standard in long term hepatocyte *in vitro* culture. In this work, a really simple long-term *in vitro* hepatocyte culture has been established, which could be easily implemented in more sophisticated *in vitro* systems such as bioreactors. In addition, with the use of rapidly evolving analysis tools and technologies in genomics and proteomics, such as gene and protein arrays, these system could be easily applied in drug screening and toxicity tests, therefore aiding pharmaceutical companies and laboratories in the drug discovery process. We suggest that these promising results are an important beginning for the application of the self-assembling peptide hydrogel in hepatic reconstruction *in vitro* for many biomedical applications.

Chapter 6: *Differentiation of an adult liver putative progenitor cell line, Lig-8, in RAD16-I self-assembling peptide scaffold*

6.1. INTRODUCTION

Liver regeneration occurrs every time there is a major loss of hepatic tissue. The most common model used to study liver regeneration is the partial hepatectomy (PHx) in which by a surgical procedure, up to the 70% of the liver mass is removed. The remaining 30% of the liver grows to restore the 100% of the mass of the original organ. In a normal status, the cells in the liver remain in a quiescent state, meaning that the cells that conform it can re-enter the cell cycle to regenerate the liver in case of partial resection. Figure 6.1. shows the kinetics of DNA synthesis of the cells that conform the liver after a PHx (Michalopoulos and DeFrances, 1997). The four major types of cells experience proliferation at different timings. Hepatocyte proliferation peaks at 24 h after PHx, while the other cells proliferate later, probably due to the synthesis of the necessary growth factors by the hepatocytes. So, liver regeneration occurrs by proliferation of mature cells and without the activation of stem cells. Only when hepatocyte proliferation is impeded or inhibited, such is the case of chronic liver injury or viral infections, then liver stem cells arise and help the process of regeneration.

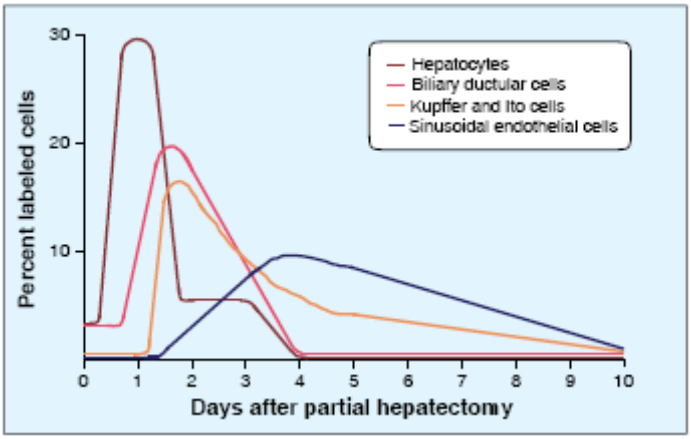

Figure 6.1. Division kinetics of the main liver cells in the process of regeneration after a partial hepatectomy (Michalopoulos and DeFrances, 1997).

Still, there is a great debate of which are the true liver stem cells, and also there is a major challenge in designing isolation, *in vitro* expansion and directed differentiation protocols for liver progenitors. There are several candidates as stem cells to direct differentiation specifically into hepatocytes, including cells from hepatic and extra-hepatic tissue (Figure 6.2.):

- Fetal liver stem cells: During development hepatoblasts give rise to the two different epithelial cell types, hepatocytes and biliary epithelial cells. Therefore, hepatoblasts are considered bipotential progenitor cells (Tosh and Strain, 2005). Furthermore, in a recent study (Malhi *et al*., 2002) human hepatoblasts were isolated, expanded and passaged *in vitro*, and gave rise to mature hepatocytes after transplantation into mice. The expansion *in vitro* of fetal progenitors proposes a very interesting approach due to the limited availability of human fetal livers.

- Oval cells are small and round cells with an oval nuclei. These cells play an important role in regeneration when the liver is severly injured. Oval cells are thought to be also bipotential, differentiating into hepatocytes or biliary epithelial cells. They are obtained by treating the animal with the carcinogen 2-acetylaminofluorene (AAF) before performing a partial hepatectomy. In this way the proliferation of oval cells is induced, and can be isolated in a higher number by liver perfusion (Qin *et al*., 2004).

- Hematopoietic stem cells (HSC) are the progenitor of the cells forming the blood including the lymphoid and myeloid lineage. There has also been investigated the possibility of differentiation of HSC into hepatocytes. The results obtained have been controversial due to the fact that in some studies it was shown to be fusion of cells rather than transdifferentiation (Michalopoulos and DeFrances, 1997; Strain *et al*., 2003). However, recent studies show clearly that HCS can differentiate into hepatocytes without any sign of cell fusion (Forbes *et al*., 2002).

- Embryonic stem cells (ESC) are pluripotent cells derived from the inner cell mass of the blastocyst that can differentiate into a multitude of cell types (Gadue *et al*., 2005; Levenberg *et al*., 2003; Schuldiner *et al*., 2000) when provided with the appropiate signals. A number of groups have been working in the direction of ESC into the hepatic lineage, demonstrated by the expression of several hepatic markers. For example, Yamamoto *et al*. (Yamamoto *et al*., 2005) differentiated mESC into the hepatocyte lineage using a cocktail of growth factors including FGF1, FGF4 and HGF. They performed microarray technology and real-time PCR, and showed that gene

expression pattern of the ES cell-derived hepatocytes was similar to that in adult mouse liver.

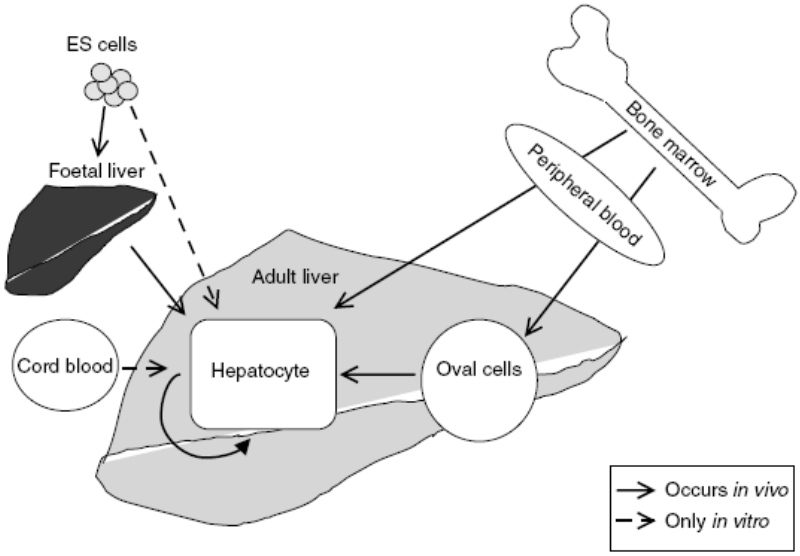

Figure 6.2. Sources of hepatocytes *in vivo* and *in vitro* (Laurson *et al*., 2005)

Recently, a putative rat liver progenitor cell line (Lig-8) was isolated and cloned by applying Suppression of Assymetric Cell Kinetics (SACK) (Lee *et al*., 2003). It is widely known that adult stem cells, while residing in their niche, present assymetric cell kinetics, where the mother cell divides to self-renew and give rise to a daughter transit progenitor cell (Figure 1.8. and Figure 6.3.). These transit cells either differentiate immediately or divide symmetrically to produce differentiating cells. The last maturation step of these progenitor or transit cells produces completely differentiated and arrested cells. Therefore, adult stem cell division kinetics limits their application and clonogenic potential, as they give rise to *in vitro* cultures with contaminating progeny, in which self-renewing adult stem cells become diluted (Figure 6.3.).

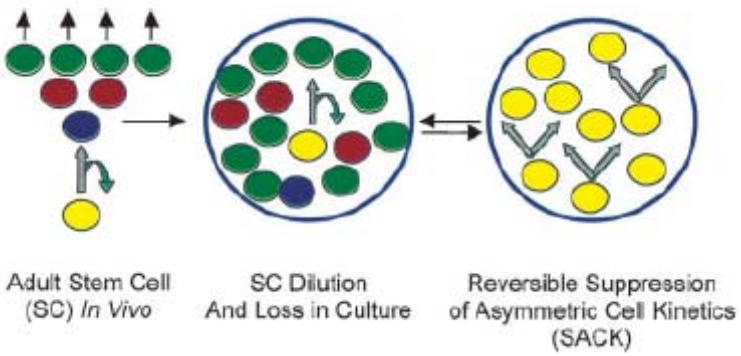

Figure 6.3. SACK strategy to obtain a clonal expansion of adult stem cells (Lee *et al*., 2003). Adult stem cells *in vivo* divide with an asymmetric cell kinetics, a mother cell divides to self-renew and give a cell with a commited fate, a progenitor cell. In culture, adult stem cells become diluted due to this asymmetric cell kinetics. The asymmetric cell kinetics can be reverted to symmetric by applying a process called Supression of Asymmetric Cell Kinetics (Lee *et al*., 2003).

Sherley and co-workers developed a strategy to revesibly convert assymetric cell kinetics to symmetric cell kinetics without the need of mutating the cells, and called it SACK (Figure 6.3). This approach is based in studies on an immortal epithelial cell line that presented symmetric cell kinetics, which reverted to asymmetric when p53 tumor supressor protein was induced (Sherley, 2002; Lee *et al*., 2003). In these studies it was demonstrated that the shift to asymmetric cell kinetics required a p53-dependent reduction of guanine nucleotide biosynthesis (Lee *et al*., 2003; Rambhatla *et al*., 2001; Sherley, 2002). The reduction in guanine nucleotide biosynthesis ocurred due to the p53-induced repression of the enzyme inosine 5'-monophosphate dehydrogenase IMPD (EC 1.1.1.205), the rate-limiting enzyme of guanine nucleotide biosynthesis. Compounds like the purine nucleoside xanthosine (Xs) was able to override the IMPD downregulation inducing the guanine nucleotide biosynthesis through other salvage pathways, causing a reversible change from asymmetric cell kinetics to symmetric cell kinetics. Therefore, p53-expressing cells which divided asymmetrically could be converted into symmetrically dividing cells in the presence of Xs (Figure 6.4.).

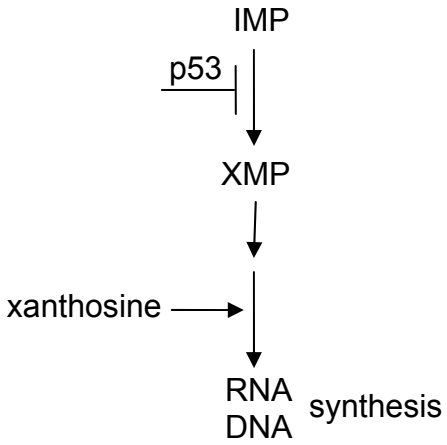

Figure 6.4. Scheme depicting that adult stem cells present an asymmetric cell kinetics due to the presence of p53 protein, which downregulates IMPD, the rate-limiting enzyme in guanine nucleotide biosynthesis. This asymmetric cell kinetics can be reverted to symmetric by the addition of the purine nucleoside xanthosine, which induces the guanine biosynthesis via salvage pathways. This change in cell kinetics can be reverted again to asymmetric cell kinetics by removing the Xs from the media.

Thus, Sherley *et al*. formulated the hypothesis that compounds like Xs might be useful in the expansion of adult stem cells, by inducing a transition from asymmetric to symmetric cell kinetics, and called it SACK (Supression of Asymmetric cell Kinetics) (Lee *et al*., 2003). Indeed, they isolated a putative rat liver derived progenitor cell line Lig-8 from the non-parenchymal fraction of a liver perfusion, and they showed that in the presence of Xs they presented exponential growth. When Xs was removed from the media, the asymmetric cell kinetics was restored, and the cells increased the expression of hepatocyte-lineage markers such as albumin and alanine aminotransferase (AAT), indicating a differentiation process (Lee *et al*., 2003).

In vivo, adult stem cells are believed to reside in a niche, in which their surrounding microenvironment (cells, soluble signals and ECM, Figure 1.8.) dictates their fate. Even though there is extensive research in understanding the differentiation processes, pathways and factors necessary for the induction of progenitor cells into an specific lineage, there is a need to obtain artificial stem cell niches which would help in the study of stem cell self-renewal, function and differentiation. The building of defined, synthetic biomaterials that provide the cells with a controlled microenvironment is clearly in that path.

In that sense, Semino *et al.* (Semino *et al*., 2003), used the self-assembling peptide scaffold RAD16-I to encapsulate Lig-8 cell line. They observed that when cells were entrapped in the peptide scaffold, they formed spheroid-like structures and reduced their division kinetics compared to 2D cultures in regular plastic dishes. Figure 6.5. **A**, C and D show Lig-8 spheroids formed in the peptide hydrogel. To easily analyze the colonies generated in the hydrogel cultures, they developed a method in which the colonies were extracted from the gel by disrupting it by pipetting it up and down several times. The result of the disruption was then plated in a tissue culture dish. In this way and after an overnight incubation, the extracted 3D-derived spheroid colonies attached to the bottom of the well, and immunofluorescence analysis could be easily performed (Figure 6.5. **A**, G and H). Using this technique, they analyzed the presence of cycling cells in both 2D cultures and in 3D-derived spheroid colonies using BrdU staining (Figure 6.5. **A**, E-H). BrdU is a thymidine analog that is incorporated to DNA when the cells are cycling (see Chapter 5). Figure 6.5. **A**, E, F shows the staining of a colony grown on 2D regular tissue culture dishes under regular culture conditions. As it can be observed, all the nuclei are positive, meaning that all the cells are cycling. However, spheroid colonies derived from 3D cultures (Figure 6.5. **A** G-H) demonstrate that just several cells are dividing, meaning that in some cells the cycle has become arrested, probably due to a differentiation process, confirming the change in cell kinetics observed by the reduction of cell doubling times in cells encapsulated in the peptide hydrogel versus cells cultured in regular tissue culture plates (Semino *et al*., 2003).

A

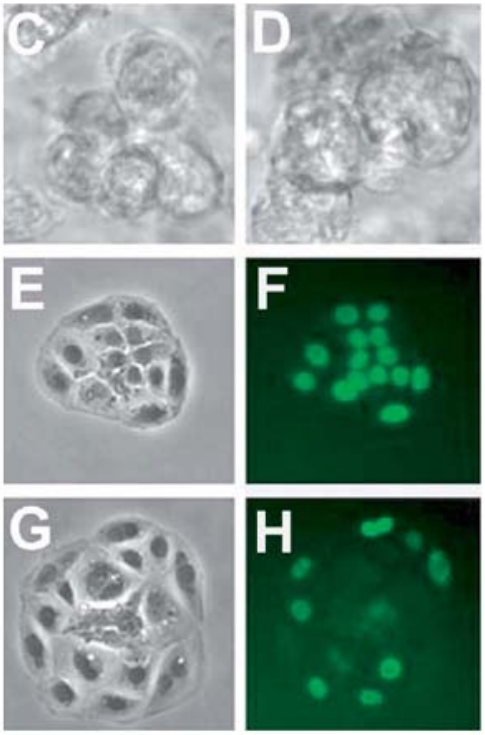

B

Table 2 Induction of hepatocyte phenotypes in RAD16-I peptide scaffolds

Marker[¥]	Standard Culture Dish	Peptide Scaffold Spheroids[§]
Hepatocyte progenitor		
α-Fetoprotein	+	+
CK8 (also mature hepatocytes)	+	+
Definitive endoderm		
HNF3β*	+	NA
Non-hepatocyte liver cell population		
ED1 (Kupffer cells)*	−	NA
GFAP (stellate cells)*	−	NA
Endodermal (liver) development		
C/EBPα	−	+++
Mature hepatocyte		
Albumin	−/+	+++
CYP1A1/CYP1A2	−/+	++
CYP2E1	−	++
Binucleated cells	−	++
Functional hepatocyte		
3-MC inducible CYP1A1	−	+
3-MC inducible CYP1A2	−	++
Caffeine metabolism (CYP1A2/2E1)	−	++

[¥] Quantification terms for marker expression: (−), not detected; (−/+), very low; (+), low; (++), medium; (+++), high expression.
[§] Cells were either grown in standard adherent culture or grown in peptide scaffold and then transferred to adherent culture for analysis as described in Methods.
* Lee et al., submitted
NA, not analyzed.

Figure 6.5. Lig-8 differentiation within RAD16-I peptide hydrogel A) C-D) Lig-8 cells forming spheroid structures when encapsulated in RAD16-I peptide hydrogel after 48 and 96 h respectively. E) Lig-8 colony cultured in regular tissue culture plates. F) BrdU staining indicating cycling nuclei of colony in E. G) Lig-8 spheroid colony derived from hydrogel cultures. H) BrdU staining of colony in H. B) Table indicating several markers absent or present in Lig-8 cells cultured in standard dishes or after being encapsulated in RAD16-I peptide hydrogel (Semino *et al*., 2003).

In the same work the authors studied several hepatocyte and non-hepatocyte markers and compared their expression both in 2D and 3D cultures (Figure 6.5. **B**, Figure 6.6.). They included the expression of C/EBPα, albumin, CYP1A1/1A2 and CYP2E1 the presence of binucleated cells as differentiation markers; as well as the inducibility of the previous cytochromes by classical inducers such as 3-methylcholantrene, or caffeine. They showed by immunofluorescence analysis significant differences in the staining of the nuclear factor C/EBPα which was higly expressed in the nuclei of 3D derived spheroid colonies and presented no staining in 2D culture colonies. Similar results were obtained in cytoplasmic staining of albumin and the cytochrome CYP1A1/1A2. In both cases, 3D derived spheroid colonies presented an upregulation of the protein expression compared to 2D cultures. They also detected the appearance of binucleated cells, a feature of mature hepatocytes, when cells were cultured in 3D hydrogels (Figure 6.5., **A** G, Figure 6.6. C and K).

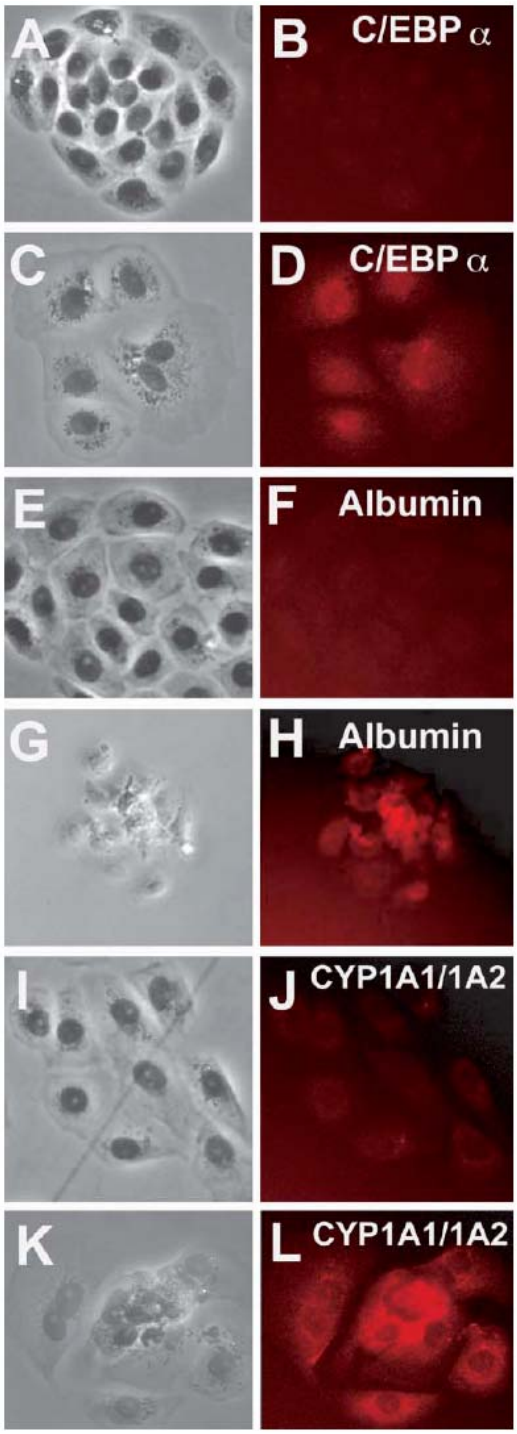

Figure 6.6. Promotion of Lig-8 differentiation into hepatocyte-like cells in RAD16-I. A, E, I) Lig-8 cells cultured in regular tissue culture plates. B, F, H) Fluorescent immunostaining of colonies in A, E, I showing expression of C/EBPα, albumin and CYP1A1/1A2 respectively. C, G, K) Lig-8 spheroid colonies derived from RAD16-I encapsulations. D, H, L) Fluorescent immunostaining of colonies in C, G, K showing expression of C/EBPα, albumin and CYP1A1/1A2 respectively.

In this part of the Thesis, we wanted to further characterize this 3D culture system and to complete this previous work by studying the effect of different media formulations in the differentiation of 3D Lig-8 cultures. Based on previous bibliography regarding to liver embryonic develpoment as well as differentiation of embryonic stem cells into an hepatic lineage, several differentiation factors were chosen for a new medium formulation. The effects they produced in the differentiation of Lig-8 cells were tested in cells cultured in regular plates (2D) as well as cells encapsulated in RAD16-I peptide hydrogel (3D). In one of the reports, Yamamoto *et al*. (Yamamoto *et al*., 2005) described a hepatocyte induction factor cocktail (HIFC) to differentiate mouse ESC into the hepatocyte lineage. This cocktail was based in the *in vivo* induction system and included FGF1 (100 ng/ml), FGF4 (20 ng/ml), HGF (50 ng/ml) and oncostatin M (10 ng/ml). Other studies suggest the use of HGF, DMSO and several FGFs to induce differentiation of hematopoietic stem cells (Strain *et al*., 2003). Therefore, HGF and FGF4 were chosen, and their effect (each growth factor alone or both combined) was tested in the differentiation of Lig-8 cell line encapsulated in the peptide hydrogel RAD16-I.

6.2. RESULTS

Lig-8 cells coming from 2D cultures in the presence of Xs were encapsulated within the peptide hydrogel RAD16-I in 96-well plates as explained in the Materials and Methods chapter. Two growth factors (HGF, FGF4) were added to the culture medium, and their effect on Lig-8 differentiation into hepatocyte-like cells was tested. Encapsulated cells, migrated, aggregated and divided along the days in culture forming spheroid-like structures. Figure 6.7. shows the spheroids that were formed after 15 days of culture. It can be observed that spheroids grown in the presence of HGF (Figure 6.7. b and d) were bigger than spheroids grown without it, as the images were all taken with the same magnification (200x). This may be due to the potent mitogen effect of HGF. Figure 6.8. shows an electron microscopy (EM) picture of a cross section of a spheroid, where the internal part of the spheroid (In) and the external portion (Ex) can be see clearly, including the remaining hydrogel nano-fibers at the exterior. The cellular section is highly polarized, showing microvilliae (Mv) in the interior of the spheroid and the presence of endoplasmic reticulum (ER) vesicles piled up in the

cytoplasm on the same side of the secreting Mv. The cell also shows many mitochondria (M) as well as polyribosomes (PR). In parallel, Lig-8 cells were also encapsulated in collagen and agarose gels as a control. In the first case (rat tail collagen-I), the cells migrated out of the gel (not shown), whereas in 0.5% agarose gels, most of the cells remained as single cells without forming spheroid structures, probably due to the higher stiffness of the material in which cells could not be able to migrate and aggregate in spheroids (Figure 6.9.). Therefore, those materials were discarded and used only the peptide hydrogel RAD16-I for the rest of the study.

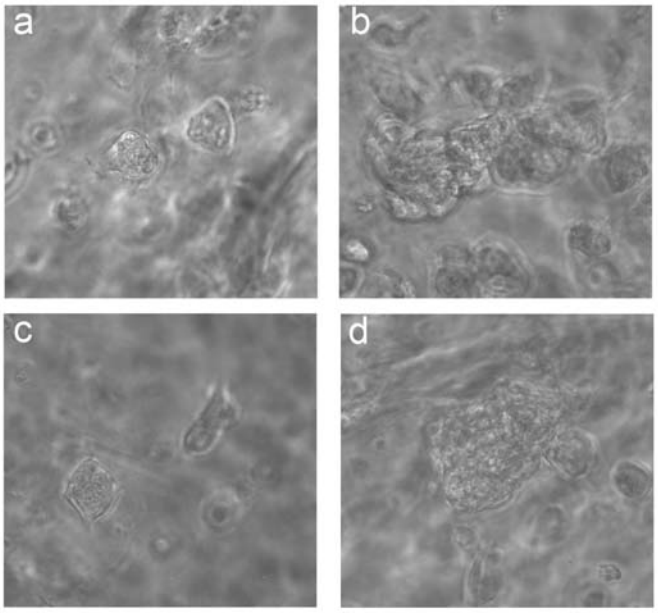

Figure 6.7. Lig-8 spheroid structures encapsulated in RAD16-I peptide hydrogel, a) in control medium without growth factors, b) with HGF, c) FGF4, d) HGF and FGF4.

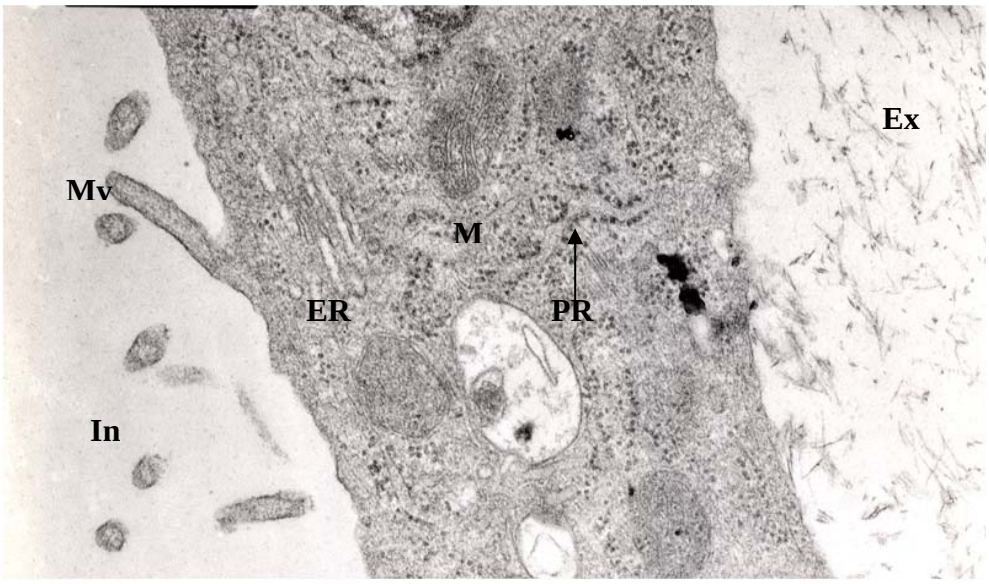

Figure 6.8. EM picture showing the ultrastructure of a cell in a spheroid. **Mv**: microvillliae, **M**: mitochondria, **PR** (arrowhead): polyribosomes, **ER**: endoplasmic reticulum.

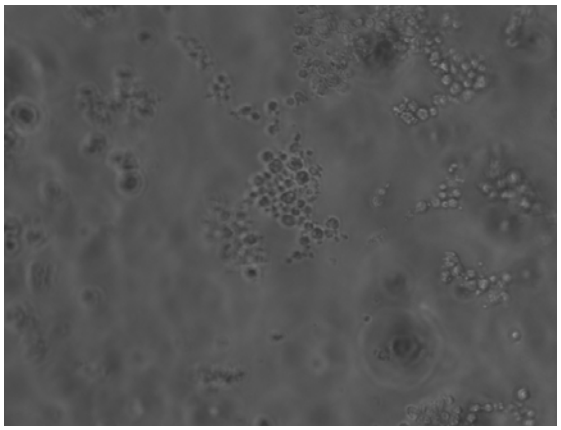

Figure 6.9. Lig-8 cells encapsulated in agarose 0.5% after 15 days in culture.

In addition, the effect of these growth factors in the expression of several cytochromes P450 was studied. As it was previously explained in Chapter 5, these enzymes, play a critical and specific role in the metabolization and clearance of endogenous chemicals (steroids, fatty acids, among others), and in the processing of exogenous chemicals such as drugs and other xenobiotics (pollutants, carcinogens, etc…, Chapter 5, Table 5.1.) (Guengerich, 1991; Guengerich, 2002). Therefore and because of their significance, there is an enormous interest in a multidisciplinary approach in the study of these enzymes. For example, and in particular for developing

drug screening *in vitro* tests it would be really important the expression of these cytochromes, specially CYP3A2, which in the rat (CYP3A4 for humans) is the responsible for the metabolization of 50% of the marketed drugs (Guengerich, 1991; Guengerich, 2002). Another important enzyme, CYP2E1, is the responsible for the metabolization of low molecular weight compounds, including solvents, and it is highly induced by ethanol. The expression of these enzymes was studied both in Lig-8 cells cultures in regular tissue culture plates (2D) as well as in the spheroids derived from a 15-day differentiation process in the self-assembling peptide hydrogel RAD16-I (3D), in the absence or presence of the differentiation factors. As it is shown in the fluorescence microscopy images, cells cultured in 2D (tissue culture plates), lacked to express CYP3A2 (Figure 6.10., **A**), meanwhile, 3D-derived spheroid colonies expressed the cytochrome in the cellular cytoplasm (Figure 6.10., **B**). In addition, in some cells it can be observed the expression of CYP3A2 in the form of granules or vesicles which may indicate the location of the enzyme in microsomes (Figure 6.10., **B** f and g). Moreover, a negative control was performed using 3D-derived spheroid colonies, in order to ensure that the fluorescent detection of the primary antibody was specific. The incubation of the cells with the primary antibody anti CYP3A2 was ommited, and the incubation with the rhodamine-conjugated secondary antibody was performed directly. After observing the colonies under the fluorescent microscope, we could not detect any fluorescence (Figure 6.11.), meaning that the CYP3A2 staining previously observed was due to the presence of CYP3A2 (Figure 6.10.). We also immunostained 2D and 3D-derived spheroid colonies to detect the presence of the cytochrome CYP2E1 (Figure 6.12.). Similarly to what it was observed for CYP3A2, CYP2E1 was not detected in 2D cultures in any condition, whereas in 3D-derived spheroid colonies a strong fluorescence was observed in all conditions indicating a differentiation process into the acquirance of liver-like functionality.

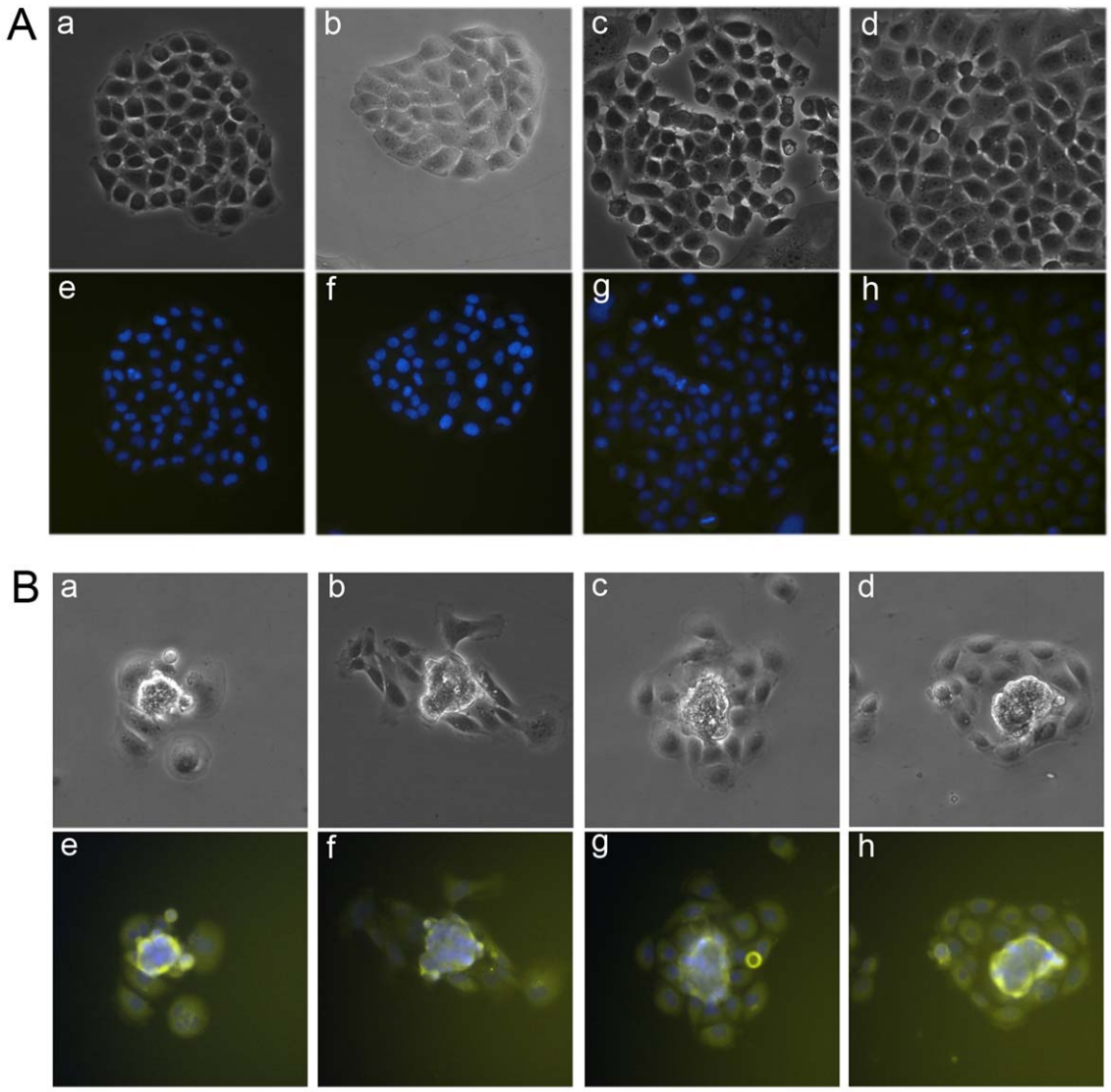

Figure 6.10. CYP3A2 immunostaining in A) Lig-8 cells cultured in 2D (regular tissue culture plates) a,e) cells cultured in control medium (without growth factors) phase and fluorescence images respectively; b, f) in the presence of HGF; c,g) in the presence of FGF4; d,h) in the presence of HGF and FGF4. B) Lig-8 cells derived from RAD16-I encapsulations after 15 days, a,e) in the absence of growth factors, b,f) with HGF; c,g) with FGF4 and d,h) with both HGF and FGF4. Nuclei were stained with DAPI.

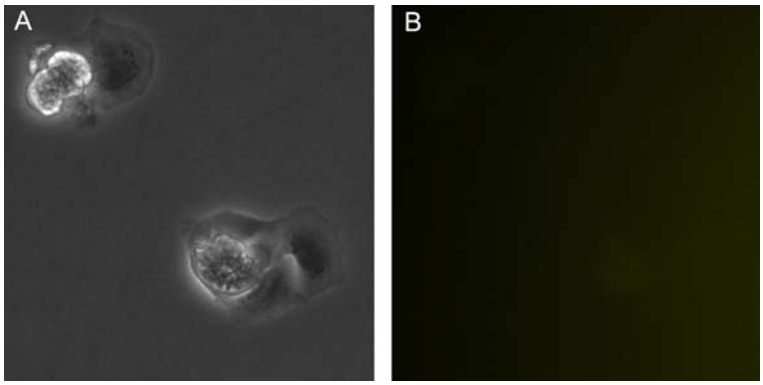

Figure 6.11. Negative control staining of CYP3A2. A) Phase image of 3D-derived spheroid colonies. B) Fluorescence image in which it is not observed fluorescence. The experiment was performed ommiting the incubation with the primary antibody anti CYP3A2.

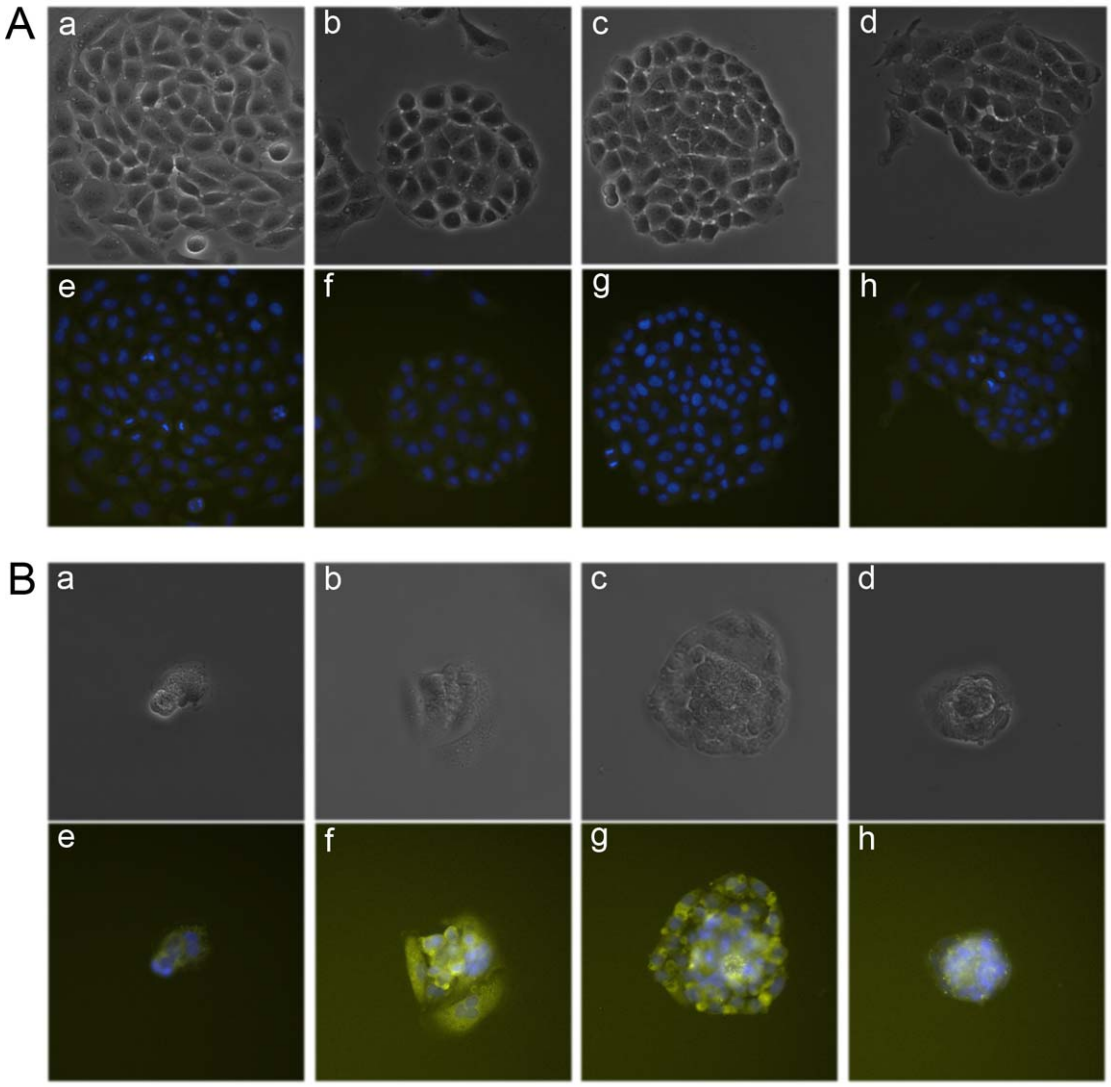

Figure 6.12. CYP2E1 immunostaining in A) Lig-8 cells cultured in 2D (regular tissue culture plates) a,e) cells cultured in control medium (without growth factors) phase and fluorescence images respectively; b, f) in the presence of HGF; c,g) in the presence of FGF4; d,h) in the presence of HGF and FGF4. B) Lig-8 cells derived from RAD16-I encapsulations after 15 days, a,e) in the absence of growth factors, b,f) with HGF; c,g) with FGF4 and d,h) with both HGF and FGF4. Nuclei were stained with DAPI.

Then, the expression of albumin on the 3D systems as well as in the 2D was tested. Cells coming from 3D cultures encapsulated within the self-assembling peptide hydrogel as well as 2D cultures were lysed to obtain protein samples. Western blots were performed probing the membrane with an anti-albumin antibody, including a sample of protein coming from a hepatocyte lysate as a positive control. As it is shown in Figure 6.13., 3D cultures presented a strong band for albumin while in 2D cultures a very weak band could be suspected (Figure 6.13.). This result suggests that Lig-8 cells encapsulated in RAD16-I peptide hydrogel undergo a process of differentiation into cells with hepatocyte-like properties such as the production of albumin, as it had been previously described (Semino *et al*., 2003).

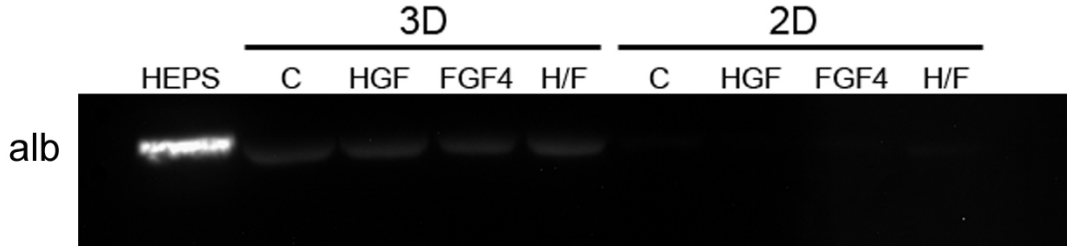

Figure 6.13. Western blot of 3D (hydrogel-encapsulated) and 2D cellular lysates against albumin. Samples cultured in the absence (C, control) or the presence of growth factors (HGF, FGF4 or both H/F) was tested. A positive control of a hepatocyte protein sample was included (HEPS). Each lane contained 5.5 μg of total protein.

Moreover, real time PCR was used to characterize the gene expression profile of the different culture conditions. Relative analysis was performed using undifferentiated cells cultured in the expansion phase (Lig-8 cells cultured in 2D in the presence of Xs) as the reference control (see Materials and Methods). The expression of three genes, albumin, CYP3A2 and CYP2E1, was analyzed and it was observed that

for the three genes tested, samples cultured in 2D were remarkably downregulated with respect to the samples cultured in 3D (Figure 6.14.). Cultures in 2D showed a slight upregulation in albumin and CYP2E1 relative to reference sample (Lig-8 +Xs), and CYP3A2 appeared downregulated when cells were cultured in the presence of growth factors (Figure 6.14.). However, in cells encapsulated within the peptide hydrogel (3D conditions), albumin appeared to be highly upregulated with respect to the reference, and the presence of HGF in the culture medium seemed to be the condition that upregulated most the expression of the gene (Figure 6.14.). CYP3A2 was at the same levels of expression or slightly upregulated than the reference, although the presence of both HGF and FGF4 seemed to downregulate the gene. Finally, CYP2E1 was also highly upregulated in all the conditions tested with respect to the reference sample. Samples cultured in the presence of HGF seemed to present a slight upregulation with respect to the other conditions tested (Figure 6.14.). These results, show that there is a gene expression change acquired in the cells when they are cultured and encapsulated in 3D. These changes are directed in the expression of liver-specific or liver-enriched genes, meaning that the encapsulation and culture of Lig-8 cells in the self-assembling peptide hydrogel induces the differentiation into cells with hepatocyte-like properties.

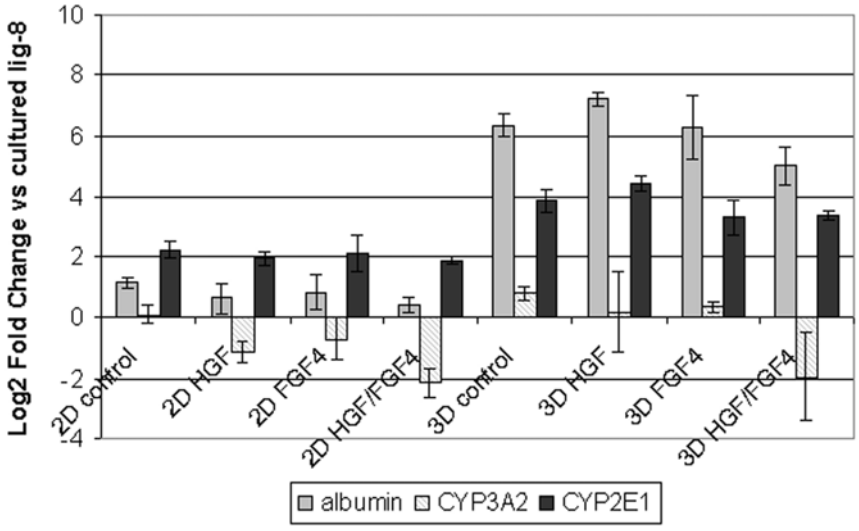

Figure 6.14. Gene expression profile of Lig-8 cells cultured in regular tissue culture plates (2D) or encapsulated within the peptide hydrogel RAD16-I, in the absence (control) or presence of different growth factors (HGF, FGF4 or both). The reference sample chosen was Lig-8 cells in the expansive phase (Lig-8 cells cultured in 2D in the presence of Xs).

The next figure (Figure 6.15., A) shows an example of the amplification plot obtained for the real time-PCR of the experiment explained above. In addition Figure 6.15. panel B, shows a melting curve which in which just one peak is observed, meaning that for each sample only one PCR product is formed. A positive control sample of freshly isolated hepatocytes was included in order to ensure the purity of the products formed.

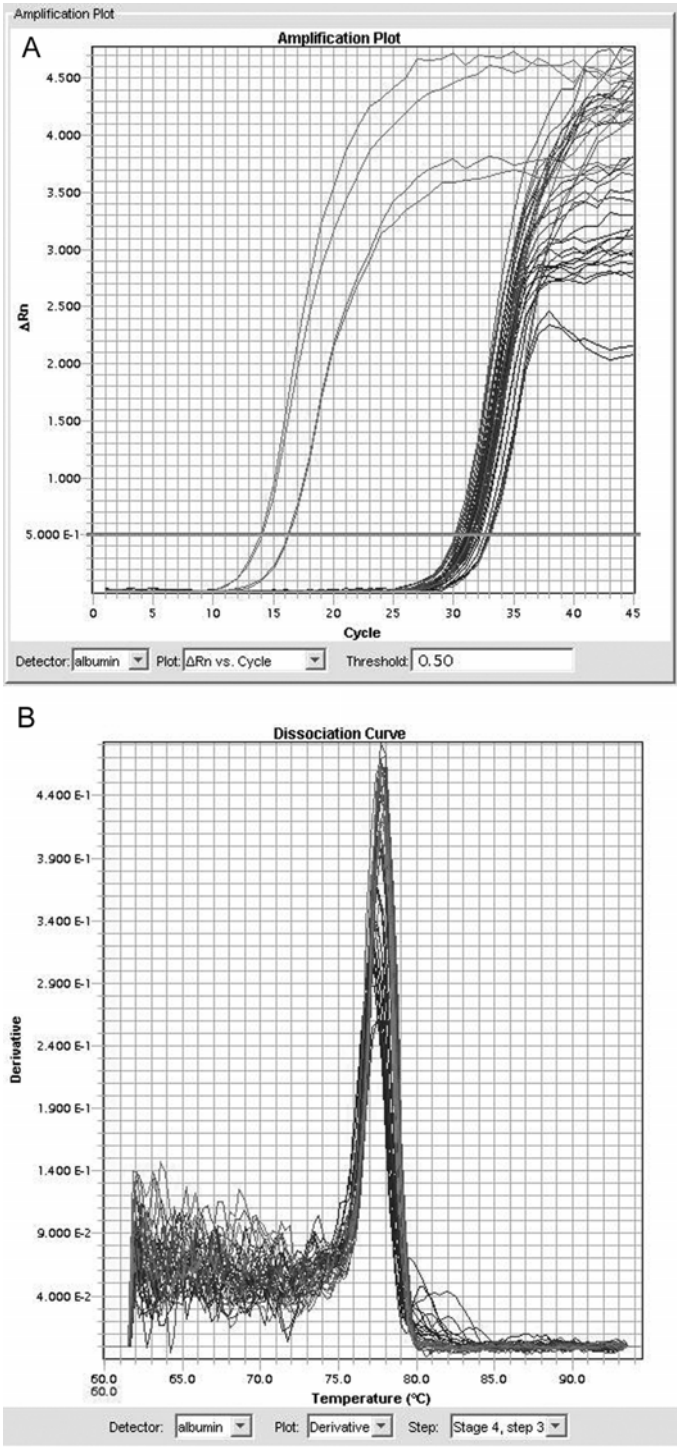

Figure 6.15. A) Real time PCR amplification plot obtained for albumin. B) Melting curve of the PCR products obtained after the real time PCR run.

However, when real time PCR data was performed relative to the gene expression of freshly isolated hepatocytes, all values appeared to be highly downregulated (Figure 6.16.). This experiment shows that even though there is some degree of differentiation, as observed with the gene expression profile when compared

with Lig-8 cells cultured in tissue culture plates (Figure 6.14.), there is a long way to go to obtain hepatocytes with complete functional liver-specific functions.

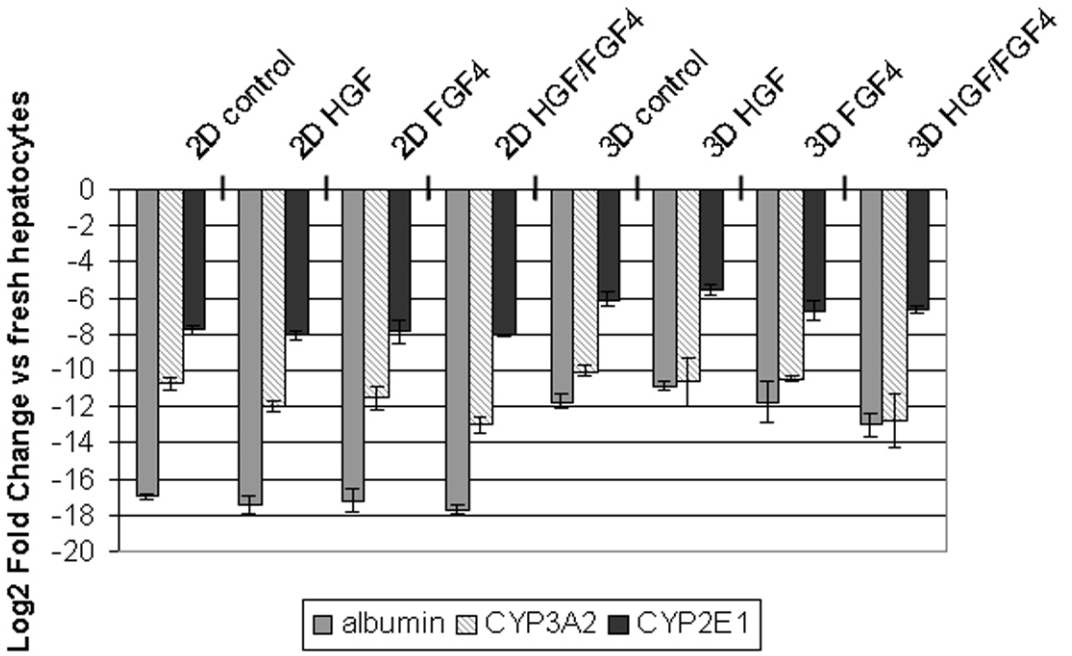

Figure 6.16. Gene expression profile of Lig-8 cells cultured in regular tissue culture plates (2D) or encapsulated within the peptide hydrogel RAD16-I, in the absence (control) or presence of different growth factors (HGF, FGF4 or both). The reference sample chosen was freshly isolated hepatocytes.

Moreover, and similarly as performed in Chapter 4, the inducibility of CYP3A2 in the presence of the dexamethasone 10 μm (which is known to be a common inducer of this enzyme) was assessed. Cells form 14-day 3D cultures were incubated for 24 hous with dexamethasone-containing medium, then, the RNA was extracted and real time PCR was performed. We observed, that in the presence of dexamethasone, CYP3A2 was upregulated relative to the reference sample (cultured Lig-8 cells), as well as relative to the same 3D conditions without the inducer (Figure 6.17.). This induction was similar in all the conditions tested.

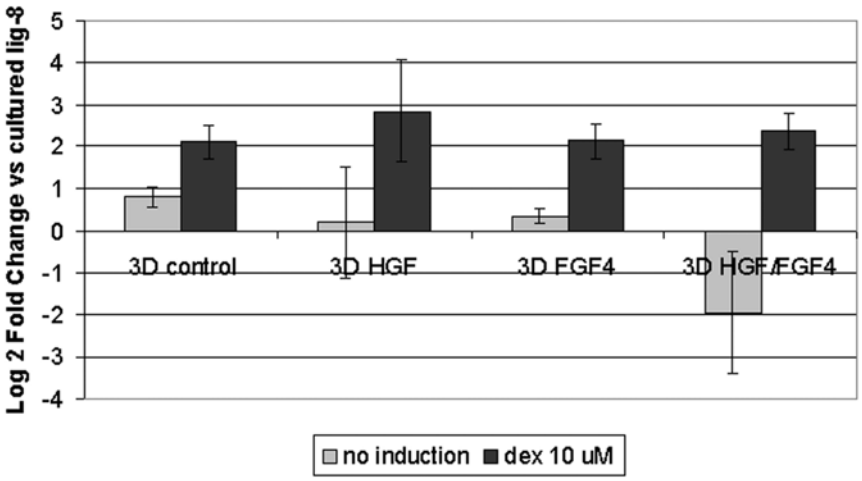

Figure 6.17. Real time-PCR relative gene expression analysis of CYP3A2 in Lig-8 3D cultures in the absence or presence of a CYP3A2 inducer (dexamethasone 10 μM).

Moreover, we performed a functional test in order to visualize differentiated cells presenting CYP1A1/1A2 activity (Semino *et al*., 2003). It had been previously shown that Lig-8 cells cultured in RAD16-I peptide scaffold were able to metabolize 7-ethoxyresorufin to the fluorescent molecule resorufin, reaction mediated by CYP1A1/1A2 (CYP1A1/1A2 dependent *O*-dealkylation of 7-ethoxyresorufin) (Semino *et al*., 2003). We incubated the cultures for 15 min with medium containing 7-ethoxyresorufin 3 μM, and observed the cells under a fluorescence microscope. Most of the cells forming the spheroids showed a strong fluorescene, but interestingly in the spheroids there were always cells that did not metabolize, 7-ethoxyresorufin (and consequently did not present fluorescence), which may be due to the undifferentiated state of those cells (Figure 6.18.).

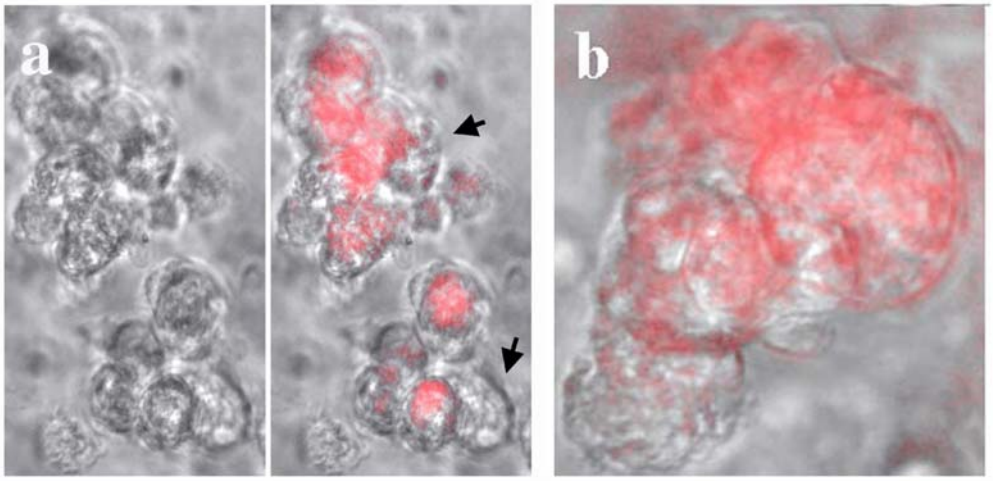

Figure 6.18. CYP1A1/1A2 dependent 7-ethoxyresoruin metabolism. a) Phase contrast and combined phase contrast-fluorescence image, showing cells that did not metabolize the substrate (arrowheads). b) Lig-8 spheroid image that combines phase contrast and resorufin fluorescence.

To further investigate the presence of proliferative undifferentiated cells in the 3D cultures, BrdU staining was used to detect cells that had gone through the cell cycle. BrdU (5-bromo-1'-deoxyuridine) is a thymidine analog which is incorporated into the DNA of cycling cells. It can be easily detected using an antibody specific against BrdU, conjugated with a fluorescent molecule. Cells (14-day cultures) were incubated overnight with medium containing BrdU 10 μM (Sigma-Aldrich, MO, 858811). After that time, the cells were fixed, and then we proceeded to immunostain the cells with an anti-BrdU FITC conjugated antibody (BD Pharmigen, 51-33284X, dilution 1:100). It was observed that in the clusters or spheroids there was always a remaining proportion BrdU-positive cells, which might suggest that these cells with proliferative capacity are somehow progenitor cells that give rise to both self-renewing and differentiated progeny (Figure 6.19.).

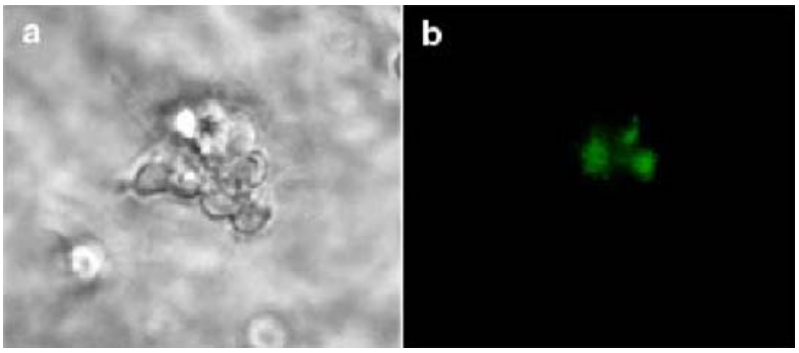

Figure 6.19. BrdU staining of Lig-8 spheroids in 3D peptide hydrogel cultures. Phase (a) and fluorescent microscopy (b) image of a Lig-8 cluster in the peptide hydrogel RAD16-I. b) shows some BrdU positive cells present in the cluster.

To further and better examine the remaining of dividing cells, we double-immunostained 3D-derived spheroid colonies which had been previously incubated overnight with a 10 μM BrdU media solution, with an antibody against CYP3A2 or CYP2E1 and an anti-BrdU antibody. The presence of CYP3A2 and CYP2E1 (Figure 6.20.) was detected, as well as some BrdU-positive cells which indicated that still some cells with proliferative capacity remained in the culture (Figure 6.20.).

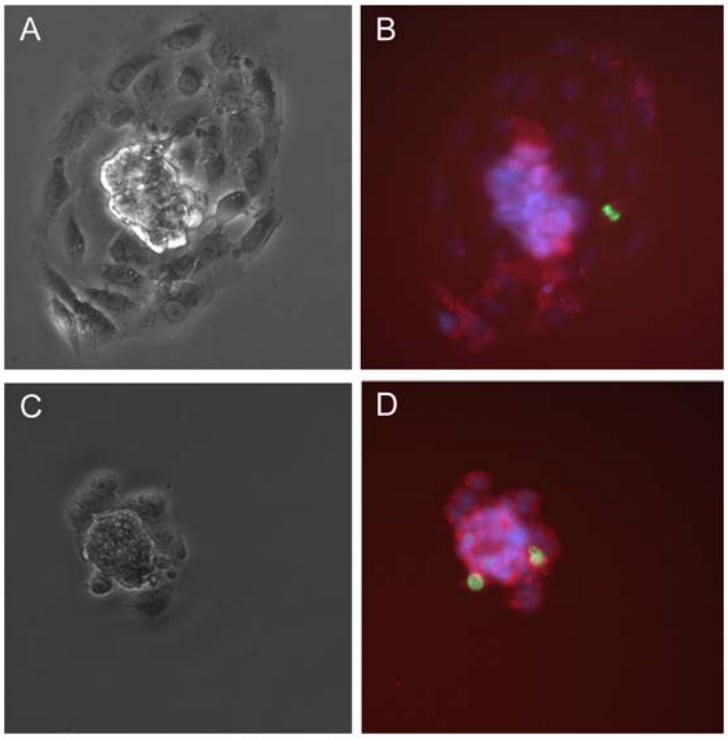

Figure 6.20. Double immunostaining of 15-day 3D-derived spheroid colonies. A) Phase and B) CYP3A2 (red) and BrdU (green) immunostaining; C) Phase, and D) CYP2E1 (red) and BrdU (green) immunostaining.

Finally, a last test was performed in order to assess the presence of remaining dividing cells in the cultures. The spheroid-like structures were trypsinized and recultured in tissue culture plates. Cells in culture were monitored for 3 days and the presence of some growing colonies with a phenotype that corresponded to Lig-8 in the expansive phase (in the presence of Xs) was observed. Besides, many cells that did not proliferate were observed as well (Figure 6.21. A and B). These results furtherly confirm that despite the 14-day differentiation process there are always remaining cells with proliferative capacity and posible progenitor phenotype. This could suggest the establishment of a regenerative stem cell compartment in the 3D-cultures, where stem cells divide assymetricaly to produce progenitor/transient cells that differentiate into hepatic-like phenotype.

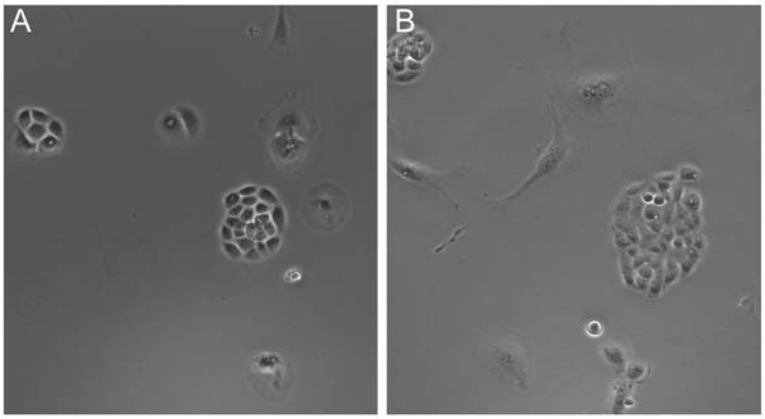

Figure 6.21. Cells derived from trypsinization of the 3D spheroids obtained after 15 days encapsulated in RAD16-I peptide hydrogel.

6.3. DISCUSSION

In this part of the work, we cultured the putative rat liver derived progenitor cell line Lig-8 within RAD16-I self-assembling peptide scaffold in the presence of several growth factors to promote differentiation into hepatocyte-like cells. We suggest that the combination of the growth factors and the self-assembling peptide hydrogel provide a microenvironment that allow the cells to aquire hepatocyte-like properties. Lig-8 cells when encapsulated in the scaffolds were able to divide, migrate and aggregate into spheroid-like structures. In contrast, cells encapsulated into agarose gels (0.5%) remained mostly as single cells or formed very small spheroids, probably due to a higher stiffness of the material. Following the work by Semino and co-workers (Semino *et al*., 2003), we wanted to study the effect of several growth factors in the differentiation of Lig-8 cells into hepatocyte-like cells. We chose HGF and FGF4 and performed different assays to assess the level of differentiation. We used immunostaining to detect the expression of the cytochromes CYP3A2 and CYP2E1 and observed that only in 3D cultures the expression was detectable (Figure 6.11.; Figure 6.12.). In some cases, the expression was detected in vesicles, which could be the presence of microsomes. Moreover, we also detected the expression of albumin only in the 3D cultures. These results altogether with the gene-expression profile observed in 2D and 3D, including the CYP3A2 induction with dexamethasone) leads us to the conclussion that 3D encapsulation in the self-assembling peptide hydrogel promotes the differentiation of Lig-8 cells into cells with hepatocyte-like properties. HGF seems to be the growth factor tried that lead the cells to a slightly higher degree of differentiation as shown by the relative real time-PCR data in Figure 6.14. Even though there is some degree of differentiation, when the results are compared with freshly isolated hepatocytes, the gene expression values are considerably below standard fresh hepatocyte levels (Figure 6.16.). Although, there is much work ahead in understanding the differentiation processes and pathways involved in the obtantion of a progeny of cells with fully hepatocyte-like features, nevertheless these progenitor cells express a substantial amount of hepatocyte-specific markers (albumin, CYP3A2, CYP2E1, as well as CYP1A1/2, C/EBP α (15)). New emerging technologies in genomics and proteomics may help in that sense, as a wider array of genes, proteins and differentiation factors involved in the process could be analyzed.

Moreover, we studied the presence of BrdU-positive proliferating cells in the gels as well as in the 3D-derived spheroid colonies. Even though most cells acquired restricted proliferative capacity (did not incorporate BrdU), consistent with the fact that

the cells become differentiated, we always detected the presence of small amounts of proliferating cells (Figure 6.18., 6.19., 6.20. and 6.21.). We hypothesize that the peptide hydrogel provides a special microenvironment that somehow recreates a "stem cell niche" maintaining in the spheroids formed, some cells with "progenitor-like" properties (Figure 6.22.). These progenitor-like cells were able to re-expand *in vitro* when spheroids in 3D cultures were disgregated by trypsinization and replated in 2D cultures, as shown in Figure 6.20.

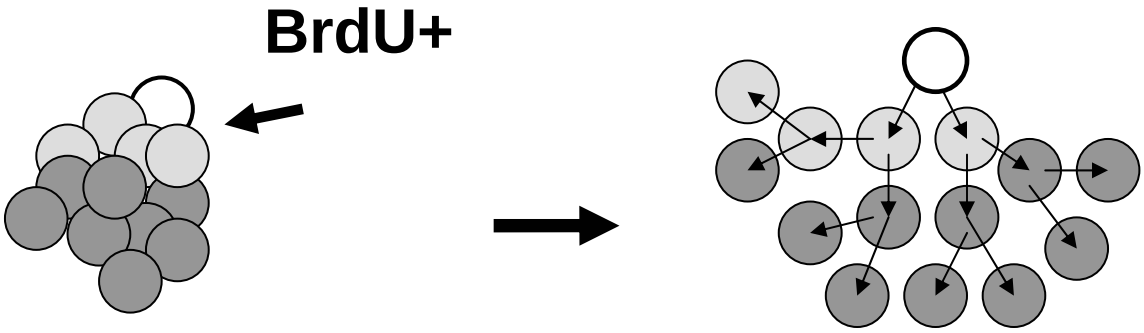

Figure 6.22. Scheme depicting the kinetics of the cells in a 3D cluster. White: progenitor cell, light grey: transit cell and grey: differentiated progeny.

The easy expansion of this cell line, and the advances in their directed differentiation in the 3D peptide hydrogel encapsulation system, could generate very interesting tools for biomedical technology, for example systems for toxicity testing, drug screening, studying molecular biology of different diseases, and generating cells with hepatocyte-like properties suitable for cell transplantation. They may be also useful in stem cell biology as they could be used in the study of stem cell niches. In addition, the easy handling and preparation of the peptide cultures in 96 well plates, would also be an advance in the application of the system in high-throughput screening analysis.

Chapter 7: *Materials and Methods*

7.1. Reagents and chemicals

Acetonitrile: HPLC-Analyzed purchased from JT Baker, 9017.
Coomassie Blue Staining Solution: 50% methanol, 40% H_2O, 10% acetic acid, 0.05% Coomassie Brilliant Blue R-50 (Gibco 15528-011).
Coomassie Blue Destaining Solution: 5% Methanol, 7% acetic acid, 88% H_2O.
BSA: Bovine Serum Albumin, Fraction V, Sigma-Aldrich, A3156.
DMEM: Dulbecco's Modified Eagle Medium, high glucose, with L-glutamine and pyridoxine hydrochloride, Invitrogen, 11965-092.
DMSO: Dimethylsulfoxide, Mallinckrodt, 4948.
EGM-2: Endothelial cell growth medium-2 from Cambrex, CC-4176. Contains, endothelial basal medium-2 (EBM-2), human epidermal growth factor (hEGF), hydrocortisone, fetal bovine serum (FBS), vascular endothelial growth factor (VEGF), basic human fibroblast growth factor (h-FGF-B), insulin-like growth factor (R^3-IGF-1), ascorbic acid, GA-1000 and heparin.
FBS: Fetal Bovine Serum, Invitrogen, 16000-044.
Glutamine: L-Glutamine 200mM, Invitrogen, 25030-081.
HCM: Hepatocyte culture medium from Cambrex, CC-3198. Contains, Hepatocyte basal medium (HBM), transferrin, hydrocortisone, bovine serum albumin (BSA), ascorbic acid, GA-100, and insulin.
PBS: Phosphate Buffered Saline, Invitrogen, 70011-044.
Penicillin-Streptomycin: Invitrogen, 15140-163.
PFA: Paraformaldehyde, Sigma-Aldrich, P6148.
Protease inhibitors: Complete Mini protease inhibitor cocktail, Roche, 1836153.
PS: Penicillin-Streptomycin, Invitrogen, 15140-163.
RIPA buffer: Radio Immunoprecipitation buffer with EDTA, containing Tris-HCl 50 mM, NaCl 150 mM, NP-40 1%, sodium deoxycholate 0.5%, SDS 0.1%, EDTA 5 mM, pH 7.4, Boston Bioproducts BP-115D.
Sucrose: Sigma-Aldrich, S0389.
TBS: Tris buffered saline, contains 100 mM Tris-HCl, 150 mM NaCl, pH 8.
TBST: Tris buffered saline with Tween-20, contains 100 mM Tris H-Cl, 150 mM NaCl, and 0.1% Tween-20, pH 8.
TFA: Trifluoroacetic acid, for protein sequence analysis, Sigma-Aldrich, 09653.
Triton-X 100: Sigma-Aldrich, T92848.
Trypsin: Trypsin from bovine pancreas, Sigma-Aldrich, T1426
Trypsin-EDTA: Invitrogen, 25300-054.
Tween-20: for molecular biology, Sigma-Aldrich, P9416.

7.2. Design and characterization of functionalized RAD16-I self-assembling peptide hydrogel

7.2.1. Peptide synthesis

All peptide sequences were obtained from SynPep (CA) with high purity and expected molecular weight determined by mass spectrometry (Table 7.1).

Table 7.1. Theoretical and obtained molecular weight by mass spectroscopy for peptide scaffolds

Peptide	Theoretical M.W.	Obtained M.W.
RAD16-I	1713	1712.9
AAS	2995.5	2996
CSR	3825.5	3826
YIG	2403.7	2404
PDS	2338.4	2339
RYV	2710.1	2711
KAF	3308.9	3309
TAG	3110.4	3110

7.2.2. Solubility and hydrogel formation

Each peptide was dissolved in deionized water at a final concentration of 1% (10 mg/ml) and sonicated for 20 min (Aquasonic, model 50T, VWR, PA). Stock solutions of peptide were always prepared in the same manner. We developed a system to test hydrogel formation on a cell culture chamber insert (10 mm diameter, 0.5 cm^2 area, pore size=0.2 μm, 136935, Nalge Nunc International, IL). A volume of 30 μl of peptide solution (0.5%) was loaded on the internal surface of the insert and allowed to form a layer (average thickness=600 μm). PBS was added at the bottom of the well to induce hydrogel formation.

7.2.3. Circular Dichroism (CD)

CD spectra were gathered on an Aviv model 202 spectropolarimeter. Samples were prepared by diluting stock peptide solutions in water (10 mg/ml) to a working concentration of 25 μM. Samples were analyzed at room temperature in a quartz cuvette with a path length of 0.3 cm and in the wavelength range 195-250 nm.

7.2.4. Atomic Force Microscopy

Peptides from stock 1% (w/v) solutions were diluted in deionized water to a final concentration of 0.01% (w/v), 1 μl of sample was loaded onto freshly cleaved mica substrate, rinsed with 100 μl of deionized water and dried in air. AFM images were obtained with a Multi 75 silicon scanning probe (MPP-21100, Nanodevices Inc., CA) with a resonance frequency of 75 KHz, spring constant 3 N/m, tip curvature radius<10 nm and 225 μm length. Images were obtained with a Multimode AFM microscope (Nanoscope IIIa, Digital Instruments, CA) operating in TappingMode. AFM scans were taken at 512x512 pixels resolution and produced topographic images of samples, which brightness of features increases as a function of height. Typical scanning parameters were as follows: tapping frequency 75 kHz, RMS amplitude before engage 1-1.2 V, setpoint 0.7-0.9 V, integral and proportional gains of 0.2-0.6 and 0.4-1 respectively, and scan rate 1.51 Hz.

7.2.5. Rheometry

Rheological assays were performed on a 50 mm parallel plate ARES strain controlled rheometer (Rheometric Scientific, NJ). Samples were dissolved in deionized water at a concentration of 2.9 mM and sonicated for 1 h the day prior to the analysis. A volume of 1 ml was loaded on the lower plate and the upper plated was set to a gap size between 0.4-0.45 mm.

A dynamic strain sweep was first performed to determine the linear viscoelastic range with the purpose to select a fixed strain. The conditions used were frequency 10 rad/s and the strain was tested from 0.001 to 10 (dimensionless). The strain selected for dynamic frequency sweep tests was 0.01.

Dynamic frequency seep tests were performed in a range of frequencies form 100 to 0.1 rad/s. RAD16-I was tested first. After the test, PBS was added around the lower

plate in order to promote gelation. The peptide was allowed to form gel for 10 min at room temperature and the test was performed once again.
The rest of the peptides were tested after the treatment with PBS in the same conditions as RAD16-I.
After every dynamic frequency sweep test, behavior of samples with time was tested. A dynamic time sweep test was performed at 10 rad/s for 5 min.

7.3. Protease degradation of RAD16-I peptide scaffold

7.3.1. Circular dichroism

Circular dichroism studies were performed on a JASCO-810 spectropolarimeter equiped with a Peltier system. Samples were diluted from a peptide stock solution (1%, 5.38 mM) in deionized water to a final concentration of 10, 25 and 100 μM and allowed to equilibrate at 20 or 90ºC for 10 min prior to analysis. CD data were acquired in a range of 195-240 nm at a band width of 1 nm and scan speed of 20 nm/s.

7.3.2. Enzymatic degradation

For degradation experiments samples were diluted from a stock solution to a final concentration of 100 μM in water. Trypsin was added in a molar ratio 1000:1 (peptide:enzyme). Samples were digested at 37ºC and samples were taken at 0, 1, 5, 10, 30 and 60 min for further analysis. Experiments were performed in duplicate.

7.3.3. MALDI-TOF

Matrix-assisted laser desorption/ionization time of flight (MALDI-TOF) trypsin-digested peptide samples prepared as explained above (7.2.2.) were performed on a Bruker Ultraflex mass spectrometer (Bremen, Germany), equipped with a pulsed nitrogen laser (337 nm). Samples were prepared by mixing 0.5 μl of the peptide solution with 1 μl of the matrix solution (0.3 mg/ml, α-cyano-4-hydroxy-cinnamic acid in ethanol/acetone 2:1). The mixture was the spotted on an anchor-chip target (Bruker), and allowed to evaporate to dryness at room temperature. Spectra were acquired in positive reflectron mode, using an acceleration voltage of 25 kV. Acquisition was performed in automated mode, using the Autoexecute software. A total of 1000 spectra, collected in 50-shot series at different positions of the sample spot, were

averaged for each sample. A mixture of standard peptides of known molecular masses in the range of 750-3500 Da (Bruker) was used for external calibration of the mass spectra.

7.3.4. AFM

To image the thermal denaturation of the self-assembling peptide RAD16-I samples were diluted in water from a stock solution (5.38 mM) to a final concentration of 100 μM. The thermal treatment consisted in subjectecting the sample to a 90ºC incubation for 10 min. Then, 1 μl of sample was deposited onto freshly cleaved mica (Grade V5 mica, Structure Probe Inc., PA, 01804-CA), rinsed twice with Milli-Q water and observed under the AFM.

For AFM imaging of the degradation experiments samples were prepared in the following manner. RAD16-I was diluted in water from a stock solution at a final concentration of 100 μM. For thermal treated samples, a 10 min denaturation step was performed prior the enzymatic degradation. Samples were cooled at room temperature and trypsin was added at a 1:1000 molar ratio (enzyme:peptide), and digestions were carried out during 1 h. Samples (Zhang *et al*., 1999) taken at 10 and 60 min and were deposited onto freshly cleaved mica, rinsed twice with Milli-Q water and scanned under the AFM.

AFM images were obtained with a silicon scanning probe (Asylum Research, CA, AC240-TS) with a resonance frequency of 70 KHz, spring constant 2 N/m, tip curvature radius <10 nm and 240 μm length. Images were obtained with a Multimode AFM microscope (Nanoscope IIIa, Digital Instruments, CA) operating in TappingMode. AFM scans were taken at 512x512 pixels resolution and produced topographic images of samples, which brightness of features increases as a function of height. Typical scanning parameters were as follows: tapping frequency 75 kHz, RMS amplitude before engage 1-1.5 V, setpoint 0.7-1 V, integral and proportional gains of 0.3-0.6 and 0.4-0.6 respectively, and scan rate 1.51 Hz.

7.4. Functional endothelial cell monolayer cultured on novel modified self-assembling peptide scaffolds

7.4.1. Cell maintenance and culture

Human aortic endothelial cells (HAEC, Cambrex, MD, CC-2535) were mantained in EBM-2 medium up to passage 5 in plastic flasks in a water-jacketed incubator at 37°C, 5% CO_2 until they reached 80% confluence. Cells were washed with fresh media without FBS before being released with trypsin (0.05%, Invitrogen, CA, 25300-054).

7.4.2. Cell culture for determining monolayer formation

The peptide hydrogel scaffolds (0.5% (w/v) in deionized water) were prepared at 100% or blended at a ratio 9:1 (RAD16-I:peptide sequence). Each solution was sonicated for 30 min, filtered (0.2 μm Acrodysc syringe filters, PALL, MI, 4192), and loaded (Gloe *et al*., 1999) into a 0.02 μm transwell insert (25 mm diameter, pore size=0.02, Nalge Nunc International, IL, 161395) and allowed to form a layer. EBM-2 medium was added to the well bottom (1 ml) to induce hydrogel formation, and after 5 min, 200 μl were added on top of the scaffold. The system was allowed to equilibrate in the incubator for 30 min and after that time the medium was changed.

Meanwhile, HAEC (Cambrex, MD, CC-2535) from routine culture conditions (passage 6) were harvested by treatment with trypsin. The released cells were washed with EBM-2 culture medium, counted and resuspended in fresh media at a final concentration of $2x10^6$ cells/ml. Cells were seeded at a density of $2x10^5$ cells/cm^2 in each tissue culture insert to study endothelial monolayer formation.

7.4.3. Cell culture system in tissue culture inserts

The scaffolds (0.5% (w/v) in deionized water) were prepared at 100% peptide sequence in the case of RAD16-I or blended with RAD16-I at a ratio 9:1 (RAD16-I:peptide sequence) for the three other cases (YIG, RYV and TAG). Each solution was sonicated 30 min, filtered (0.2 μm Acrodysc syringe filters, PALL, MI, 4192), loaded (Farkas *et al*., 2005) into a transwell insert (10 mm diameter, Nalge Nunc International, IL, 136935) and allowed to form a layer. EBM-2 media was added to the bottom of the well to induce hydrogel formation. After that time, medium was exchanged twice and the gels were allowed to equilibrate in the incubator for 1 h. Collagen-I (Rat Tail collagen, BD Biosciences, MA, 354236) and Matrigel matrix from EHS mouse tumour (BD Biosciences, MA, 354234) scaffolds were prepared following the manufacturer's recommendations. Briefly, the solutions were loaded (Farkas *et al*., 2005) on top of the same cell culture chamber insert and incubated at 37ºC to allow gel formation.

Meanwhile, HAEC from routine culture conditions (passage 5-6) were harvested and loaded on top of the preformed scaffolds at a density of $8x10^4$ cells/cm^2 and cultured in the incubator at 37ºC and 5% CO_2.

7.4.4. Low density lipoprotein (LDL) uptake staining

Cells cultured as above described in section 7.4.3., were used to perform cell staining. Cells were incubated for 4 h with medium containing 8 μg/ml of acetylated low density lipoprotein labeled with 1,1'-dioctadecyl-3,3,3',3'-tetramethylindo-carbocyanine perchlorate (DiI-Ac-LDL, Biomedical Technologies Inc, MA, , BT-902).
After that time, cells were fixed for 1 h with 2% PFA, permeabilized for 10 min with 0.1% Triton-X 100 and blocked for 1 h with blocking solution (20% BCS, 0.1% Triton-x 100 and 1% DMSO in PBS). DAPI staining (4',6-diamidino-2-phenylindole dihydrochloride, Molecular Probes, OR, D-1306) was used to visualize cell nuclei. Samples were incubated with 10 μg/ml DAPI in PBS for 5 minutes and analyzed under a Nikon Epi-Fluorescence microscope TE300 (Nikon, NY).

7.4.5. Cell attachment

Scaffolds were prepared as in section 7.4.3. Cell attachment assays were performed 1 h after the initial cell loading. In this case, the covering medium was removed, cells washed with PBS (Without Ca^{2+} and Mg^{2+}) and incubated with

trypsin/EDTA (0.25%/0.1%, Invitrogen, CA, 25200-0.56) for 30 min until most of the monolayer dettached. Cell counting was performed on a hematocytometer after Trypan Blue (Sigma-Aldrich, MO, T9906) exclusion assay staining.

7.4.6. Competition assays

The cellular scaffolds were prepared as described in section 7.4.3. For each scaffold the respective soluble motif (YIGSR, RYVVLPR, TAGSCLRKFSTM) and the non-respective sequence motifs were added independently to the culture medium at a concentration of 400 μg/ml. HAEC cells (passage 6) were loaded into the tissue culture insert at a density of $8x10^4$ cells/cm^2. Half of the medim was changed every other day. After the third day of culture, the medium was removed and fresh EBM-2 medium without FBS nor ascorbic acid, and containing 400 μg/ml of soluble peptide was added. The next day, cell numbers were evaluated as described above in section 7.4.5. Each condition was tested in triplicate.

7.4.7. DNA analysis

Cells were harvested and treated as described in competition assays section. Cells were resuspended in 40 μl of lysis buffer (0.1% Triton-X 100, protease inhibitors) together with the scaffold. Samples were sonicated for 20 min before proceeding to analyze the sample in order to disassemble the scaffold and to ensure the disruption of the cells. DNA was quantified by detection with ethidium bromide fluorescence. To perform the analysis, 45 μl of a 5 μg/ml ethidium bromide (Sigma, MO, E 1510) in TNE buffer were placed on a microtiter plate and 5 μl of sample was added to each well. The excitation and emission wavelengths used were 544 and 590 respectively. Fluoresce was measured on a Fluoroskan II (MTX Labs Inc., VI).

7.4.8. SDS PAGE elecrophoresis and Western Blotting

Harvested HAEC for each culture condition were counted and lysated with sample buffer (Invitrogen, CA, NP0007) containing 2% (v/v) β-mercaptoethanol and a cocktail of protease inhibitors to avoid proteolysis. Cell lysates containing equal amounts of cells were loaded on 10% polyacrylamide gel electrophoresis system (PAGE, Invitrogen, CA, NP0301) to analyze protein contents. A volume of sample equivalent to the cell number was loaded into the wells and MOPS

buffer (Invitrogen, CA, NP0001) was used to obtain better resolution on high molecular weight proteins. Proteins were transferred to a polyvinyliden difluoride membrane (Invitrogen, CA, LC2002) and used to perform western blot. The membranes were first blocked for 3h with blocking solution (2% BSA and 0.1% Triton-X 100 in PBS). Then they were incubated independently for 1h at room temperature with several primary antibodies diluted in the same blocking buffer: mouse monoclonal IgG_{2a} anti human laminin-1 (1:1000 dilution, Chemicon, CA, MAB1920), mouse monoclonal IgG_1 and anti human collagen IV (2 μg/mL, Chemicon, CA, MAB3326). Each membrane was then washed three times with blocking buffer. A secondary antibody HRP conjugated was used for detection by chemiluminiscence. Goat polyclonal anti mouse IgG-HRP conjugated (1:5000 dilution, Santa Cruz Biotechnology, CA, sc-2302) was used for both laminin-1 and collagen IV detection. The membranes were incubated for 30 min with the secondary antibody, then washed three times for 20 min with blocking buffer and twice with PBS. Western blots were developed using a chemiluminiscent system (Santa Cruz Biotechnology, CA, sc-2048) and protein bands visualized by exposure to an X-ray film (Biomax Film, Kodak, NY).

7.4.9. NO_x release

Media samples isolated as described above in competition assays section, was used to analyze NO_x release using a commercially available assay kit following the manufacturers instructions (Calbiochem, CA, 482702). Briefly, the assay is based on the detection of nitrites by the Griess method. In biological systems, the final products of NO *in vivo* are nitrate (NO_3^-) and nitrite (NO_2^-). The relative proportions of these two products is variable. Hence, the best index of total NO produced is the sum of both NO_2^- and NO_3^-. The assay is performed by a first reduction of NO_3^- to NO_2^- using nitrate reductase followed by an incubation with a lactate dehydrogenase solution (LDH) which destroys the excess of NADPH cofactor that interferes with the Griess reagents. A colorimetric reading at 540 nm can be performed after incubating the samples with the Griess reagents. Each condition was tested in triplicate.

7.5. A synthetic functionalized self-assembling peptide hydrogel culture system maintains hepatocyte specific functions

7.5.1. Hepatocyte isolation

Hepatocytes were isolated from 160-230 g male Fischer rats. The rats were anesthesized by intraperitoneal administration of sodium pentobarbitol. Livers were perfused through the inferior vena cava with Ca^{2+} free buffer for 7 minutes at 37 ºC. After that time, Liberase Blendzyme 3 (Roche Applied Science, IN, 1814184) solution in Ca^{2+} containing buffer was then added and the perfusion continued for another 10 minutes at 37 ºC. Hepatocytes were released and suspended in DMEM containing 0.2% BSA and Gentamycin. The suspension was centrifuged 2 times at 50 g for 3 minutes at 4 ºC and cell viability was assesed by trypan blue exclusion.

All hepatocyte isolations were performed by Laura Vineyard in Dr. L. Griffith's laboratory at MIT.

7.5.2. Hepatocyte culture on a collagen monolayer

Collagen (Rat tail collagen, BD Biosciences, MA, 354236) substrates were prepared at a concentration of 2 mg/ml following the manufacturer's instructions. Briefly, the collagen solution was diluted and neutralized with 1M NaOH. Then, 100 μl of the collagen solution were added at the bottom of a tissue culture insert (Millipore, MA, PICM 1250) and placed in the incubator at 37 ºC for 30 min to induce gellation. After that time the collagen was equilibrated with the hepatocyte culture medium (HCM) and 65000 cells/cm^2 were added into the insert.

7.5.3. Hepatocyte culture in a collagen sandwich

Collagen substrates (2 mg/ml) were prepared as explained above (7.5.2.). Briefly, the collagen solution was diluted in water and PBS 10X, and neutralized with 1M NaOH. 80 or 40 μl of the collagen solution were loaded into the botton of tissue culture insert (Millipore, MA, PICM 1250) and the collagen was allowed to gellify at 37ºC for 30 min. The 80 μl and 40 μl gels provided 1 mm and 0.5 mm-thick gels respectively, and will be refered by height in the text. Then, 65000 cells/cm^2 were loaded into the tissue culture insert. Cultures were incubated at 37ºC overnight. The next day, the unattached cells were removed by washing two times with sucrose 10%

and another layer (80 or 40 μl) of collagen were added on top and allowed to gellify in the incubator for 30 min. After that time medium was added to the bottom of the well and inside the insert.

7.5.4. Hepatocyte culture on a peptide monolayer

Peptide scaffolds were prepared by diluting in sucrose 20% the peptide stock solution 1% to a final concentration of 0.5%. When the modified peptides were used, they were mixed in a proportion 95:5 with the prototypic peptide. 40 μl of peptide were loaded into the bottom of a tissue culture insert and 200 μl of medium were added underneath the insert membrane to initiate gellation. After the peptide was gelled (10-15 min), 200 μl were added into the insert, and the gels were allowed to equilibrate for 30 min in the incubator at 37ºC. After that time, medium was changed and a volume of hepatocyte cell suspension was added at a final density of 65000 cells/cm^2. The cultures were mantained for two weeks.

7.5.5. Hepatocyte culture in a peptide sandwich

Peptide scaffolds were prepared by diluting in sucrose 20% the peptide hydrogel RAD16-I (Puramatrix, BD Biosciences, MA, 354250) stock solution 1% to a final concentration of 0.5%. When the modified peptides were used, they were mixed in a proportion 95:5 with the prototypic peptide (RAD16-I). The peptide solution becomes a hydrogel when it contacts a salt solution, such as a buffer or culture media. Thus, 80 or 40 μl of peptide were loaded into the bottom of a tissue culture insert and 200 μl of HCM were added underneath the insert membrane to initiate gellation (Millipore, PICM 1250), giving rise to 1 mm and 0.5 mμm-thick gels. After the peptide was gelled (10-15 min), 200 μl of HCM were added into the insert, and the gels were allowed to equilibrate for 30 min in the incubator at 37ºC. After that time, medium was changed and a volume of hepatocyte cell suspension was added at a final density of 65000 cells/cm^2 and were left to attach in the incubator overnight. The next day, unattached cells were washed by rinsing them three times with sucrose 10%. Then, 80 or 40 μl of peptide were added on top, entrapping the cells into a sandwich fashion. 200 μl of medium were added below the insert membrane, and the solution was allowed to gellify for 30 minutes. After that time the peptide was equilibrated by carefuly adding 20 μl of medium on top, were left for 20 minutes, then the process was repeated one more time. Finally, 50 μl of medium were carefuly added into the insert and 650 μl were

added outside of it. The medium was changed every day by removing the outside 650 μl and letting flow the media inside the insert, to avoid disturbing the upper peptide layer.

7.5.6. Cytochrome CYP3A2 induction with dexamethasone

Peptide and collagen sandwiches were prepared as explained above. Cells (65000 cells/cm^2) were cultured for a week with daily media changes. Cytochrome CYP3A2 was induced by incubating day 6 cultures with 10 μM dexamethasone (MP Biomedicals, 190040) in HCM media for 24 hours. RNA samples were taken at day 7 to study the expression of the cytochrome CYP3A2.

7.5.7. RNA isolation and real time-PCR analysis

RNA was obtained by treating the cells with Trizol Reagent (Invitrogen, CA, 15596-026), followed by a extraction with an RNEasy kit (Qiagen, CA, 74104). The obtained RNA was quantified, digested with DNAse I to remove contaminant DNA, and 100 ng were reverse transcribed with an Omniscript reverse transcription kit (Qiagen, CA, 205111) using random hexamers. Finally q-PCR was carried out using QuantiTect SYBR Green PCR kit (Qiagen, CA, 204143) in a MJ Opticon Monitor instrument. PCR primers were designed to obtain 150-200 base pair product. Forty five cycles were run with the following parameters: 2 min at 50ºC, 10 min at 94ºC, and for each cycle, 15 sec at 94ºC for denaturation, 30 s at 51-55 ºC for annealing and 30 s at 72ºC for extension. Finally a melting curve analysis was performed to test the specificity of the PCR products. The primer sequences were the following: albumin forward 5'-GGTGCAGGAAGTAACAGACTTTG-3' and reverse 5'-TAACTTGTCTCCGAAGAGAGTGTG-3'; HNF4-a forward 5'-CTGAGACTCCACAGCCATCA-3' and reverse 5'-CTAGATGGCTTCCTGCTTGG-3', CYP3A2 forward 5'-GTAGTACTCTTTCCATTCCTCACCC-3' and reverse 5'-GGTGCTTATGCTTAGAATCCAGAC-3'; TAT forward 5'-CATCGTGGACAACATGAAGG-3' and reverse 5'-TTGTACTTCCCCGAGTCCAG-3'; MDR2 forward 5'-CTTTGTGGTGGGGACACTCT-3' and reverse 5'-CCAAGAAGACCAGCGAGAAC-3'; 18s forward 5'-GCAATTATTCCCCATGAACG-3' and reverse 5'-GGCCTCACTAAACCATCCAA-3'. Primers sequences and PCR contidions were designed and optimized by Dr. A. Sivaraman, in Dr. L. Griffith's laboratory at MIT (Sivaraman Anand, 2004; Sivaraman *et al*., 2005).

Relative gene fold enrichments were determined by the $2^{-\Delta\Delta Ct}$ method using the ribosomal unit 18s as a housekeeping gene. Samples were compared to the gene expression in freshly isolated hepatocytes corresponding to the respective isolation. Experiments were performed in duplicate and the values were evaluated also in duplicate. PCR product sizes were checked by running 2% agarose gels.

7.5.8. Albumin secretion

Media samples corresponding to day 3, 5, 7 and 10 were kept at -20 ºC for further analysis. Albumin synthesis was measured with a rat albumin ELISA kit (Bethyl Laboratories, TX, E110-125). Briefly, 96-well plates were coated with a sheep anti-rat albumin antibody (1:100 in a carbonate-bicarbonate buffer pH 9.6) for an hour. After that, the wells were washed 3 times with washing buffer (50 mM Tris, 0.14M NaCl, 0.05% Tween-20 pH 8) and they were blocked for 30 min with blocking solution (50 mM Tris, 0.14M NaCl, 0.05% Tween-20, 1% BSA, pH 8). Then, 100 μl of standards and samples were incubated for 1 h, following 5 washes with washing solution. Then, the wells were incubated for another h with 100 μl of a secondary antibody HRP conjugated solution (1:50000), and the wells were washed again 5 times with washing buffer. Finally, wells were incubated 15 min with 100 μl of TMB substrate, and the reaction was stopped by adding 100 μl of H_2SO_4 2M. Absorbances were assesed by reading at 450 nm wavelength in a plate reader. Values were normalized using the cellular lysate total protein content value. Each experiment was performed in duplicate.

7.5.9. Urea production

Media samples from hepatocyte sandwich cultures were collected from peptide and collagen cultures and stored at -20ºC until analysis. Urea was quantitated with using a urease method. Briefly, 10 μl of sample were incubated with 25 μl of urease solution (Sigma-Aldrich, MO, US-3383) for 20 min at r.t. After that time, 50 μl of phenol nitroprusside (Sigma-Aldrich, P6994), 50 μl of alkaline hypochlorite (Sigma-Aldrich, MO, A1727) and 200 μl of MQ water were added to each well, and were incubated for 30 min at room temperature. Absorbance was measured at 590 nm. Absorbance values were quantitated using a calibration curve ranging from 0 to 150 mg urea/L, and values were normalized against the cell lysate total protein value. Each experiment was performed in duplicate.

7.5.10. Total protein quantification

Hepatocyte cultures were lysated using 300 μl of RIPA buffer containing protease inhibitors. Lysates were sonicated for 5 min and the solutions were centrifuged for 10 min at 10000 rpm to remove cell and scaffold debris. Total protein contained in the supernatant was quantified using the BCA assay kit (Pierce Biotechnology, 23225) following the manufacturers instructions.

7.5.11. Analysis of secreted protein by a proteomic approach

Media samples from hepatocyte collagen and RAD16-I sandwich cultures were electrophoresed using a 12% Bis-Tris gels and MOPS buffer. A sample of fresh HCM was added as a control to differentiate proteins present in the regular culture medium. Gels were stained with coomasie blue staining solution. Differential bands from samples to HCM control were cut and identidified using a proteomic approach. Briefly, bands were desalted and digested with trypsin, and eluted using a Agilent 1100 Nanoflow HPLC system connected to a Thermo Electron LTQ Ion Trap mass spectrometer. Ions were scanned in a range molecular weigth range from 500-3500 Da. Probability-based validation of protein identifications were performed using a modified SEQUEST algorithm to match the fragmentation patterns with the theoretical fragment patterns of tryptic peptides in the Uniprot Rat protein database. Ions were considered valid when Xcorr was 2.0 for peptides with m/z=1, 2.5 for peptides with m/z=2 and 3.5 for peptides with m/z=3. Experiments were performed at MIT's Biopolymers laboratory.

7.5.12. SDS-elecrophoresis and Western Blotting

Hepatocytes for each culture condition were lysated using RIPA buffer containing a cocktail of protease inhibitors (Roche Complete mini, Roche Applied Science, IN, 1836153) to avoid proteolysis, samples were sonicated, centrifuged to remove cell and scaffold debris, and maintained at -20ºC until analyzed. Total protein was quantitated with a BCA Protein Assay kit Pierce Biotechnology, IL, 23225). Volumes containg 5 μg of protein were mixed with sample buffer (Invitrogen, CA, NP0007) boiled for 5 minutes and loaded into a 12% Bis-Tris gel electrophoresis system (NuPAGE, Invitrogen, CA, NP0301). Proteins were electophoresed using MOPS buffer (Invitrogen, CA, NP0001), and then they were transferred for 2 h to a

polyvinyliden difluoride membrane (Invitrogen, CA, LC2002) and used to perform western blot. The membranes were first blocked for 3 h with blocking buffer (5% dry skim milk in TBST buffer). Then they were incubated independently overnight at 4ºC with several antibodies diluted in the same blocking buffer: sheep anti rat albumin-HRP conjugated antibody (1:20000 dilution, Bethyl Laboratories, TX, A110-134P), goat anti HNF4-a antibody (1:200 dilution, Santa Cruz Biotechnology, sc-6556), goat anti actin antibody (1:500 dilution, Santa Cruz Biotechnology, sc-1615). Each membrane was then washed three times with blocking buffer. A secondary antibody HRP conjugated was used for detection by chemiluminiscence. Goat polyclonal anti mouse IgG-HRP conjugated (1:1000 dilution, Santa Cruz Biotechnology, CA, sc-2302) was used for HNF4-α and actin detection. The membranes were incubated for 6 hours with the secondary antibody, then washed once for 20 min with blocking buffer and twice with TBS. Western blots were developed using a chemiluminiscent system (Supersignal West Pico Chemiluminiscent Substrate, Pierce Biotechnology, 34080) and protein bands visualized using an FluorChem gel imaging system (Fluorchem, Alpha Innotech).

For biotin dependent carboxylases detection, the membranes were blocked with blocking buffer for 3 h and then incubated overnight at 4ºC with avidin-HRP conjugated in TBS (1:2000 dilution, Peprotech, NJ). Membranes were washed 3 times with TBS and bands were visualized as explained above.

7.5.13. Bile canaliculi staining

Transport in bile canaliculi was visualized by treatment of the cultures with fluorescein diacetate. Briefly, to assess functional transportation by bile canaliculi, medium containing 2.5 μg/ml of fluorescein diacetate (Molecular Probes, CA, F1303) was added to 7 day peptide sandwich cultures. Cells were incubated for 20 min and visualized under a Nikon Epifluorescence microscope.

7.6. Differentiation of a rat-liver derived cell line Lig-8 in RAD16-I peptide scaffold

7.6.1. Lig-8 cell line culture

The derivation of adult rat liver stem cell line Lig-8 is described in detail elsewhere (Lee *et al*., 2003). Lig-8 cells were maintained in DMEM supplemented with 10% dialyzed fetal bovine serum (dFBS, 43605-100, JR Scientific, CA) and 200 μM xanthosine (X0750, Sigma, MO) in a water-jacketed incubator at 37°C and 5% CO_2.

7.6.2. Peptide scaffold culture

Cells from routine culture conditions (~80% confluence) were harvested by treatment with trypsin. The released cells were washed with complete culture medium, counted, resuspended in 20% (w/v) sucrose (S 5391, Sigma, MO) at final concentration of $2x10^6$ cells/ml, and mixed with an equal volume of a 1% peptide solution. Then, the cell suspension in the peptide was loaded into a 96 well plate (50 μl/well), the bottom of the wells had been previously soaked with 10 μl of medium to initiate gellation. After 15 min, 100 μl of culture medium (DMEM containing 10% dFBS, 4 mM glutamine and penicillin streptomycin) were added. The culture medium was changed three times during the first 60 min of culture. Medium was changed every other day. In addition, cells were cultured in the presence of 20 ng/mL hepatocyte growth factor (HGF, Chemicon, GF116), 10 ng/mL fibroblast growth factor 4 (FGF4) or a combination of both growth factors.

7.6.3. Spheroid-colony isolation from scaffold cultures

Peptide scaffold cell cultures were disrupted mechanically with a micropipette by several up and down aspirations. For immunofluorescence analysis, the cell/cluster suspension was placed on regular culture plates and incubated overnight in the same medium. The next day, the remaining scaffold was removed by washing the wells with fresh medium, and the attached cells/clusters were fixed with 1% PFA to perform immunostaining.

7.6.4. Immunofluorescence analysis

Spheroid-colonies obtained as described above were fixed with 1% PFA in PBS for 2 h, washed with PBS, permeabilized and blocked with blocking buffer (20% FBS, 0.1% Triton X-100; 1% DMSO in PBS) for 4 h at room temperature. The cells were then incubated overnight at 4ºC with different antibodies, rabbit anti rat cytochrome P450 CYP3A2 (dilution 1:200, Chemicon, AB1276), rabbit anti-CYP2E1 (dilution 1:200, Chemicon, CA, AB1252). Then, they were washed three times with bocking buffer, incubated for 5h at room temperature with a rhodamine conjugated secondary antibody (donkey anti-rabbit IgG-R, sc-2095, dilution 1:1000; or donkey anti-goat IgG-R, sc-2094, dilution 1:1000). Nuclei were stained with DAPI for 15 min at room tempertaure (Molecular probes, OR, D-1306) for detection under a Nikon microscope TE300. Controls incubating the cells with only secondary antibody were performed in order to confirm the specificity of the antibody.

For BrdU uptake analysis, cells were incubated overnight with culture medium containing BrdU at a final concentration of 10 μM (Sigma-Aldrich, MO, B9285). Cells were fixed with a 1% PFA solution and then, they were treated with HCl 2N for 30 min, blocked with blocking buffer and incubated overnight with a mouse anti BrdU-FITC conjugated antibody (BD Pharmigen, 51-33284X, dilution 1:100). Cells were then visulaized under a fluorescence microscope.

For CYP1A1/1A2-dependent metabolization of 7-ethoxyresorufin, cultures were incubated for 15 min with medium containing 7-ethoxyresorufin 3 μM (Sigma-Aldrich, MO, 46121). After that time, cells were visualized under a fluorescence microscope using the rhodamine filter.

7.6.5. SDS-elecrophoresis and Western Blotting

Lig-8 cells for each culture condition were lysated using RIPA buffer containing a cocktail of protease inhibitors (Roche Complete mini, Roche Applied Science, IN, 1836153) to avoid proteolysis, samples were sonicated and maintained at -20ºC until analyzed. Total protein was quantitated with a BCA Protein Assay kit Pierce Biotechnology, IL, 23225). Volumes containg 5.5 μg of protein were mixed with sample buffer (Invitrogen, CA, NP0007) boiled for 5 min and loaded into a 12% Bis-Tris gel electrophoresis system (NuPAGE, Invitrogen, CA, NP0301). Proteins were electophoresed using MOPS buffer (Invitrogen, CA, NP0001), and then they were transferred for 2 h to a polyvinyliden difluoride membrane (Invitrogen, CA, LC2002) and used to perform western blot. The membranes were first blocked for 3 h with blocking

buffer (5% dry skim milk in TBST buffer). Then they were incubated overnight at 4ºC with a sheep anti rat albumin-HRP conjugated antibody (1:20000 dilution, Bethyl Laboratories, TX, A110-134P). The membranes were washed once for 20 min with blocking buffer and twice with TBS. Western blots were developed using a chemiluminiscent system (Supersignal West Pico Chemiluminiscent Substrate, Pierce Biotechnology, 34080) and protein bands visualized using an FluorChem gel imaging system (Fluorchem, Alpha Innotech).

7.6.6. RNA isolation and real-time PCR analysis

RNA of lig-8 cultures was obtained by treating the cells with Trizol Reagent (Invitrogen, CA, 15596-026), followed by a extraction with an RNEasy kit (Qiagen, CA, 74104). The obtained RNA was quantified, digested with DNAse I to remove contaminant DNA, and 100 ng were reverse transcribed with an Omniscript reverse transcription kit (Qiagen, CA, 205111) using random hexamers. Finally q-PCR was carried out using QuantiTect SYBR Green PCR kit (Qiagen, CA, 204143) in an Applied Biosystems instrument. PCR primers were designed to obtain 150-200 base pair product. Forty five cycles were run with the following parameters: 2 min at 50 ºC, 10 min at 94 ºC, and for each cycle, 15 s at 94 ºC for denaturation, 1 min at 51-55 ºC for annealing and 30 s at 72ºC for extension. Finally a melting curve analysis was performed to test the specificity of the PCR products. The primer sequences were the following: albumin forward 5'-GGTGCAGGAAGTAACAGACTTTG-3' and reverse 5'-TAACTTGTCTCCGAAGAGAGTGTG-3'; CYP3A2 forward 5'-GTAGTACTCTTTCCATTCCTCACCC-3' and reverse 5'-GGTGCTTATGCTTAGAATCCAGAC-3'; CYP2E1 forward 5-TATCTACGATACCTACCTGGAAGCC-3' and reverse 5-CTCTATGAGGAGACAGTCAGTCACA-3'; 18s forward 5'-GCAATTATTCCCCATGAACG-3' and reverse 5'-GGCCTCACTAAACCATCCAA-3'. Primers were designed and optimized by Dr. A. Sivaraman, in Dr. L. Griffith's laboratory at MIT (Sivaraman Anand, 2004; Sivaraman *et al*., 2005).

Relative gene fold enrichments were determined by the $2^{-\Delta\Delta Ct}$ method using the ribosomal unit 18s as a housekeeping gene. Samples were compared to the gene expression in lig-8 in standard 2D cultures in the presence of Xs. They were also compared to samples of RNA from freshly isolated hepatocytes. Experiments were performed in duplicate and the values were evaluated also in duplicate. PCR product sizes were checked by running 2% agarose gels.

7.6.7. Dexamethasone induction

Lig-8 cultures were prepared as above described in section 7.6.2. At day 14, medium containing 10 μM dexamethasone was added for 24 h. After that time, RNA was isolated by treating the cells with Trizol reagent followed by an extraction using the RNEasy kit (Qiagen, CA, 74104).

7.6.8. Growth of 3D-derived Lig-8 cells

Lig-8 cultures were prepared as above described in section 7.6.2. At day 14, scaffolds were disrupted and incubated for 15 min with trypsin. Trypsin was stopped by adding culture medium, centrifugated and resuspended in fresh medium. Samples were re-cultured in regular tissue culture plates and monitored for three days.

CONCLUSIONS

- The self-assembling peptide hydrogel RAD16-I was functionalized in order to obtain a new generation of synthetic extracellular matrix analogs (Chapter 2). The new peptide scaffolds were succesfully tailored by extending the RAD16-I peptide sequence at the amino-terminal with laminin-1 and collagen-IV motifs, two of the main proteins from the basement membrane.

- Some physicochemical properties of the new functionalized peptides were studied. The peptides that were soluble in water formed hydrogels, presented a β-sheet secondary structure and formed nanofibers. In general the addition of peptide motifs caused distortion in these parameters, resulting in changes in the β-sheet structure as well in the capacity to form hydrogels and nanofibers. Nevertheless, those changes didn't affect the capacity to use these peptides in blending conditions with RAD16-I where the functionalized peptides were added in small percentages (5-10%)

- In Chapter 3, thermal stability and proteolysis of the scaffold was evaluated. It was shown that diluted solutions of the peptide undergo a thermal denaturation when treated at high temperatures (Laurson *et al*., 2005) by a change of secondary structure analyzed by CD and confirmed by AFM.

- Trypsin proteolytic activity on RAD16-I was evaluated monitoring the degradation reaction with two techniques MALDI-TOF and AFM. The impressive differences in proteolysis shown by AFM, added to the results obtained by circular dichroism, may indicate that the change in secondary structure from β-sheet from random coil influlences the proteolytic process. Indeed, the loss of the β-sheet, may leave the cleavage sites accessible for the enzymatic attack. For untreated samples the proteolytic process may be due to an equilibrium β-sheet-random coil in the ends of the fibers. We hipotesized that the transition from β-sheet to random coil occurs at the ends of the fibers causing the peptide to enter in solution and accessible to the enzymatic cleavage.

- In Chapter 4, the use of the novel functionalized peptides as basement membrane analogs for the culture of HAEC was described. Blends containing a 10% of functionalized peptides (YIG, RYV, TAG) with the prototypic RAD16-I were prepared and used in order to culture and obtain HAEC monolayers. Experiments were performed side to side to RAD16-I as well as Collagen I and Matrigel (being last two matrices considered as positive controls). It was observed, that cell attachment for all

the surfaces tested was close to 100% suggesting that the modifications are not playing an important role in cell attachment under the culture conditions tested.

- The functionalized peptide scaffolds promoted the maintenance and growth of HAEC over time in culture. In particular, sub-confluent seeded cultures of HAEC developed into confluent monolayers with elevated cell number when compared with the non-functionalized scaffold (RAD16-I), suggesting their role in increasing growth rates. In addition, growth rates in the non-functionalized RAD16-I scaffold did not change over time, suggesting that cells under this condition remain mainly inactive, probably they do not spread or migrate well, and, as a consequence do not proliferate.

- Competition assays with each corresponding soluble motif designed to block specific interactions between cells and the functionalized scaffolds demonstrated that growth rates were reduced to levels similar to control RAD16-I scaffold, suggesting that the cells indeed recognized the exposed adhesion motifs attached to each scaffold. Therefore, it appeared that endothelial cell growth was modulated through the biomimetic surface matrix only when the sequence was physically attached to the nanofiber, and that specific interaction in each case can be disrupted by adding the same soluble non-attached peptide motif.

- Moreover, and generally speaking, the peptide scaffolds enhanced endothelial cell phenotype and function, indicated in terms of basement membrane components deposition (laminin-1 and collagen IV), as well as NO synthesis. These results suggest that these peptide matrix conditions recreate better the endothelial microenvironement as it has been shown by the functional tests performed.

- In Chapter 5, completely synthetic extracellular matrix analogs were used in order to recreate the most commonly used hepatocyte culture system *in vitro*, the collagen sandwich. In this study, all experiments were performed in parallel to the same sandwich system built of a rat tail collagen-I gel, which is considered today, as the gold standard for the culture of hepatocytes *in vitro*.

- It was observed that in peptide cultures, hepatocyte morphology appeared to be polygonal and with a vast network of bile canaliculi, as it happens in the control collagen cultures. These canaliculi proved to be functional by the fact that they were able to metabolize and transport fluorescein diacetate through them, as it had been previously shown for collagen sandwich cultures.

- In terms of gene expression, the levels of relative expression to freshly isolated hepatocytes of the genes studied was comparable in collagen and peptide hydrogel cultures, except for hepatocytes cultured in peptide hydrogel sandwiches containing the peptide YIG, which presented some degree of upregulation specially in MDR2 and TAT.

- Generally speaking for all the functional experiments tested, hepatocytes in peptide sandwich cultures behaved correspondingly similar to collagen sandwich cultures. The same happened in terms of gene and protein expression, and in relation to the proteomic profile secreted to the culture medium.

- CYP3A2 gene expression appears to be highly downregulated in both collagen an peptide hydrogel sandwiches. However, CYP3A2 can be induced in this system by using common cytochrome inducers such as dexamethasone.

- This peptide sandwich model represents an enormous advance, meaning that defined and synthetic extracellular matrix analogs are being used, obtaining a truly comparable system to what is considered the gold standard in long term hepatocyte *in vitro* culture.

- In Chapter 6, the putative rat liver derived progenitor cell line Lig-8 was encapsulated within RAD16-I self-assembling peptide scaffold in the presence of several growth factors (HGF and FGF4) to promote differentiation into hepatocyte-like cells.

- Lig-8 cells when encapsulated in the scaffolds were able to divide, migrate and aggregate into spheroid-like structures. In contrast, cells encapsulated into agarose gels (0.5%) remained mostly as single cells or formed very small spheroids, probably due to a higher stiffness of the material.

- The degree of differentiation was evaluated using different assays. We used immunostaining to detect the expression of the cytochromes CYP3A2 and CYP2E1 and observed that only in 3D cultures the expression was detectable. In some cases, the expression was detected in vesicles, which could be the presence of microsomes. Moreover, analyzed the presence of albumin in the cellular lysates and we also detected the expression of albumin only in the 3D cultures. In terms of gene expression, 3D cultures presented a remarkable upregulation in albumin and CYP2E1 relative to lig-8 cells cultured in the presence of Xs. Even though there is some degree

of differentiation, when the PCR results were calculated relative to freshly isolated hepatocytes, the gene expression values were considerably below standard fresh hepatocyte levels. As well as it is observed with hepatocytes, CYP3A2 was inducible by dexamethasone.

- The presence of small amounts of remaining proliferating cells was always detected. We hypothesize that the peptide hydrogel provides a special microenvironment that somehow recreates a “stem cell niche” maintaining in the spheroids formed some cells with “progenitor-like” properties.

- We conclude that tailor-made peptide scaffolds represent a new generation of cell-responsive materials, easy to synthesize and purify and likely to have an impact on biomedical technologies. Moreover, this technological platform may serve to build novel scaffolds functionalized with other biomolecules such as carbohydrates, lipids, etc… to obtain materials with a wide range of biological properties.

REFERENCES

Abraham,L.J., Bradshaw,A.D., Shiels,B.R., Northemann,W., Hudson,G., and Fey,G.H. (1990). Hepatic transcription of the acute-phase a1-inhibitor III gene is controlled by a novel combination of cis-acting regulatory elements. Molecular and Cellular Biology *10*, 3483-3491.

Abu-Absi,S.F., Hu,W.S., and Hansen,L.K. (2005). Dexamethasone Effects on Rat Hepatocyte Spheroid Formation and Function. Tissue Engineering *11*, 415-426.

Ajees,A.A., Anantharamaiah,G.M., Mishra,V.K., Hussain,M.M., and Murthy,H.M.K. (2006). Crystal structure of human apolipoprotein A-I: Insights into its protective effect against cardiovascular diseases. Proceedings of the National Academy of Sciences of the United States of America *103*, 2126-2131.

Alper,C.A., Peters,J.H., Birtch,A.G., and Gardner,F.H. (1965). Haptoglobin synthesis. I. In vivo studies of the production of haptoglobin, fibrinogen, and g-globulin by the canine liver. Journal of Clinical Investigation *44*, 574-581.

Auth Marcus,K.H., Woitaschek,D., Beste,M., Schreiter,T., Kim,H.S., Oppermann,E., Joplin,R.E., Baumann,U., Hilgard,P., Nadalin,S., Markus,B.H., and Blaheta,R.A. (2005). Preservation of the synthetic and metabolic capacity of isolated human hepatocytes by coculture with human biliary epithelial cells. Liver transplantation : official publication of the American Association for the Study of Liver Diseases and the International Liver Transplantation Society *11*, 410-419.

Baker,D.E., Harrison,N.J., Maltby,E., Smith,K., Moore,H.D., Shaw,P.J., Heath,P.R., Holden,H., and Andrews,R.W. (2007). Adaptation to culture of human embryonic stem cells anda oncogenesis *in vivo*. Nature Biotechnology *25*, 207-215.

Barter,P.J. and Rye,K.A. (2006). The rationale for using apoA-I as a clinical marker of cardiovascular risk. Journal of Internal Medicine *259*, 447-454.

Barth,C.A. and Schwarz,L.R. (1982). Transcellular transport of fluorescein in hepatocyte monolayers: evidence for functional polarity of cells in culture. Proceedings of the National Academy of Sciences of the United States of America *79*, 4985-4987.

Baumgartner,M.R., Almashanu,S., Suormala,T., Obie,C., Cole,R.N., Packman,S., Baumgartner,E.R., and Valle,D. (2001). The molecular basis of human 3-methylcrotonyl-CoA carboxylase deficiency. Journal of Clinical Investigation *107*, 495-504.

Beck,K., Hunter,I., and Engel,J. (1990). Structure and function of laminin: anatomy of a multidomain glycoprotein. The FASEB journal : official publication of the Federation of American Societies for Experimental Biology *4*, 148-160.

Bell,S.E., Mavila,A., Salazar,R., Bayless,K.J., Kanagala,S., Maxwell,S.A., and Davis,G.E. (2001). Differential gene expression during capillary morphogenesis in 3D collagen matrices: regulated expression of genes involved in basement membrane matrix assembly, cell cycle progression, cellular differentiation and G-protein signaling. Journal of cell science *114*, 2755-2773.

Ben Ze'ev,A., Robinson,G.S., Buchter,N.L.R., and Farmer,S.R. (1988). Cell-cell and cell-matrix interactions differentially regulate the expression of hepatic and cytoskeletal

genes in primary cultures of rat hepatocytes. Proceedings of the National Academy of Sciences of the United States of America *85*, 2161-2165.

Berthiaume,F., Moghe,P.V., Toner,M., and Yarmush,M.L. (1996). Effect of extracellular matrix topology on cell structure, function, and physiological responsiveness: hepatocytes cultured in a sandwich configuration. FASEB Journal *10*, 1471-1484.

Bhatia,S.N., Balis,U.J., Yarmush,M.L., and Toner,M. (1999). Effect of cell-cell interactions in preservation of cellular phenotype: cocultivation of hepatocytes and nonparenchymal cells. FASEB Journal *13*, 1883-1900.

Binning,G.B., Quate,C.F., and Gerber,C.H. (1986). Atomic Force Microscope. Phys. Rev. Lett. *12*, 930.

Boeynaems,J.M. and Pirotton,S. (1994). Regulation of the Vascular Endothelium: Signals and Transduction Mechanisms.

Bogenriender,T. and Herlyn,M. (2003). Axis of evil: molecular mechanism of cancer metastasis. Oncogene *22*, 6524-6536.

Braciak,T.A., Northemann,W., Hudson,G.O., Shiels,B.R., Gehring,M.R., and Fey,G.H. (1988). Sequence and acute phase regulation of rat alpha 1-inhibitor III messenger RNA. The Journal of biological chemistry *263*, 3999-4012.

Busse,R. and Fleming,I. (2003). Regulation of endothelium-derived vasoactive autacoid production by hemodynamic forces. Trends in Pharmacological Sciences *24*, 24-29.

Cai,J., Weiss,M.L., and Rao,M.S. (2004). In search of "stemness". Experimental hematology *32*, 585-598.

Calero,M., Tokuda,T., Rostagno,A., Kumar,A., Zlokovic,B., Frangione,B., and Ghiso,J. (1999). Functional and structural properties of lipid-associated apolipoprotein J (clusterin). Biochemical Journal *344*, 375-383.

Caplan,M.R., Moore,P.N., Zhang,S., Kamm,R.D., and Lauffenburger,D.A. (2000). Self-Assembly of a b-Sheet Protein Governed by Relief of Electrostatic Repulsion Relative to van der Waals Attraction. Biomacromolecules *1*, 627-631.

Caplan,M.R., Schwartzfarb,E.M., Zhang,S., Kamm,R.D., and Lauffenburger,D.A. (2002). Control of self-assembling oligopeptide matrix formation through systematic variation of amino acid sequence. Biomaterials *23*, 219-227.

Cassell,O.C.S., Hofer,S.O.P., Morrison,W.A., and Knight,K.R. (2003). Vascularisation of tissue-engineered grafts: the regulation of angiogenesis in reconstructive surgery and in disease states. British journal of plastic surgery *55*, 603-610.

Charonis,A.S., Tsilibary,E.C., Yurchenco,P.D., and Furthmayr,H. (1985). Binding of laminin to type IV collagen: a morphological study. Journal of Cell Biology *100*, 1848-1853.

Chung,Y., Klimanskaya,I., Becker,S., Marh,J., Lu,S.J., Johnson,J., Meisner,L., and Lanza,R. (2006). Embryonic and extraembryonic stem cell lines derived from single mouse blastomeres. Nature (London, United Kingdom) *439*, 216-219.

Cines,D.B., Pollak,E.S., Buck,C.A., Loscalzo,J., Zimmerman,G.A., McEver,R.P., Pober,J.S., Wick,T.M., Konkle,B.A., Schwartz,B.S., Barnathan,E.S., McCrae,K.R., Hug,B.A., Schmidt,A.M., and Stern,D.M. (1998). Endothelial cells in physiology and in the pathophysiology of vascular disorders. Blood *91*, 3527-3561.

Colton,C.K. (1996). Implantable biohybrid artificial organs. Cell transplantation *4*, 415-436.

Cunningham,C.C. and Van Horn,C.G. (2004). Energy availability and alcohol-related liver pathology. Alcohol research & health : the journal of the National Institute on Alcohol Abuse and Alcoholism *27*, 291-299.

Davis,G.E., Bayless,K.J., and Mavila,A. (2002). Molecular basis of endothelial cell morphogenesis in three-dimensional extracellular matrices. Anatomical Records *268*, 252-275.

Davis,G.E. and Black,S.M.B.K. (2000). Capillary morphogenesis during human endothelial cell invation of three-dimensional collagen matrices. In Vitro Cell Developmental Biology Animal *36*, 513-519.

De Bartolo,L., Morelli,S., Rende,M., Gordano,A., and Drioli,E. (2004). New modified polyetheretherketone membrane for liver cell culture in biohybrid systems: adhesion and specific functions of isolated hepatocytes. Biomaterials *25*, 3621-3629.

De Bartolo,L., Morelli,S., Gallo,M.C., Campana,C., Statti,G., Rende,M., Salerno,S., and Drioli,E. (2005). Effect of isoliquiritigenin on viability and differentiated functions of human hepatocytes maintained on PEEK-WC-polyurethane membranes. Biomaterials *26*, 6625-6634.

De Bartolo,L., Salerno,S., Morelli,S., Giorno,L., Rende,M., Memoli,B., Procino,A., Andreucci,V.E., Bader,A., and Drioli,E. (2006). Long-term maintenance of human hepatocytes in oxygen-permeable membrane bioreactor. Biomaterials *27*, 4794-4803.

DeLeve,L.D., Wang,X., Hu,L., McCuskey,M.K., and McCuskey,R.S. (2004). Rat liver sinusoidal endothelial cell phenotype is maintained by paracrine and autocrine regulation. American Journal of Physiology *287*, G757-G763.

Domarus, A. V., Farreras, P., and Rozman, C. Medicina Interna. (1973).

Donovan,P.J. and Gearhart,J. (2001). The end of the beginning for pluripotent stem cells. Nature (London, United Kingdom) *414*, 92-97.

Drury,J.L. and Mooney,D.J. (2003). Hydrogels for tissue engineering: scaffold design variables and applications. Biomaterials *24*, 4337-4351.

Dunn,J.C.Y., Tompkins,R.G., and Yarmush,M.L. (1991). Long-term in vitro function of adult hepatocytes in a collagen sandwich configuration. Biotechnology Progress *7*, 237-245.

Dunn,J.C.Y., Yarmush,M.L., Koebe,H.G., and Tompkins,R.G. (1989). Hepatocyte function and extracellular matrix geometry: long-term culture in a sandwich configuration. FASEB Journal *3*, 174-177.

Dziadek,M. and Timpl,R. (1986). Expression of nidogen and laminin in basement membranes during mouse embryogenesis and in teratocarcinoma cells. Developmental biology *111*, 372-382.

Eichner,J.E., Dunn S Terence, Perveen,G., Thompson,D.M., Stewart,K.E., and Stroehla,B.C. (2002). Apolipoprotein E polymorphism and cardiovascular disease: a HuGE review. American journal of epidemiology *155*, 487-495.

Eiselt,P., Kim,B.S., Chacko,B., Isenberg,B., Peters,M.C., Greene,K.G., Roland,W.D., Loebsack,A.B., Burg,K.J.L., Culberson,C., Halberstadt,C.R., Holder,W.D., and Mooney,D.J. (1998). Development of Technologies Aiding Large-Tissue Engineering. Biotechnology Progress *14*, 134-140.

Engel,J. (1992). Laminins and other strange proteins. Biochemistry *31*, 10643-10651.

Engel,J., Odermatt,E., Engel,A., Madri,J.A., Furthmayr,H., Rohde,H., and Timpl,R. (1981). Shapes, domain organizations, and flexibility of laminin and fibronectin, two multifunctional proteins of the extracellular matrix. Journal of Molecular Biology *150*, 97-120.

Falkenberg,C., Grubb,A., and Aakerstroem,B. (1990). Isolation of rat serum a1-microglobulin. Identification of a complex with a1-inhibitor-3, a rat a2-macroglobulin homolog. Journal of Biological Chemistry *265*, 16150-16157.

Farkas,D., Bhat,V.B., Mandapati,S., Wishnok,J.S., and Tannenbaum,S.R. (2005). Characterization of the Secreted Proteome of Rat Hepatocytes Cultured in Collagen Sandwiches. Chemical Research in Toxicology *18*, 1132-1139.

Ferenczy,A., Bertrand,G., and Gelfand,M.M. (1979). Proliferation kinetics of human endometrium during the normal menstrual cycle. Am J Obstet Gynecol *133*, 859-867.

Flanagan,N. (2003). Engineering methods for tissue and cell repair. Genetic Engineering News *23*, 10-13.

Forbes,S., Vig,P., Poulsom,R., Thomas,H., and Alison,M. (2002). Hepatic stem cells. The Journal of pathology *197*, 510-518.

Frank,P.G. and Marcel,Y.L. (2000). Apolipoprotein A-I: structure-function relationships. Journal of Lipid Research *41*, 853-872.

Friedman,S.L., Roll,F.J., Boyles,J., and Bissell,D.M. (1985). Hepatic lipocytes: the principal collagen-producing cells of normal rat liver. Proceedings of the National Academy of Sciences of the United States of America *82*, 8681-8685.

Fujiwara,S., Wiedemann,H., Timpl,R., Lustig,A., and Engel,J. (1984). Structure and interactions of heparan sulfate proteoglycans from a mouse tumor basement membrane. European journal of biochemistry / FEBS *143*, 145-157.

Gadue,P., Huber,T.L., Nostro,M.C., Kattman,S., and Keller,G.M. (2005). Germ layer induction from embryonic stem cells. Experimental Hematology (New York, NY, United States) *33*, 955-964.

Garreta,E., Genove,E., Borros,S., and Semino,C.E. (2006). Osteogenic Differentiation of Mouse Embryonic Stem Cells and Mouse Embryonic Fibroblasts in a Three-Dimensional Self-Assembling Peptide Scaffold. Tissue Engineering *12*, 2215-2227.

Genove,E., Shen,C., Zhang,S., and Semino,C.E. (2005). The effect of functionalized self-assembling peptide scaffolds on human aortic endothelial cell function. Biomaterials *26*, 3341-3351.

Gloe,T., Riedmayr,S., Sohn,H.Y., and Pohl,U. (1999). The 67-kDa laminin-binding protein is involved in shear stress-dependent endothelial nitric-oxide synthase expression. J Biol Chem *274*, 15996-16002.

Godbey,W.T. and Atala,A. (2002). In vitro systems for tissue engineering. Annals of the New York Academy of Sciences *961*, 10-26.

Grant,D.S., Kinsella,J.L., Fridman,R., Auerbach,R., Piasecki,B.A., Yamada,Y., Zain,M., and Kleinman,H.K. (1993). Interaction of endothelial cells with a laminin A chain peptide (SIKVAV) in vitro and induction of angiogenic behavior in vivo. Journal of Cellular Physiology *153*, 614-625.

Grant,D.S., Tashiro,K., Segui-Real,B., Yamada,Y., Martin,G.R., and Kleinman,H.K. (1989). Two different laminin domains mediate the differentiation of human endothelial cells into capillary-like structures in vitro. Cell *58*, 933-943.

Greenfield,N.J. and Fasman,G.D. (1969). Computed circular dichroism spectra for the evaluation of protein conformation. Biochemistry *8*, 4108-4116.

Griffith,L.G. and Naughton,G. (2002). Tissue engineering--current challenges and expanding opportunities. Science *295*, 1009-1014.

Griffith,L.G. and Swartz,M.A. (2006). Capturing complex 3D tissue physiology in vitro. Nature Reviews Molecular Cell Biology *7*, 211-224.

Guan,J. and Wagner,W.R. (2005). Synthesis, characterization and cytocompatibility of polyurethaneurea elastomers with designed elastase sensitivity. Biomacromolecules *6*, 2833-2842.

Guengerich,F.P. (1991). Reactions and significance of cytochrome P-450 enzymes. Journal of Biological Chemistry *266*, 10019-10022.

Guengerich,F.P. (2002). Cytochrome P450 enzymes in the generation of commercial products. Nature Reviews Drug Discovery *1*, 359-366.

Guengerich,F.P. (2004). Cytochrome P450: what have we learned and what are the future issues? Drug metabolism reviews *36*, 159-197.

Hatzis,P. and Talianidis,I. (2001). Regulatory mechanisms controlling human hepatocyte nuclear factor 4a gene expression. Molecular and Cellular Biology *21*, 7320-7330.

Havel,H.A. (1996). Spectroscopic Methods for Determining Protein Structure in Solution.

Hayhurst,G.P., Lee,Y.H., Lambert,G., Ward,J.M., and Gonzalez,F.J. (2001). Hepatocyte nuclear factor 4a (nuclear receptor 2A1) is essential for maintenance of hepatic gene expression and lipid homeostasis. Molecular and Cellular Biology *21*, 1393-1403.

Hedberg,E.L., Shih,C.K., Lemoine,J.J., Timmer,M.D., Liebschner,M.A.K., Jansen,J.A., and Mikos,A.G. (2005). In vitro degradation of porous poly(propylene fumarate)/poly(-lactic-co-glycolic acid) composite scaffolds. Biomaterials *26*, 3215-3225.

Hernández, R. Design and fabrication of a new bioreactor for vascular tissue engineering. (2006). Universitat Ramon Llull, Barcelona.

Holmes,T.C. Novel peptide-based biomaterial scaffolds for tissue engineering. Trends in biotechnology *20*, 16-21.

Holmes,T.C., De Lacalle,S., Su,X., Liu,G., Rich,A., and Zhang,S. (2000). Extensive neurite outgrowth and active synapse formation on self-assembling peptide scaffolds. Proceedings of the National Academy of Sciences of the United States of America *97*, 6728-6733.

Hooiveld,G.J.E.J., van Montfoort,J.E., Meijer,D.K.F., and Muller,M. (2001). Function and Regulation of ATP-binding cassette transport proteins involved in hepatobiliary transport. [Erratum to document cited in CA134:216682]. European Journal of Pharmaceutical Sciences *12*, 523, 525-523, 543.

Iwamoto,Y., Robey,F.A., Graf,J., Sasaki,M., Kleinman,H.K., Yamada,Y., and Martin,G.R. (1987). YIGSR, a synthetic laminin pentapeptide, inhibits experimental metastasis formation. Science (Washington, DC, United States) *238*, 1132-1134.

Jiang,H., Rao,K.S., Yee,V.C., and Kraus,J.P. (2005). Characterization of Four Variant Forms of Human Propionyl-CoA Carboxylase Expressed in Escherichia coli. Journal of Biological Chemistry *280*, 27719-27727.

Jitrapakdee,S. and Wallace,J.C. (1999). Structure, function and regulation of pyruvate carboxylase. Biochemical Journal *340*, 1-16.

Jonnalagadda,S. and Robinson,D.H. (2004). Effect of thickness and PEG addition on the hydrolytic degradation of PLLA. Journal of Biomaterials Science, Polymer Edition *15*, 1317-1326.

Kan,P., Miyoshi,H., and Ohshima,N. (2004). Perfusion of Medium with Supplemented Growth Factors Changes Metabolic Activities and Cell Morphology of Hepatocyte-Nonparenchymal Cell Coculture. Tissue Engineering *10*, 1297-1307.

Kanemoto,T., Reich,R., Royce,L., Greatorex,D., Adler,S.H., Shiraishi,N., Martin,G.R., Yamada,Y., and Kleinman,H.K. (1990). Identification of an amino acid sequence from the laminin A chain that stimulates metastasis and collagenase IV production. Proceedings of the National Academy of Sciences of the United States of America *87*, 2279-2283.

Kapron,J.T., Hilliard,G.M., Lakins,J.N., Tenniswood,M.P.R., West,K.A., Carr,S.A., and Crabb,J.W. (1997). Identification and characterization of glycosylation sites in human serum clusterin. Protein Science *6*, 2120-2133.

Kavanagh,G.M. and Ross-Murphy,S.B. (1998). Rheological characterization of polymer gels. Progress in Polymer Science *23*, 533-562.

Kim,K., Yu,M., Zong,X., Chiu,J., Fang,D., Seo,Y.S., Hsiao,B.S., Chu,B., and Hadjiargyrou,M. (2003). Control of degradation rate and hydrophilicity in electrospun non-woven poly(d,l-lactide) nanofiber scaffolds for biomedical applications. Biomaterials *24*, 4977-4985.

Kim,S. and Healy,K.E. (2003). Synthesis and Characterization of Injectable Poly(N-isopropylacrylamide-co-acrylic acid) Hydrogels with Proteolytically Degradable Cross-Links. Biomacromolecules *4*, 1214-1223.

Kisiday,J., Jin,M., Kurz,B., Hung,H., Semino,C., Zhang,S., and Grodzinsky,A.J. (2002). Self-assembling peptide hydrogel fosters chondrocyte extracellular matrix production

and cell division: implications for cartilage tissue repair. Proceedings of the National Academy of Sciences of the United States of America *99*, 9996-10001.

Klein,G., Ekblom,M., Fecker,L., Timpl,R., and Ekblom,P. (1990). Differential expression of laminin A and B chains during development of embryonic mouse organs. Development (Cambridge, United Kingdom) *110*, 823-837.

Kleinman,H.K., Graf,J., Iwamoto,Y., Sasaki,M., Schasteen,C.S., Yamada,Y., Martin,G.R., and Robey,F.A. (1989). Identification of a second active site in laminin for promotion of cell adhesion and migration and inhibition of in vivo melanoma lung colonization. Archives of Biochemistry and Biophysics *272*, 39-45.

Klimanskaya,I., Chung,Y., Becker,S., Lu,S.J., and Lanza,R. (2006). Human embryonic stem cell lines derived from single blastomeres. Nature (London, United Kingdom) *444*, 512.

Koliakos,G.G., Kouzi-Koliakos,K., Furcht,L.T., Reger,L.A., and Tsilibary,E.C. (1989). The binding of heparin to type IV collagen: domain specificity with identification of peptide sequences from the a1(IV) and a2(IV) which preferentially bind heparin. Journal of Biological Chemistry *264*, 2313-2323.

Kreis,T. and Vale,R. (2000). Guidebook to the Extracellular Matrix, Anchor, and Adhesion Proteins; Second Edition.

Kweon,H., Yoo,M.K., Park,I.K., Kim,T.H., Lee,H.C., Lee,H.S., Oh,J.S., Akaike,T., and Cho,C.S. (2003). A novel degradable polycaprolactone networks for tissue engineering. Biomaterials *24*, 801-808.

Lanza,R., Langer,R., and Vacanti,C.A. (2000). Principles of tissue engineering. (San Diego: Academic Press).

Laurson,J., Selden,C., and Hodgson Humphrey,J.F. (2005). Hepatocyte progenitors in man and in rodents--multiple pathways, multiple candidates. International journal of experimental pathology *86*, 1-18.

LeCluyse,E.L., Audus,K.L., and Hochman,J.H. (1994). Formation of extensive canalicular networks by rat hepatocytes cultured in collagen-sandwich configuration. The American journal of physiology *266*, C1764-C1774.

LeCluyse,E.L., Bullock,P.L., and Parkinson,A. (1996). Strategies for restoration and maintenance of normal hepatic structure and function in long-term cultures of rat hepatocytes. Advanced Drug Delivery Reviews *22*, 133-186.

Lee,H.S., Crane,G.G., Merok,J.R., Tunstead,J.R., Hatch,N.L., Panchalingam,K., Powers,M.J., Griffith,L.G., and Sherley,J.L. (2003). Clonal expansion of adult rat hepatic stem cell lines by suppression of asymmetric cell kinetics (SACK). Biotechnology and Bioengineering *83*, 760-771.

Lee,K.Y. and Mooney,D.J. (2001). Hydrogels for Tissue Engineering. Chemical Reviews (Washington, D. C.) *101*, 1869-1879.

Levenberg,S., Huang,N.F., Lavik,E., Rogers,A.B., Itskovitz-Eldor,J., and Langer,R. (2003). Differentiation of human embryonic stem cells on three-dimensional polymer scaffolds. Proceedings of the National Academy of Sciences of the United States of America *100*, 12741-12746.

Li,R.H., Altreuter,D.H., and Gentile,F.T. (1996). Transport characterization of hydrogel matrixes for cell encapsulation. Biotechnology and Bioengineering *50*, 365-373.

Logdberg,L.E., Akerstrom,B., and Badve,S. (2000). Tissue distribution of the lipocalin alpha-1 microglobulin in the developing human fetus. Journal of Histochemistry and Cytochemistry *48*, 1545-1552.

Lutolf,M.P. and Hubbell,J.A. (2005). Synthetic biomaterials as instructive extracellular microenvironments for morphogenesis in tissue engineering. Nature Biotechnology *23*, 47-55.

Lutolf,M.P., Lauer-Fields,J.L., Schmoekel,H.G., Metters,A.T., Weber,F.E., Fields,G.B., and Hubbell,J.A. (2003). Synthetic matrix metalloproteinase-sensitive hydrogels for the conduction of tissue regeneration: Engineering cell-invasion characteristics. Proceedings of the National Academy of Sciences of the United States of America *100*, 5413-5418.

Malarkey,D., Johnson,K., Ryan,L., Boorman,G., and Maronpot,R. (2005). New insights into functional aspects of liver morphology. Toxicologic Pathology *33*, 27-34.

Malhi,H., Irani,A.N., Gagandeep,S., and Gupta,S. (2002). Isolation of human progenitor liver epithelial cells with extensive replication capacity and differentiation into mature hepatocytes. Journal of cell science *115*, 2679-2688.

Malinda,K.M., Nomizu,M., Chung,M., Delgado,M., Kuratomi,Y., Yamada,Y., Kleinman,H.K., and Ponce,M.L. (1999). Identification of laminin alpha1 and beta1 chain peptides active for endothelial cell adhesion, tube formation, and aortic sprouting. The FASEB journal : official publication of the Federation of American Societies for Experimental Biology *13*, 53-62.

Marshak,D.R., Gardner,R.L., Gottieb,D., and Editors. (2001). Stem Cell Biology. [In: Cold Spring Harbor Monogr. Ser., 2001; 40].

Martin,G.R. and Timpl,R. (1987). Laminin and other basement membrane components. Annual Review of Cell Biology *3*, 57-85.

Massia,S.P., Rao,S.S., and Hubbell,J.A. (1993). Covalently immobilized laminin peptide Tyr-Ile-Gly-Ser-Arg (YIGSR) supports cell spreading and co-localization of the 67-kilodalton laminin receptor with alpha-actinin and vinculin. J Biol Chem *268*, 8053-8059.

Michalopoulos,G.K. and DeFrances,M. (2005). Liver regeneration. Advances in Biochemical Engineering/Biotechnology *93*, 101-134.

Michalopoulos,G.K. and DeFrances,M.C. (1997). Liver regeneration. Science (Washington, D. C.) *276*, 60-66.

Min,B.H., Jeong,S.Y., Kang,S.W., Crabo,B.G., Foster,D.N., Chun,B.G., Bendayan,M., and Park,I.S. (1998). Transient expression of clusterin (sulfated glycoprotein-2) during development of rat pancreas. Journal of Endocrinology *158*, 43-52.

Muller,M. and Jansen,P.L.M. (1997). Molecular aspects of hepatobiliary transport. American Journal of Physiology *272*, G1285-G1303.

NG,C.P., Helm,C.E., and Swartz,M.A. (2004). Interstitial flow differentially stimulates blood and lymphatic endothelial cell morphogenesis in vitro. Microvascular Research *68*, 258-264.

Nomizu,M., Utani,A., Shiraishi,N., Kibbey,M.C., Yamada,Y., and Roller,P.P. (1992). The all-D-configuration segment containing the IKVAV sequence of laminin A chain has similar activities to the all-L-peptide in vitro and in vivo. Journal of Biological Chemistry *267*, 14118-14121.

Nomizu,M., Yokoyama,F., Suzuki,N., Okazaki,I., Nishi,N., Ponce,M.L., Kleinman,H.K., Yamamoto,Y., Nakagawa,S., and Mayumi,T. (2001). Identification of Homologous Biologically Active Sites on the N-Terminal Domain of Laminin Alpha Chains. Biochemistry *40*, 15310-15317.

Pachence,J.M. (1996). Collagen-based devices for soft tissue repair. Journal of Biomedical Materials Research *33*, 35-40.

Parenteau,N. Skin: the first tissue-engineered products. Scientific American *280*, 83-84.

Parker,G. and Picut,C. (2005). Liver Immunobiology. Toxicologic Pathology *33*, 52-62.

Paulsson,M., Aumailley,M., Deutzmann,R., Timpl,R., Beck,K., and Engel,J. (1987). Laminin-nidogen complex. Extraction with chelating agents and structural characterization. European Journal of Biochemistry *166*, 11-19.

Ponce,M.L., Nomizu,M., Delgado,M.C., Kuratomi,Y., Hoffman,M.P., Powell,S., Yamada,Y., Kleinman,H.K., and Malinda,K.M. (1999). Identification of endothelial cell binding sites on the laminin g1 chain. Circulation Research *84*, 688-694.

Poschl,E., Mayer,U., Stetefeld,J., Baumgartner,R., Holak,T.A., Huber,R., and Timpl,R. (1997). Site-directed mutagenesis and structural interpretation of the nidogen binding site of the laminin gamma1 chain. The EMBO journal *15*, 5154-5159.

Powers,M.J., Janigian,D.M., Wack,K.E., Baker,C.S., Beer,S.D., and Griffith,L.G. (2002). Functional behavior of primary rat liver cells in a three-dimensional perfused microarray bioreactor. Tissue Engineering *8*, 499-513.

Pratt,A.B., Weber,F.E., Schmoekel,H.G., Mueller,R., and Hubbell,J.A. (2004). Synthetic extracellular matrixes for in situ tissue engineering. Biotechnology and Bioengineering *86*, 27-36.

Qin,A.L., Zhou,X.Q., Zhang,W., Yu,H., and Xie,Q. (2004). Characterization and enrichment of hepatic progenitor cells in adult rat liver. World Journal of Gastroenterology *10*, 1480-1486.

Rambhatla,L., Bohn,S.A., Stadler,P.B., Boyd,J.T., Coss,R.A., and Sherley,J.L. (2001). Cellular senescence: Ex vivo p53-dependent asymmetric cell kinetics. Journal of Biomedicine & Biotechnology *1*, 28-37.

Reed,M.J. and Sage,E.H. (1996). SPARC and the extracellular matrix: implications for cancer and wound repair. Current Topics in Microbiology and Immunology *213*, 81-94.

Rosso,F., Giordano,A., Barbarisi,M., and Barbarisi,A. (2004). From cell-ECM interactions to tissue engineering. Journal of Cellular Physiology *199*, 174-180.

Rouet,P., Raguenez,G., Ruminy,P., and Salier,J.P. (1998). An array of binding sites for hepatocyte nuclear factor 4 of high and low affinities modulates the liver-specific enhancer for the human a1-microglobulin/bikunin precursor. Biochemical Journal *334*, 577-584.

Russell, P, Batchelor, D, and Thornton, J. SEM and AFM: complementary techniques for high resolution surface investigations. www.veeco.com, (2001).

Sakamoto,N., Iwahana,M., Tanaka,N.G., and Osada,Y. (1991). Inhibition of angiogenesis and tumor growth by a synthetic laminin peptide, CDPGYIGSR-NH2. Cancer Research *51*, 903-906.

Saxena,R., Theise,N.D., and Crawford,J.M. (2000). Microanatomy of the human liver-exploring the hidden interfaces. Hepatology (Baltimore, Md.) *30*, 1339-1346.

Schmitmeier,S., Langsch,A., Jasmund,I., and Bader,A. (2006). Development and characterization of a small-scale bioreactor based on a bioartificial hepatic culture model for predictive pharmacological in vitro screenings. Biotechnology and Bioengineering *95*, 1198-1206.

Schramm,G. (1994). A practical approach to rheology and rheometry. (Karlsruhe.

Schuldiner,M., Yanuka,O., Itskovitz-Eldor,J., Melton,D.A., and Benvenisty,N. (2000). Effects of eight growth factors on the differentiation of cells derived from human embryonic stem cells. Proceedings of the National Academy of Sciences of the United States of America *97*, 11307-11312.

Semino,C. (2003). Can we build artificial stem cell compartments. Journal of Biomedicine and Biotechnology *3*, 164-169.

Semino,C.E., Kamm,R.D., and Lauffenburger,D.A. (2006). Autocrine EGF receptor activation mediates endothelial cell migration and vascular morphogenesis induced by VEGF under interstitial flow. Experimental Cell Research *312*, 289-298.

Semino,C.E., Kasahara,J., Hayashi,Y., and Zhang,S. (2004). Entrapment of Migrating Hippocampal Neural Cells in Three-Dimensional Peptide Nanofiber Scaffold. Tissue Engineering *10*, 643-655.

Semino,C.E., Merok,J.R., Crane,G.G., Panagiotakos,G., and Zhang,S. (2003). Functional differentiation of hepatocyte-like spheroid structures from putative liver progenitor cells in three-dimensional peptide scaffolds. Differentiation (Berlin, Germany) *71*, 262-270.

Sherley,J.L. (2002). Asymmetric cell kinetics genes: the key to expansion of adult stem cells in culture. Stem cells (Dayton, Ohio) *20*, 561-572.

Sherlock,S. and Dooley,J. (2007). Diseases of the Liver and Biliary System.

Ship,N.J., Toprak,A., Lai,R.P., Tseng,E., Kluger,R., and Pang,K.S. (2005). Binding of acellular, native and cross-linked human hemoglobins to haptoglobin: Enhanced distribution and clearance in the rat. American Journal of Physiology *288*, G1301-G1309.

Silva,G.A., Czeisler,C., Niece,K.L., Beniash,E., Harrington,D.A., Kessler,J.A., and Stupp,S.I. (2004). Selective differentiation of neural progenitor cells by high-epitope density nanofibers. Science (Washington, DC, United States) *303*, 1352-1355.

Silva,J.M., Morin,P.E., Day,S.H., Kennedy,B.P., Payette,P., Rushmore,T., Yergey,J.A., and Nicoll-Griffith,D.A. (1998). Refinement of an in vitro cell model for cytochrome P450 induction. Drug Metabolism and Disposition *26*, 490-496.

Sipe,J.D. (2002). Tissue engineering and reparative medicine. Annals of the New York Academy of Sciences *961*, 1-9.

Sivaraman Anand. A microfabricated 3D microfabricated "Liver on a Chip": high information content assays for in vitro drug metabolism studies. (2004). Massachusetts Institute of Technology, Cambridge, MA.

Sivaraman,A., Leach,J.K., Townsend,S., Iida,T., Hogan,B.J., Stolz,D.B., Fry,R., Samson,L.D., Tannenbaum,S.R., and Griffith,L.G. (2005). A microscale in vitro physiological model of the liver: predictive screens for drug metabolism and enzyme induction. Current Drug Metabolism *6*, 569-591.

Skubitz,A.P.N., McCarthy,J.B., Zhao,Q., Yi,X.Y., and Furcht,L.T. (1990). Definition of a sequence, RYVVLPR, within laminin peptide F-9 that mediates metastatic fibrosarcoma cell adhesion and spreading. Cancer Research *50*, 7612-7622.

Soprano,D.R., Soprano,K.J., and Goodman,D.S. (1986). Retinol-binding protein messenger RNA levels in the liver and in extrahepatic tissues of the rat. Journal of Lipid Research *27*, 166-171.

Strain,A.J., Crosby,H.A., Nijjar,S., Kelly,D.A., and Hubscher,S.G. (2003). Human liver-derived stem cells. Seminars in Liver Disease *23*, 373-383.

Sudo,R., Mitaka,T., Ikeda,M., and Tanishita,K. (2005). Reconstruction of 3D stacked-up structures by rat small hepatocytes on microporous membranes. FASEB Journal *19*, 1695-1697, 10.

Tamkun,J.W. and Hynes,R.O. (1983). Plasma fibronectin is synthesized and secreted by hepatocytes. Journal of Biological Chemistry *258*, 4641-4647.

Tashiro,K., Sephel,G.C., Weeks,B., Sasaki,M., Martin,G.R., Kleinman,H.K., and Yamada,Y. (1989). A synthetic peptide containing the IKVAV sequence from the A chain of laminin mediates cell attachment, migration, and neurite outgrowth. Journal of Biological Chemistry *264*, 16174-16182.

Timpl,R. (1989). Structure and biological activity of basement membrane proteins. European Journal of Biochemistry *180*, 487-502.

Timpl,R. (1996). Macromolecular organization of basement membranes. Current Opinion in Cell Biology *8*, 618-624.

Tosh,D. and Strain,A. (2005). Liver stem cells--prospects for clinical use. Journal of Hepatology *42 Suppl*, S75-S84.

Tsilibary,E.C., Koliakos,G.G., Charonis,A.S., Vogel,A.M., Reger,L.A., and Furcht,L.T. (1988). Heparin-type IV collagen interactions. Equilibrium binding and inhibition of type IV collagen self-assembly. Journal of Biological Chemistry *263*, 19112-19118.

Tsilibary,E.C., Reger,L.A., Vogel,A.M., Koliakos,G.G., Anderson,S.S., Charonis,A.S., Alegre,J.N., and Furcht,L.T. (1990). Identification of a multifunctional, cell-binding peptide sequence from the a1(NC1) of type IV collagen. Journal of Cell Biology *111*, 1583-1591.

Tsitlanadze,G., Machaidze,M., Kviria,T., Djavakhishvili,N., Chu,C.C., and Katsarava,R. (2004). Biodegradation of amino-acid-based poly(ester amide)s: In vitro weight loss and preliminary in vivo studies. Journal of Biomaterials Science, Polymer Edition *15*, 1-24.

Tsuji,A., Akamatsu,T., Nagamune,H., and Matsuda,Y. (1994). Identification of targeting proteinase for rat a1-macroglobulin in vivo. Mast-cell tryptase is a major component of the a1-macroglobulin-proteinase complex endocytosed into rat liver lysosomes. Biochemical Journal *298*, 79-85.

Turncliff,R.Z., Meier,P.J., and Brouwer,K.L.R. (2004). Effect of dexamethasone treatment on the expression and function of transport proteins in sandwich-cultured rat hepatocytes. Drug Metabolism and Disposition *32*, 834-839.

Uyama,N., Shimahara,Y., Kawada,N., Seki,S., Okuyama,H., Iimuro,Y., and Yamaoka,Y. (2002). Regulation of cultured rat hepatocyte proliferation by stellate cells. Journal of Hepatology *36*, 590-599.

Van Amersfoort,E.S., Van Berkel,T.J.C., and Kuiper,J. (2003). Receptors, mediators, and mechanisms involved in bacterial sepsis and septic shock. Clinical Microbiology Reviews *16*, 379-414.

Wang,Y., Liu,H., Guo,H., Wen,H., and Liu,J. (2004). Primary hepatocyte culture in collagen gel mixture and collagen sandwich. World journal of gastroenterology : WJG *10*, 699-702.

Watt,A.J., Garrison,W.D., and Duncan,S.A. (2003). HNF4: A central regulator of hepatocyte differentiation and function. Hepatology (Philadelphia, PA, United States) *37*, 1249-1253.

Watt,F.M. and Hogan,B.L. (2000). Out of Eden: stem cells and their niches. Science *287*, 1427-1430.

Weissman,I.L. (2000). Translating stem and progenitor cell biology to the clinic: barriers and opportunities. Science (Washington, D. C.) *287*, 1442-1446.

Werb,Z. (1997). ECM and cell surface proteolysis: regulating cellular ecology. Cell (Cambridge, Massachusetts) *91*, 439-442.

West,J.L. and Hubbell,J.A. (1999). Polymeric Biomaterials with Degradation Sites for Proteases Involved in Cell Migration. Macromolecules *32*, 241-244.

Yamada,K.M. (1991). Adhesive recognition sequences. Journal of Biological Chemistry *266*, 12809-12812.

Yamada,Y. and Kleinman,H.K. (1992). Functional domains of cell adhesion molecules. Current Opinion in Cell Biology *4*, 819-823.

Yamamoto,Y., Teratani,T., Yamamoto,H., Quinn,G., Murata,S., Ikeda,R., Kinoshita,K., Matsubara,K., Kato,T., and Ochiya,T. (2005). Recapitulation of in vivo gene expression during hepatic differentiation from murine embryonic stem cells. Hepatology (Hoboken, NJ, United States) *42*, 558-567.

Yang,S., Leong,K.F., Du,Z., and Chua,C.K. (2002). The design of scaffolds for use in tissue engineering. Part I. Traditional factors. Tissue Engineering *7*, 679-689.

Yasumitsu,T., Nomizu,M., Gullberg,D., MacKrell,A.J., Keene,D.R., Yamada,Y., and Fessler,J.H. (1996). Conserved neuron promoting activity in Drosophila and vertebrate laminin alpha-1. J Biol Chem *271*, 18074-18081.

Yurchenco,P.D. and Cheng,Y.S. (1993). Self-assembly and calcium-binding sites in laminin. A three-arm interaction model. Journal of Biological Chemistry *268*, 17286-17299.

Yurchenco,P.D. and O'Rear,J.J. (1994). Basement membrane assembly. Methods in Enzymology *245*, 489-518.

Zeisberg,M., Kramer,K., Sindhi,N., Sarkar,P., Upton,M., and Kalluri,R. (2006). De-differentiation of primary human hepatocytes depends on the composition of specialized liver basement membrane. Molecular and Cellular Biochemistry *283*, 181-189.

Zhang,S. and Altman,M. (1999). Peptide self-assembly in functional polymer science and engineering. Reactive & Functional Polymers *41*, 91-102.

Zhang,S., Holmes,T., Lockshin,C., and Rich,A. (1993). Spontaneous assembly of a self-complementary oligopeptide to form a stable macroscopic membrane. Proceedings of the National Academy of Sciences of the United States of America *90*, 3334-3338.

Zhang,S., Holmes,T.C., DiPersio,C.M., Hynes,R.O., Su,X., and Rich,A. (1995). Self-complementary oligopeptide matrixes support mammalian cell attachment. Biomaterials *16*, 1385-1393.

Zhang,S., Lockshin,C., Herbert,A., Winter,E., and Rich,A. (1992). Zuotin, a putative Z-DNA binding protein in Saccharomyces cerevisiae. EMBO Journal *11*, 3787-3796.

Zhang,S., Yan,L., Altman,M., Lassle,M., Nugent,H., Frankel,F., Lauffenburger,D.A., Whitesides,G.M., and Rich,A. (1999). Biological surface engineering: a simple system for cell pattern formation. Biomaterials *20*, 1213-1220.

The data presented in this Thesis has been published or is under process of publication. The following list indicates the state of publication by Chapter:

- Chapter 2 and Chapter 4:

  Genové, E., Shen, C., Zhang, S., Semino, C.; (2005); The effect of functionalized self-assembling peptide scaffolds on human aortic endothelial cells. *Biomaterials*, **26**, 3341-3351

  Hernández Vera, R., Genové, E., Alvarez, L., Borrós, S., Lauffenburger, D., Semino, C. Interstitial fluid flow intensity modulates endothelial sprouting in restricted Src activated cell clusters during capillary morphogenesis. *In preparation.*

- Chapter 3:

  Genové E., Borrós, S., Semino, C. β-sheet to random coil transition in self-assembling peptide scaffolds influences protease degradation. *In preparation.*

- Chapter 5:

  Genové E., Sala, A., Schmitmeier, S., Borrós, S., Bader, A., Griffith, L.G., Semino, C. A synthetic functionalized self-assembling peptide hydrogel enhance hepatocyte activity *in vitro. Under review.*

- Chapter 6:

  Genové, E., Semino, C. Differentiation of an adult liver putative progenitor cell line, Lig-8, in RAD16-I self-assembling peptide scaffold. *In preparation.*

Other papers published by the author of this Thesis in collaboration with other members of the group:

- Garreta E., Genové, E., Borrós, S., Semino, C. (2006), Osteogenic Differentiation of Mouse Embryonic Stem Cells and Mouse Embryonic Fibroblasts in a Three-Dimensional Self-Assembling Peptide Scaffold. *Tissue Engineering,* **12**, 2215-2227

- Quintana, L., Fernández-Muiños, T., Genové, E., Olmos, M., Borrós, S., Semino, C. A Soft Nanofiber Matrix Promote Mouse Embryonic Fibroblast Self-Organization into a 3D-Bilateral Structure With Patterned Paraxial Cartilage-like Tissue. *In preparation.*